# Interactions between human 2D- and 3D-cultured jaw periosteal and dendritic cells

**Thesis submitted as requirement to fulfill the degree
„Doctor of Philosophy" (Ph.D.)**


**at the
Faculty of Medicine
Eberhard Karls University
Tübingen**


**by**


**Dai, Jingtao**


**from
Guangdong, P. R. China**


**2021**

Dean: Professor Dr. B.  Pichler

First reviewer: Prof. Dr. D. Alexander-Friedrich

Second reviewer: Prof. Dr. A. Nüssler


Date of oral examination: 23.04.2021

**Table of Contents**

# 1. Introduction

## 1.1. Bone tissue engineering

Bone tissue is a critical organ of the skeletal system, participating in several physiological processes, which include mechanical support and protection to the body, facilitating movement, mineral homeostasis and hematopoiesis, etc. Clinically, bone defects represent the most frequent organ injuries due to oncological surgeries, malformations, osteomyelitis or trauma, affecting hundreds of millions of people worldwide per year. Although bone tissue possesses a good self-repair and regeneration capacity, some bone defects exceed bone self-healing capacity. The defect repair using the bone tissue engineering (BTE) approach is as assumed to be a feasible approach. The demand for BTE is closely linked to increasing cases of bone injuries due to a higher life expectancy and the increased world population.

Undoubtedly, the gold standard to repair a bone defect is an autologous bone graft due to not only its excellent biocompatibility and osteogenesis but also ideal mechanical properties. Nevertheless, autologous bone is facing several issues for treatments of the bone defect. The limitations mainly include their additional surgery, postoperative complications at the donor site and a limited amount of material available. Therefore, to overcome the disadvantages above, BTE has been proposed to develop new functional bone substitutes exhibiting excellent biocompatibility with a high bone regenerative potential [1, 2]. Although xenografts (i.e., bovine bone) and alloplasts (i.e., beta-tricalcium phosphate (β-TCP) and hydroxyapatite) with excellent osteoconduction have been used in clinical, the demand for bone substitutes with osteoinductive and osteoinductive properties is increasing. Numerous studies demonstrated that mesenchymal stem cells (MSCs) possess the ability to undergo osteogenic differentiation that makes them appropriate for bone tissue engineering purposes.

Hitherto, MSC-based bone constructs have been further proposed as an ideal treatment for bone defects [1, 2]. As shown in Figure 1.1, The MSC-based bone constructs (bioactive constructs) highlight three critical roles: 1)

cells: tissue-derived stem cells; 2) scaffolds: biocompatible materials mimicking the natural bone extracellular matrix, providing cell growth and mechanical integrity; 3) bioactive factors: growth factors (signalling molecules) can regulate osteoprogenitor proliferation, migration and differentiation. Additionally, the assembly method between cells and scaffolds has been considered and developed, i.e. cell seeding, bioprinting and microspheres [3]. The use of MSC-based bone constructs for patient safety, including immunogenicity, sterility and carcinogenesis, is another aspect [3].
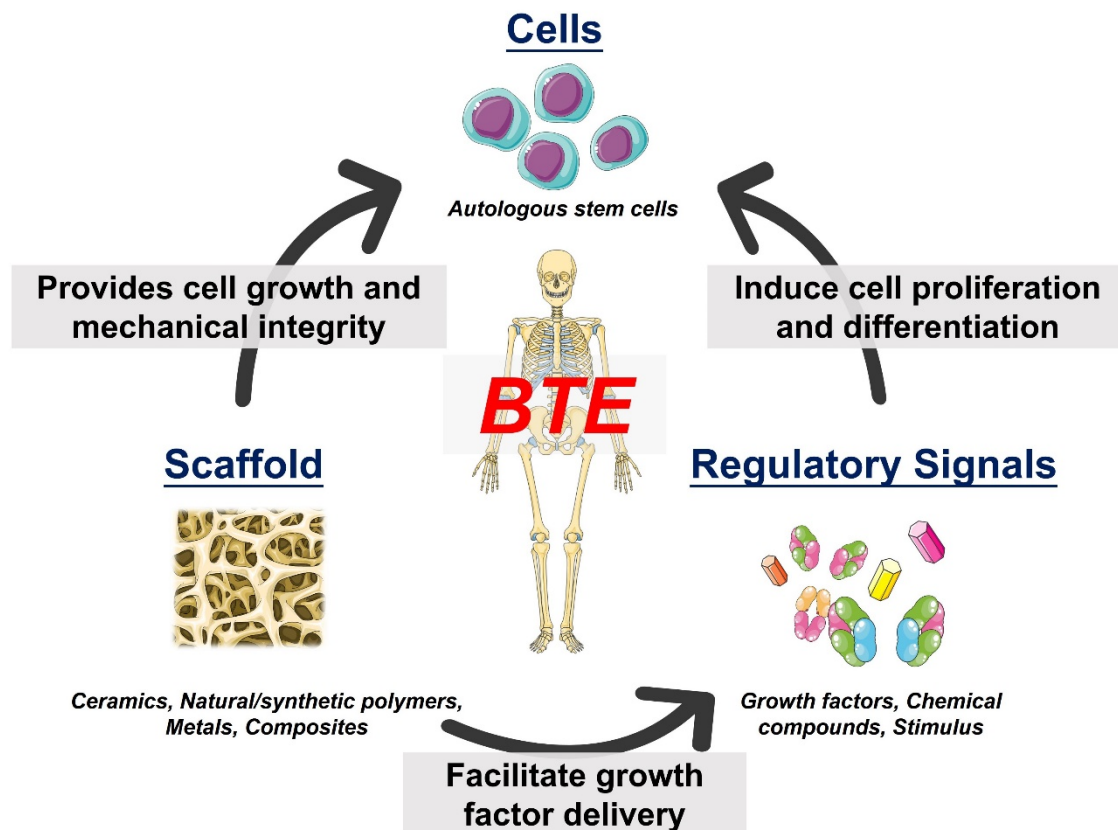


**Figure 1.1**. Schematic representation of the development of cells-based bone constructs for bone tissue engineering.

## 1.2. Cells

### 1.2.1. Cell sources used in bone tissue engineering

Regarding BTE, cells seeded into scaffolds are tissue-derived stem cells, which can be of autologous, allogenic, xenogenic origin or alloplasts [4]. Considering the risk of immunogenicity, autologous cells are the best option for BTE. Different somatic and stem cells can be classified according to their differentiation capabilities, as summarized in Table 1.1. To date, stem cells are the first choice for cell sources in BTE due to their high capacity for expansion as well as potency. The application of embryonic and fetal tissue has been limited due to safety concerns and ethical issues. Current research efforts gradually focus on induced pluripotent stem cells (iPSCs), developed by reprogramming of somatic cells to a state of pluripotency and multilineage potential. However, the immunogenicity of iPSCs has been controversially discussed because of their possible tumorigenicity [5]. As a source with lower stem cell potential , the use of adult tissue-derived stem cells in BTE has been considered to be the most suitable also considering the lacking ethical concerns. Numerous research has focused on different mesenchymal tissue-derived stem cells, such as bone marrow, adipose tissue, umbilical cord, dental pulp and periosteum, which are able to differentiate into the bone tissue.

**Table 1.1.** Comparision of different cell sources used in BTE [6].

| Cell Type | Cell potency | Advantages | Limitations |
|---|---|---|---|
| Autologous osteoblasts | None | Lack of immune rejection<br>Low cost<br>No requirement for development | Need to be expanded ex vivo<br>Time-consuming procedure |
| Embryonic stem cells (e.g. Morula) | Totipotent | Unlimited differentiating capability<br>Unlimited proliferation potential | Ethical objections<br>The risk of tumorigenicity<br>Difficult culturing |
| Fetal adnexa-derived adult stem cells (e.g. Umbilical cord-derived stem cells) | Pluripontent or multipotent | High proliferation rates<br>Immuno-privileged properties | Ethical concerns<br>Difficult to isolate<br>Limited phenotype |
| Adult tiusse derived stem cells | Multipotent | No ethical concerns<br>Ease availability | Limited phenotype<br>Lack of specific identification |

| (e.g. Bone marrow-derived stem cells) | | Immunosuppressive capacity | markers<br>Partially difficult isolation from tissue |
|---|---|---|---|
| Induced pluripotent stem cells (iPSC) | Pluripontent | Ability to differentiate into cells of all three primary germ layers<br>Suggested to not cause immunological rejection<br>Lack of ethical issues | Risk of tumorigenicity<br>Safety issues about in the case of retroviral transfection |

### 1.2.2. Periosteum derived stem cells

Periosteum refers to a highly vascularized connective tissue that covers bone surfaces. As shown in Figure 1.2, the thin membrane is divided into an outer fibrous layer and an inner cellular layer [7]. The fibrous layer mainly contains tissue fibroblasts, elastic fibres and microvessels. The cellular layer is composed of periosteum derived progenitor cells (PDPCs), which play a critical role in fracture healing and bone development [8].
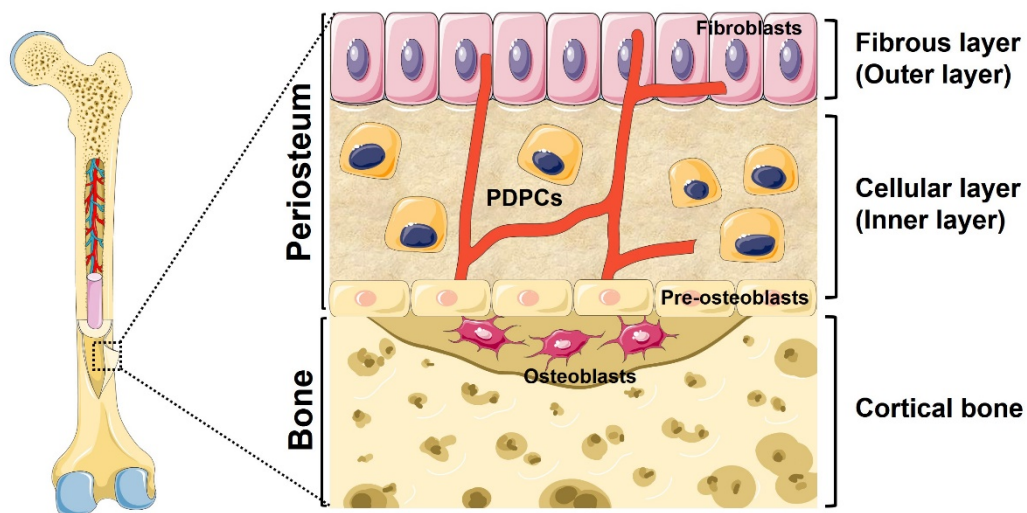


**Figure 1.2.** Schematic representation of periosteum.

In fact, the significance of the periosteum during bone healing has been firstly reported in 1800, showing that new bone growth can be induced by transplanted periosteal tissue [8]. The osteogenic potential of cells derived from the periosteum was firstly documented in the 1900s [9]. Although the application of autologous periosteum graft is well known in orthopaedic surgery, the use of periosteal cells for BTE attracted more attention only in the last decades. Previous studies demonstrated that periosteal cells have a multi-potential capacity playing a critical role in the initial callus formation. Also,

these cells are involved in the intramembranous bone formation [10, 11] and can induce endochondral ossification after bone fracture [11]. Thereby, the use of PDPCs has been considered as a promising alternative in bone tissue regeneration owing to their excellent biological characteristics, including easy isolation and expansion, relatively high proliferative capacity and high osteogenic potential [6].

Jaw periosteal cells (JPCs) could represent a suitable stem cell source for applications in the maxillofacial area due to its simple tissue harvesting and cell isolation [10]. Previous studies by Alexander's group have long-lasting focused on the bone regenerative application of JPCs, and continuously optimized the detection methods, cell culture conditions and related biomaterial applications [12-16]. In 2007, the *in vitro* osteogenic potential of human JPCs has been demonstrated, and the harvest of JPCs is relatively simple [17]. JPCs seeded in three dimensional (3D)-scaffold materials showed mineralization capacity *in vitro*, indicating the feasibility of JPCs-based bone substitutes [12, 18, 19]. To define specific differentiation markers, previous studies reported that as the low-affinity nerve growth factor receptor (LNGFR/CD271) [20] and the human mesenchymal stem cell antigen-1/tissue non-specific alkaline phosphatase (MSCA-1/TNAP) [14, 21], could be predictors of the progenitor subpopulation isolated from the periosteum tissue. Based on the above mentioned findings, further investigations reported from a magnetic separation method using MSCA-1 specific antibodies for the effective isolation of osteoprogenitor cells from the periosteal tissue [22]. Furthermore, to optimize the *in vitro* culture conditions and to facilitate later clinical applications, the selection of cell culture medium, i.e. serum-free culture conditions or human platelet lysate, was undertaken and influences of the *in vitro* expansion and even mineralization potential were observed [15, 23, 24]. Thus, JPCs can be considered as a promising stem cell source for BTE.

In principle, various immune cells (i.e., macrophages and dendritic cells (DCs)) can react against implanted constructs in order to eliminate the foreign body objects. DCs have been recognized as the most efficient antigen-presenting cells, which are involved in the initiation of adaptive immune

response by naïve T cells as well as by integrating innate immune signals into this process [25].

Mesenchymal stem cells (MSCs) can not only participate in regenerative therapeutic approaches but they are considered to be able to contribute as therapeutic options for the treatment of autoimmune diseases or as an additive for organ transplantations. This specific MSC potential is based on the knowledge that MSCs exhibit immunoregulatory and/or immunosuppressive effects through both cell-to-cell interactions and by released immunomodulatory factors [26, 27]. MSCs exert these immunosuppressive activities by affecting major immune cell populations such as, T cells, B cells and DCs [28]. MSCs suppress B and T cell proliferation by mitogen [29, 30]. Specifically, the T-cell suppressive effects of MSCs include both T helper (Th) cells and cytotoxic T lymphocytes (CTLs). Fiorina et al. [31] reported a shift in pro-inflammatory Th1 cell and anti-inflammatory Th2 cell balance toward Th2 cell response, due to allogeneic MSC administration in non-obese diabetic (NOD) mice. Additionally, MSCs inhibit the development of CTLs by secreting soluble factors and hamper in CTL-associated lysis of target cells in the early activating phase [32]. Furthermore, MSCs participate in immunosuppressive responses through the induction of $CD4^+$ regulatory T cells (Treg), which are responsible for maintaining homeostasis and self-tolerance [33]. Previous studies demonstrated that MSCs can inhibit DC maturation [34, 35], then immature DCs can induce T-cell anergy or regulatory T cells [36, 37]. Studies demonstrated that the production of IL-10 by DCs increase in the presence of MSCs [38] and IL-10 may directly inhibit T-cell proliferation [39]. Moreover, Djouad et al. [40] demonstrated that bone marrow-derived MSCs can inhibit DC maturation via an interleukin-6-dependent mechanism.

To the best of our knowledge, there were no published studies investigating the interactions between JPCs and DCs before we started our research in this area. In order to move further step by step towards the clinical use of JPCs, their immunoregulatory properties have to be analyzed in detail.

## 1.3. Scaffold

1.3.1. Scaffold materials

In bone tissue regeneration, ideal scaffolds should not only provide sufficient strength to maintain mechanical support but also possess excellent biological characteristics, including osteoconductive and osteoinductive features [2, 24]. Without a doubt, autologous bone is still recognized as the gold standard due to its combined osteoconductive and osteoinductive properties. The use of autologous bone grafts is widely applied, however, it has some limitations causing morbidity of the donor site and limited availability concerning the amount of the isolated bone biopsies. To address these limitations, synthetic bone substitutes have been investigated and developed during the past decades. As listed in Table 1.2, the biological properties of the most frequently used scaffolds have been reported [2, 24].

**Table 1.2.** Comparision of biological properties scaffold materials used in BTE [2, 24].

| Types | Mechanical support | Osteo-conduction | Osteo-induction | Osteo-genesis | Limitations |
|---|---|---|---|---|---|
| Autologous bone grafts | | | | | |
| Autologous cortical | +++ | + | + | + | Limited availability and donor site morbidity |
| Autologous cancellous | - | +++ | +++ | +++ | Same as above |
| Allogeneic bone grafts | | | | | |
| Allogeneic cortical | +++ | + | - | - | Risk of immune reaction and disease transmission |
| Allogeneic cancellous | - | + | + | - | Same as above |
| Demineralized bone matrix | - | + | ++ | - | Variable osteoinductivity |
| Synthetic bone substitutes | | | | | |
| Calcium sulfate | + | + | - | - | Rapid resorption and osteoconductive only |
| Hydroxyapatite | ++ | + | - | - | Slow resorption and osteoconductive only |

| CaP ceramic | ++ | + | - | - | Osteoconductive only |
| CaP cement | + | + | - | - | Osteoconductive only |

### 1.3.2. JPCs-based bone constructs

To establish the osteoinductive ability, human JPCs seeded in different types of scaffolds have been investigated. Previously, the osteoinductive effects of JPCs in 3D scaffolds were evaluated by using different scaffold materials, i.e., polylactic acid (PLA), collagen composites of a mixture of type I and III collagens and calcium phosphate, respectively. JPCs seeded on PLA scaffolds showed the highest proliferation rates and newly formed bone-like nodules, indicating that PLA might be a promising biodegradable material for JPCs [12]. Furthermore, PLA scaffolds were coated with RGD peptides to enhance cell adhesion, proliferation and mineralization. The results indicated that the surface coating with linear RGD peptides using a poly-L-lysine spacer might be a suitable surface modification for functionalizing the PLA scaffolds [16]. Additionally, the surface biofunctionalization of beta-tricalcium phosphate (β-TCP) as a scaffolding material has been investigated by using the surface immobilization with the aptamer 74 or graphene oxide [19, 41]. These results indicated that JPC mineralization can be induced on 3D constructs. Therefore, JPCs-based bone constructs could be a suitable basis in the field of BTE. However, to date, the interactions between JPCs-based bone constructs and cells of the immune system have not been described in the literature.

## 1.4. Regulatory signals

Regulatory signals, such as biological, biochemical, and biophysical factors within the extracellular matrix, can directly influence cellular behavior of stem cells, including cell viability, proliferation, migration and differentiation [1]. To improve cellular behavior, various regulatory signals are used in BTE, which act as an important third component (Figure 1.1). In general, tissue regeneration can be modulated by biochemical (growth factors and cytokines) or biophysical stimuli which are able to regulate gene and protein expression in target cells. Among the bone relevant growth factors, recombinant human bone morphogenetic proteins (rhBMPs) are the most widely used and some of them FDA-approved [42]. Nonetheless, the clinical use of BMPs still has various drawbacks, such as supraphysiological dosage, adverse clinical complications and high costs [43]. Also, other growth factors or growth factor cocktails, such as parathyroid hormone, vascular endothelial growth factor and platelet-rich plasma have been taken into considerations while they are also facing several issues and challenges. Additionally, the use of trace elements such as physiological metallic ions have gained increasing attention as biochemical stimuli.

The local delivery of bioinorganic ions in bone regeneration has been considered as a natural and safer approach. Previously, physiological functions of various human metallic ions, such as magnesium (Mg), strontium (Sr), copper (Cu) and zinc (Zn) have been unravelled. These metallic ions not only belong to human essential elements but are also involved in the process of new bone formation. Metallic Zn ions have gained increasing interest as regulatory signals based on the following consideration: Firstly, Zn ions belong to the essential trace elements in the human body, mainly regulating the physiological functions, i.e., enzymatic catalysis and nucleic acid metabolism [44]. Moreover, Zn is involved in the structural and catalytic regulation of the enzyme alkaline phosphatase (ALP). ALP represents a zinc-containing enzyme playing a critical role in the process of mineralization [45]. More importantly, previous studies demonstrated that Zn ion release can stimulate the osteogenic differentiation, leading to new bone formation *in vivo*

[46, 47]. Thus, Zn ions attracted attention as a potent osteoinductive factor.

## 1.5. Objetives

Human jaw periosteal cells (JPCs) are considered to be a suitable stem cell source for clinical applications in oral and maxillofacial surgeries due to a higher osteogenic capacity and easy harvesting. Due to excellent biocompatibility and osteoconductive properties, β-tricalcium phosphate (β-TCP) has been widely used and we proposed to choose this material for the generation of JPC-seeded constructs. Since the immunoregulatory properties of two- and three-dimensionally cultured JPCs are completely unknown, this was the focus of the following two studies:

1. To investigate the immunoregulatory properties of untreated and osteogenically differentiated JPCs on monocyte-derived dendritic cell maturation by analyzing numbers and gene expression of differentiated dendritic cells (corresponding to study I).

2. To evaluate the impact of untreated and osteogenically induced JPCs seeded in β-TCP constructs on dendritic cell maturation by the analysis of gene expression, the obtained phenotype, and differentiation level (corresponding to study II).

Since the potential osteoinductive capability of Zn ions on JPCs is still unknown, the following study was undertaken:

3. To clarify the effects of different Zn ion concentrations on cell metabolic and mineralization activities, as well as on osteogenesis-related gene expression of human periosteal cells (corresponding to study III).

## 2. Study I: Effects of Jaw Periosteal Cells on Dendritic Cell Maturation

***The part is a reprint of the following publication:***

---

**Abstract:**

Clinical application of tissue engineering products requires the exclusion of immune responses after implantation. We used jaw periosteal cells (JPCs) as a suitable stem cell source and analyzed herein the effects of JPCs on dendritic cell maturation after co-culturing of both cell types. Peripheral blood mononuclear cells (PBMCs) were differentiated to dendritic cells (DCs) by the addition of differentiation cocktails for 7 days in co-culturewith undifferentiated and osteogenically induced JPCs. The effects of JPCs on DC maturation were analyzed at the beginning (day 7), in the middle (day 14), and at the end (day 21) of the osteogenesis process. We detected significantly lower DC numbers after co-culturing with JPCs that have previously been left untreated or osteogenically differentiated for 7, 14, and 21 days. Using gene expression analyses, significantly lower IL-12p35 and -p40 and pro-inflammatory cytokine (IFN-γ and TNF-α) levels were detected, whereas IL-8 mRNA levels were significantly higher in DCs. Furthermore, osteogenic media conditions enhanced significantly IL-10 gene expression. We concluded that undifferentiated and osteogenically differentiated JPCs had an overall inhibiting influence on dendritic cell maturation. Further studies should clarify the underlaying mechanism in depth.

## 2.1. Introduction

In the clinical application of tissue engineering (TE) products, it is crucial to prevent an immune rejection of the *in vitro* developed constructs. Biomaterials used for the generation of TE products, could induce an immune reaction. Efforts should be undertaken to develop biomaterials with low immunogenic potential. Some strategies involve the integration of immunosuppressive factors within the core material of biomaterials. However, these attempts fail, due to temporary but not persistent protection. On the other site, the potential of mesenchymal stromal stem cells (MSCs) could help to create an immunosuppressive environment, thus avoiding an immune response.

For TE purposes, the use of autologous instead of allogeneic stem cell sources should be preferred. However, it has been proven repeatedly in the past that MSCs have the potential to inhibit or ameliorate immune responses after allogeneic administration, for instance, in graft-versus- host-disease [48, 49]. This observation is based on the immunoregulatory properties of MSCs on players of the innate and adaptive immune system [50]. It has been shown that MSCs are capable to downregulate cyclin D2, and therefore arrest stimulated T cells at the G1 phase [51]. Additionally, MSCs from bone marrow significantly suppressed CD4$^+$ and CD8$^+$ T cell proliferation [30], whereby soluble factors secreted by them were probably involved in this phenomenon and not the induction of apoptosis [30].

It has been demonstrated that MSCs also exert their regulatory functions by inhibition of the complement system. MSCs bind through the receptors C3aR and C5aR the complement components C3 and C5, protecting them from apoptosis and promoting their proliferation [52]. Tu and co-authors detected constitutive expression of the complement inhibitor factor H by MSCs [53]. The depletion of factor H abolished the complement inhibitory capacities of MSCs and a pro-inflammatory environment containing interferon-γ and TNF-α enhanced production of factor H by MSCs.

The immunosuppressive properties of MSCs target not only T cells, but also antigen presenting cells. They inhibit, for instance, the differentiation of

13

CD34^{+} hematopoietic progenitors or monocytes into mature dendritic cells [34]. DCs are key regulators bridging the innate and adaptive immune system. Mice lacking dendritic cells develop systemic autoimmunity [54]. Whereas, immature DCs possessing high endocytic activity and expressing low levels of HLA-DR and co-stimulatory factors, maintain self-tolerance, mature DCs trigger immune responses by T cell activation.

Since harvesting of bone marrow for the isolation of MSCs requires surgeries, which lead to chronic pain in some patients (bone marrow aspirates from iliac crest), the use of mesenchymal stem cells derived from periosteum harbors several advantages. The harvest procedure is minimally invasive leaving no chronic pain [55]. Periosteal tissue is predestinated for bone reconstruction therapies [56, 57], since it is its natural function to form new bone tissue after injury and/or to remodel bone tissue continuously. Furthermore, it has been shown that the osteogenic capacity of periosteum tissue depends on the tissue source [58]. In this study, periosteal tissue from load-bearing areas, such as tibia and femur, showed a higher osteogenic capacity compared to that harvested from calvarial and rib bones. In the light of this experience and the high mechanical loading occurring within the jaw, we are convinced that jaw periosteal cells represent the most suitable stem cell source for clinical applications in oral and maxillofacial surgery.

Meanwhile, profound knowledge of the immunoregulatory properties of MSCs from bone marrow already exists. Even when it can be speculated that periosteal cells behave similarly concerning their immunomodulatory features, no investigations have been performed. Therefore, we analyzed in the present study for the first time the effects of untreated and osteogenically differentiated JPCs on monocyte-derived DC differentiation.

## 2.2. Materials and Methods

### 2.2.1. Isolation and Culture of JPCs

The study was approved by the local ethics committee (Ethik-Kommission der Medizinischen Fakultaet Tuebingen; approval number 194/2008BO2). After obtaining written informed consent from all donors, the human jaw periosteum biopsy from 3 donors was obtained during routine interventions. The pieces (<1 cm$^2$) of jaw periosteal tissue were cut in Dulbecco's phosphate-buffered saline (DPBS w/o Mg$^{2+}$, Ca$^{2+}$, Sigma-Aldrich, Merck, Darmstadt, Germany) and enzymatically digested using 1500 U/mL type XI collagenase (Sigma-Aldrich, Merck, Darmstadt, Germany) for 90 min. The isolated JPCs were then plated in 75 cm$^2$ cell culture flasks (Corning, Kaiserslautern, Germany) and cultivated under standard cell culture conditions (37 °C, 5% $CO_2$, a humidified atmosphere of 95%). JPCs were routinely cultured in a 1:1 mixture of Dulbecco's Modified Eagle Medium and Nutrient Mixture F-12 (Ham), containing GlutaMAX (DMEM/F-12, (Invitrogen-BioSource Europe, Thermo Fisher, Darmstadt, Germany) supplemented with 10% fetal bovine serum (FBS, Sigma-Aldrich, Merck, Darmstadt, Germany), 1% 250 µg/mL amphotericin B (Biochrom GmbH, Berlin, Germany), and 1% 10,000 U/mL penicillin/streptomycin (Lonza, Basel, Switzerland), for up to 4 passages. After reaching 80% confluence, JPCs were passaged with trypsin-versene EDTA (Lonza, Basel, Switzerland). Pooled JPCs from the three donors of passage 5 were used for all co-culture experiments, and cell medium was changed three times per week. The osteogenic potential of the used JPCs was tested and alizarin staining after 21 days of osteogenic differentiation is shown in Figure 2.1.
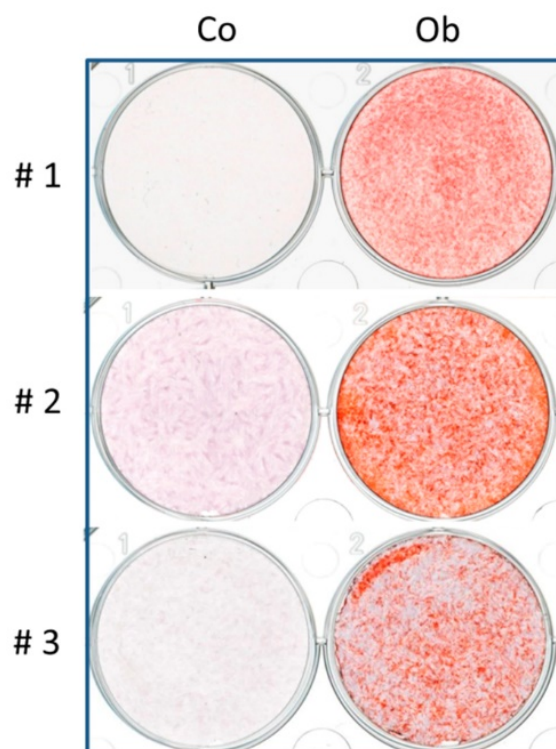
**Figure 2.1.** Alizarin staining of undifferentiated (co) and osteogenically differentiated (ob, 21 days) jaw periosteal cells (JPCs) derived from the 3 donors (#1, 2, 3) used for the following co-culture experiments.

2.2.2.  Isolation and Culture of PBMCs, Dendritic Cell Differentiation

Peripheral blood mononuclear cells (PBMCs) were collected and isolated from the blood of 6 normal healthy donors after informed consent. A whole blood sample was diluted 1:1 with DPBS and carefully layered over with 12 mL of 1.077 g/mL Ficoll-Paque PLUS (GE Healthcare, Freiburg, Germany). Plasma and red blood cells were separated from the PBMCs by density gradient centrifugation (no break, 810 g, 20 °C) for 20 min. The PBMCs were carefully harvested and transferred into another 50 mL tube. The cells were washed 3 times with DPBS, and then cultured in x-vivo 15 chemically defined, serum-free medium (Biozym, Hamburg Belgium) with 1% 10,000 U/mL penicillin/streptomycin and 3% autologous plasma. For flow cytometric analyses of dendritic cell marker expression, the PBMCs were grown in 75 cm$^2$ culture flasks at a cell seeding density of $5 \times 10^6$ cells per flask. For co-cultivation experiments, 6-well Transwell co-culture plates (0.4 µm pore size membrane, Corning, Kaiserslautern, Germany) with a cell seeding density of

$1 \times 10^6$ cells per well were used. To stimulate monocyte-derived dendritic cell differentiation, the first medium change was performed after 24 h, using x-vivo medium supplemented with 1% 10,000 U/mL penicillin/streptomycin, 3% autologous plasma, and the first DC differentiation cocktail containing 100 ng/mL GM-CSF (Sigma-Aldrich, Darmstadt, Germany) and 40 ng/mL IL-4 (Sigma-Aldrich, Darmstadt, Germany). At day 6, the second DC differentiation cocktail, containing 100 ng/mL GM-CSF, 40 ng/mL IL-4, 10 ng/mL TNF-α (Tebu Bio, Offenbach, Germany), 10 ng/mL IL-1β (Tebu Bio, Offenbach, Germany), 10 ng/mL IL-6 (Tebu Bio, Offenbach, Germany), and 1 µg/mL PGE2 (BioTrend, Köln, Germany) was added for another 24 h to stimulate DCs maturation. For co-culture experiments, pooled JPCs from 3 donors (upper chamber) and unpooled PBMCs from 6 donors were used in total. Co-cultures of PBMCs from one donor in the lower chamber with pooled JPCs from 3 donors (for all experiments the same donors) in the upper chamber were referred to as one independent experiment.

### 2.2.3. Flow Cytometric Analyses of Dendritic Marker Expression

PBMCs (derived from 4 donors) cultured under undifferentiated (day 1) and DC differentiation conditions (day 7) were collected from cell culture flasks. After centrifugation for 7 min (1400 rpm, 4 °C), cells were resuspended in 20 µL of 10% Gamunex (human immune globulin solution, Talecris Biotherapeutics, Frankfurt am Main, Germany) and incubated for 15 min at 4 °C. The cells were incubated at 4 °C with specific phycoerythrin (PE)-labeled mouse anti-human CD80, CD83, CCR-7 (BD Biosciences Pharmingen, Heidelberg, Germany) and HLA-DR (MACS Miltenyi Biotec, Bergisch Gladbach, Germany), and allophycocyanin (APC)-labeled mouse anti-human HLA-1, CD14 and CD86 (BioLegend, San Diego, CA, USA) for 15 min after adding 100 µL FACS buffer (DPBS, 0.1% sodium azide, 0.1% BSA). Subsequently, the cells were centrifuged for 7 min (1400 rpm, 4 °C) and washed two times with FACS buffer and then resuspended in 200 µL FACS buffer. The flow cytometric analyses were performed with the guava easyCyte 6HT-2L instrument (Merck Millipore, Germany). GuavaSoft 2.2.3 (InCyte 2.2.2) software was used for data evaluation.

### 2.2.4.   Co-Cultivation of JPCs and PBMCs

The Transwell system was used to prevent JPCs from contacting PBMCs directly. Pooled JPCs ($2 \times 10^4$ in 1 mL of DMEM/F12) from 3 donors were seeded in the upper compartments of the 6-well Transwell co-culture plates. PBMCs ($1 \times 10^6$ per well in 2 mL of x-vivo medium) from 6 donors were cultured in the lower chambers (the ratio of JPCs to PBMCs was 1:50) in x-vivo medium with 1% 10,000 U/mL penicillin/streptomycin, 3% autologous plasma, and two DC differentiation cocktails (see above) for 7 days at 37 °C and 5% $CO_2$, under four different upper chamber conditions:

1.  JPC-free culture with complete DMEM/F12 medium (Monoculture_co);

2. JPC-free culture with osteogenic medium (ob—complete DMEM/F12 medium containing 100 mM L-ascorbic acid 2-phosphate, 10 mM β-glycerophosphate, and 4 μM dexamethasone, Sigma-Aldrich) (Monoculture_ob);

3. Co-culture with undifferentiated JPCs (Coculture_co);

4. Co-culture with osteogenic differentiated JPCs (Coculture_ob).

After 24 h of PBMCs (into the lower chamber) and JPCs (into the upper chamber) seeding in separate plates, a co-cultivation experiment was started, and the medium change in the upper chamber was performed on day 1 and day 3, respectively. To evaluate the effect of osteogenically differentiated，JPCs on DCs, JPCs were either treated with osteogenic differentiation medium directly in the co-culture plates for day 7 of examination, or cells were induced in inserts from separate transwell plates for 7 and 14 days, before transferring the inserts to the co-culture plates with PBMCs/DCs for day 14 and 21 of examination. JPCs cultured without any osteogenic compounds for the same time period served as undifferentiated controls (co).

### 2.2.5.  RNA Isolation and Quantitative Gene Expression Analyses in PBMCs

RNA isolation from PBMCs was performed with the NucleoSpin RNA XS kit (Macherey-Nagel, Hoerdt, France) following the manufacturer's instructions. The isolated RNA was photometrically measured and quantified (GE Healthcare, Freiburg, Germany), and 200 ng of RNA were used for cDNA

synthesis using the SuperScript VILO Kit (Invitrogen, Thermo Fisher, Darmstadt, Germany) following the manufacturer's instructions. mRNA expression levels were quantified by the real-time LightCycler System (Roche Diagnostics, Mannheim Germany). DNA Master Sybr Green 1 (Roche, Mannheim, Germany) and commercial primer kits (Search LC, Heidelberg, Germany) were used for the PCR reactions. The following genes were analyzed: interleukin 12 subunit p35 (IL-12p35), interleukin 12 subunit p40 (IL-12p40), interleukin 12 receptor beta 1 (IL-12Rβ1), interleukin 12 receptor beta 2 (IL-12Rβ2), interferon-gamma (IFN-γ), tumor necrosis factor-alpha (TNF-α), interleukin 27 (IL-27), interleukin 8 (IL-8), and interleukin 10 (IL-10). Then, 40 cycles of PCR product amplification were carried out. The ratios of target genes versus the housekeeping gene glyceraldehyde 3-phosphate dehydrogenase (GAPDH, Search LC, Heidelberg, Germany) were calculated, and the ratios of PBMC monocultures (with normal (co) or osteogenic (ob) medium) were set as 1 (control) and induction factors (x-fold) in relation to this control were calculated.

### 2.2.6.  IL-8 Protein Release in JPCs and PBMCs

The supernatants from JPCs and PBMCs were collected at day 1 and day 7, centrifuged (1400 rpm, 8 °C, 7 min), and kept at -80 °C before being assayed. IL-8 production in the medium was evaluated according to kit instructions (Invitrogen, Thermo Fisher, Darmstadt, Germany). All determinations were performed in duplicates. ELISA plates were read immediately with a Microplate ELISA reader (BioTek, Friedrichshall, Germany) at OD 450 nm. Concentrations of IL-8 were quantified with known standards, with the lowest detection limit of 15.63 pg/mL.

### 2.2.7.  Statistical Analyses

All data were tested for normal distributions and variance equality. The results for surface marker expression were analyzed using the student's t-test. Cell numbers and densities were analyzed by one-way analysis of variance (ANOVA) with culture type as an independent factor, whilst IL-8 concentrations were analyzed by two-way ANOVA with culture time and culture type as independent factors, followed by the Tukey HSD post-hoc test.

The results of gene expression were analyzed using the Kruskal-Wallis test, followed by the Nemenyi post-hoc comparisons. Descriptive statistics were shown as the mean values ± standard error of mean of four (FACS analyses) or six independent experiments (co-culture experiments). Statistical analyses were performed using SPSS v.22.0 (IBM Corp., New York, NY, USA) at a level of significance of $p < 0.05$.

## 2.3. Results

2.3.1.  Effect of DC Differentiation Cocktails on the Phenotype of Monocyte

To compare the phenotype of monocyte before and after DC differentiation, the cell surface marker expression was analyzed (from 4 donors). As shown in Figure 2.2, the expression of the costimulatory molecules CD80 and CD86, and of the DC maturation marker CD83, and of the MHC II receptor HLA-DR were significantly up-regulated after 7 days of DC cultivation with the differentiation cocktails (CD80: day 7 $58.71 \pm 18.17\%$ versus day 1 $0.19 \pm 0.41\%$, $p < 0.05$; CD86: day 7 $96.78 \pm 0.29\%$ versus day 1 $23.13 \pm 9.42\%$, $p < 0.05$; CD83: day 7 $58.82 \pm 18.29\%$ versus day 1 $2.15 \pm 0.94\%$, $p < 0.05$; HLA-DR: day 7 $97.82 \pm 1.04\%$ versus day 1 $16.71 \pm 3.44\%$, $p < 0.05$). The difference in CD14 surface expression was not significant at day 7 compared to day 1 (day 7 $10.24 \pm 3.27\%$ versus day 1 $16.30 \pm 6.36\%$, n.s.). These results indicated that monocyte-derived DCs develop the typical expression profile after stimulation with both DC differentiation cocktails, providing a basis for the further co-cultivation experiments.
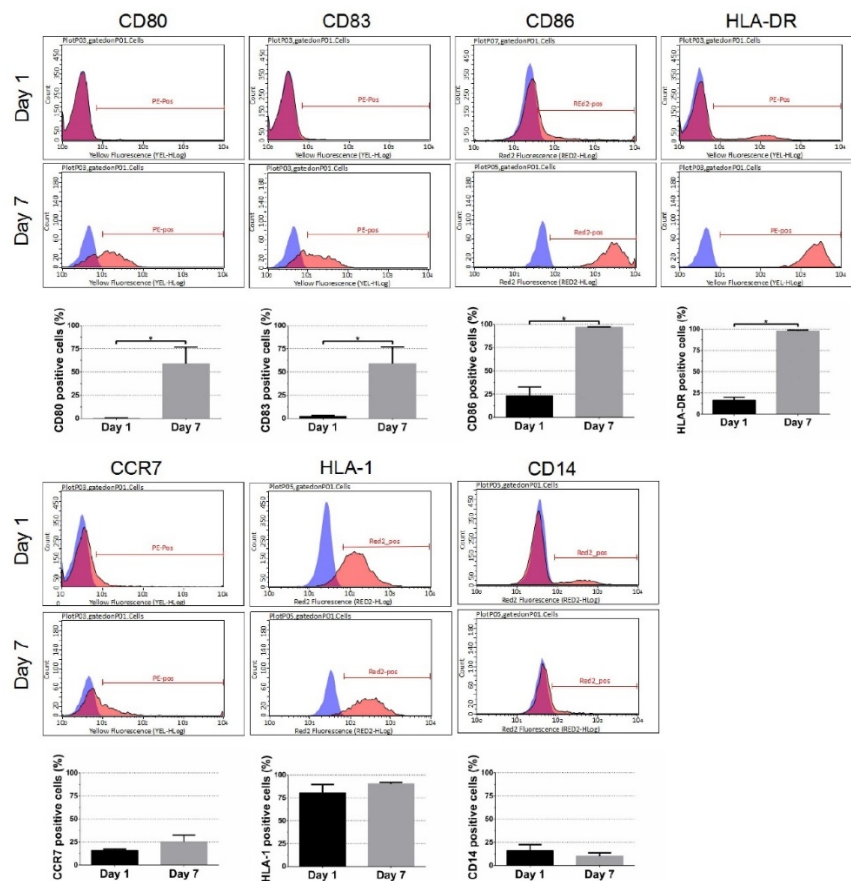
**Figure 2.2.** Flow cytometric analysis of cell surface marker expression before (day 1) and after DC differentiation (day 7). Representative flow cytometric histograms are illustrated for dendritic cell marker CD80, CD83, and CD86 expression. Furthermore, HLA-DR, CCR7, and the ubiquitous HLA-1 expression were analyzed. CD14 as a marker for mature monocytes is the only marker showing a decreasing tendency in expression. Results were averaged from 4 independent.

## 2.3.2. Effect of JPCs on the Morphology, Number, and Size of DC

To investigate whether undifferentiated and osteogenically induced and/or differentiated JPCs inhibit the maturation of DCs, JPCs were cultured under normal (co) and osteogenic conditions (ob) for 7 days, 14 days, and 21 days, respectively. Light microscopy was used to identify DC, and the full-length cell sizes of mono- and co-cultured PBMCs from 6 donors were measured using ImageJ software (n = 30 per image). As shown in Figure 2.3A, Figure 2.4A, and Figure 2.5A, similar images were obtained, and the cells were found at day 1 as small round cells among all groups, whereas the cells were found to increase in size at day 7 compared to day 1; most importantly, less differentiated DCs were observed both in co-cultures with JPCs under untreated and osteogenic culture conditions. Furthermore, significantly reduced cell numbers were detected in co-cultures with JPCs at day 6 (Figure 2.4B co: co-culture 14,286 ± 3266 versus monoculture 50,947 ± 11,966, $p < 0.05$; Figure 2.4B ob: co-culture 13,236 ± 2629 versus monoculture 40,579 ± 9482, $p < 0.05$; Figure 2.5B co: co-culture 19,380 ± 2577 versus monoculture 47,491 ± 6801, $p < 0.05$; Figure 2.5B ob: co-culture 18,100 ± 1809 versus monoculture 46,109 ± 6461, $p < 0.05$) and day 7 (Figure 2.4B co: co-culture 19,995 ± 5389 versus monoculture 90,707 ± 15,196, $p < 0.05$; Figure 2.4B ob: co-culture 24,987 ± 9389 versus monoculture 73,272 ± 8384, $p < 0.05$; Figure 2.5B co: co-culture 39,785 ± 7803 versus monoculture 95,469 ± 13,045, $p < 0.05$; Figure 2.5B ob: co-culture 39,452 ± 5838 versus monoculture 65,489 ± 7465, $p < 0.05$). Whereas results from Figure 2.3B showed no statistically significant differences, co-cultures with JPCs still showed a lower cell density compared to monocultures (day 6 co: co-culture 28,198 ± 8753 versus

monoculture 48,490 ± 12,841, n.s.; day 6 ob: co-culture 25,638 ± 8673 versus monoculture 42,034 ± 14,027, n.s.; day 7 co: coculture 56,580 ± 22,120 versus monoculture 94,931 ± 32,730, n.s.; day 7 ob: co-culture 50,896 ± 16,351 versus monoculture 86,354 ± 27,696, n.s.). In addition, as illustrated in Figure 2.3C, Figure 2.4C, and Figure 2.5C, the same tendency was observed, the cells had a diameter of 10 µm at day 0 and day 1. After treatment of monocytes with DC differentiation cocktails, an increased diameter (day 3: 20 µm; day 6 and day 7: 30 µm) was detected. However, the cell sizes were similar among all groups at the same time point of examination.



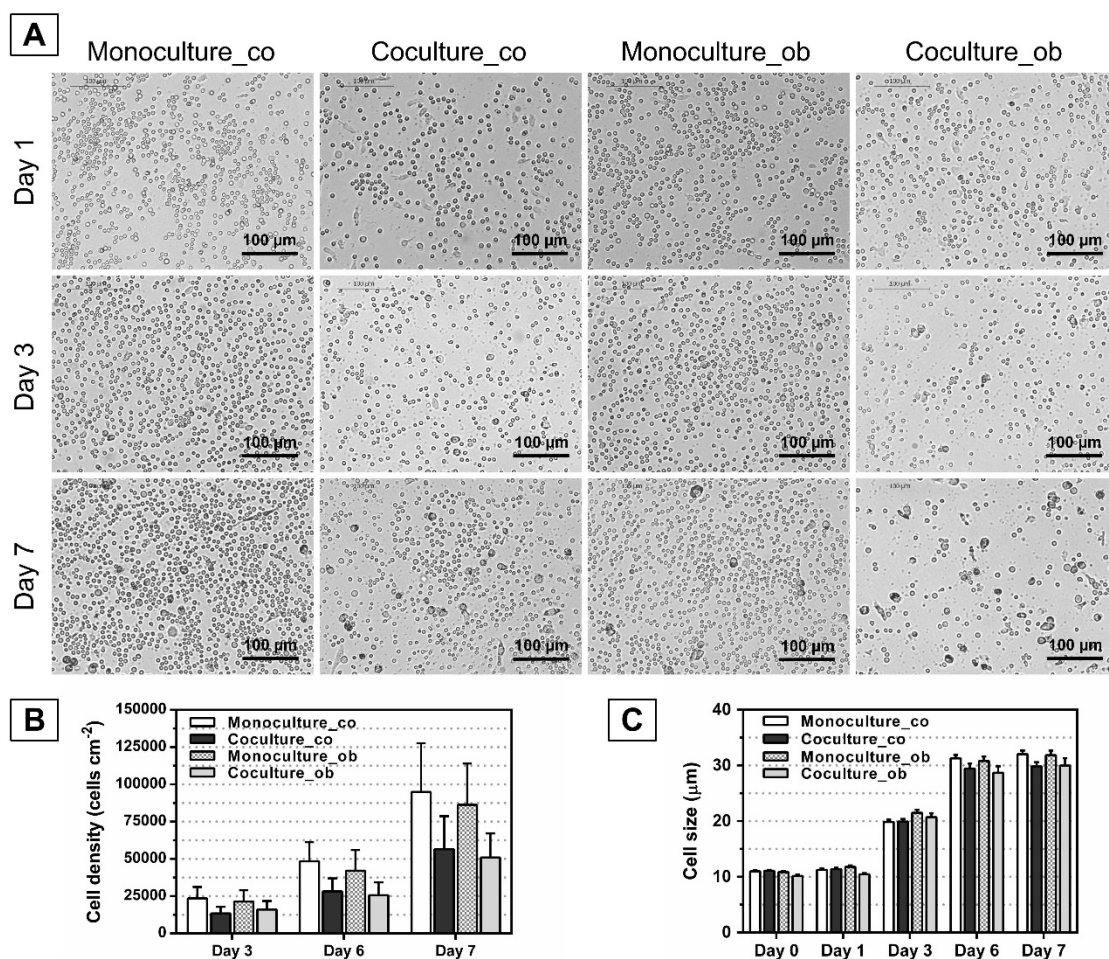**Figure 2.3**. Morphology, cell numbers, and sizes of peripheral blood mononuclear cells (PBMCs) during DC differentiation in monocultures or co-cultures with untreated (co) and osteogenically induced JPCs for 7 days (ob). Microscopic images of PBMCs during DC differentiation on day 1, day 3, and 7 are shown (part A). Resulting cell numbers (cells/cm², part B) and determination of cell sizes (µm,

part C) in mono- and co-cultures were quantified using the ImageJ software. Results were averaged from 6 independent experiments. Scale bar, 100 µm.
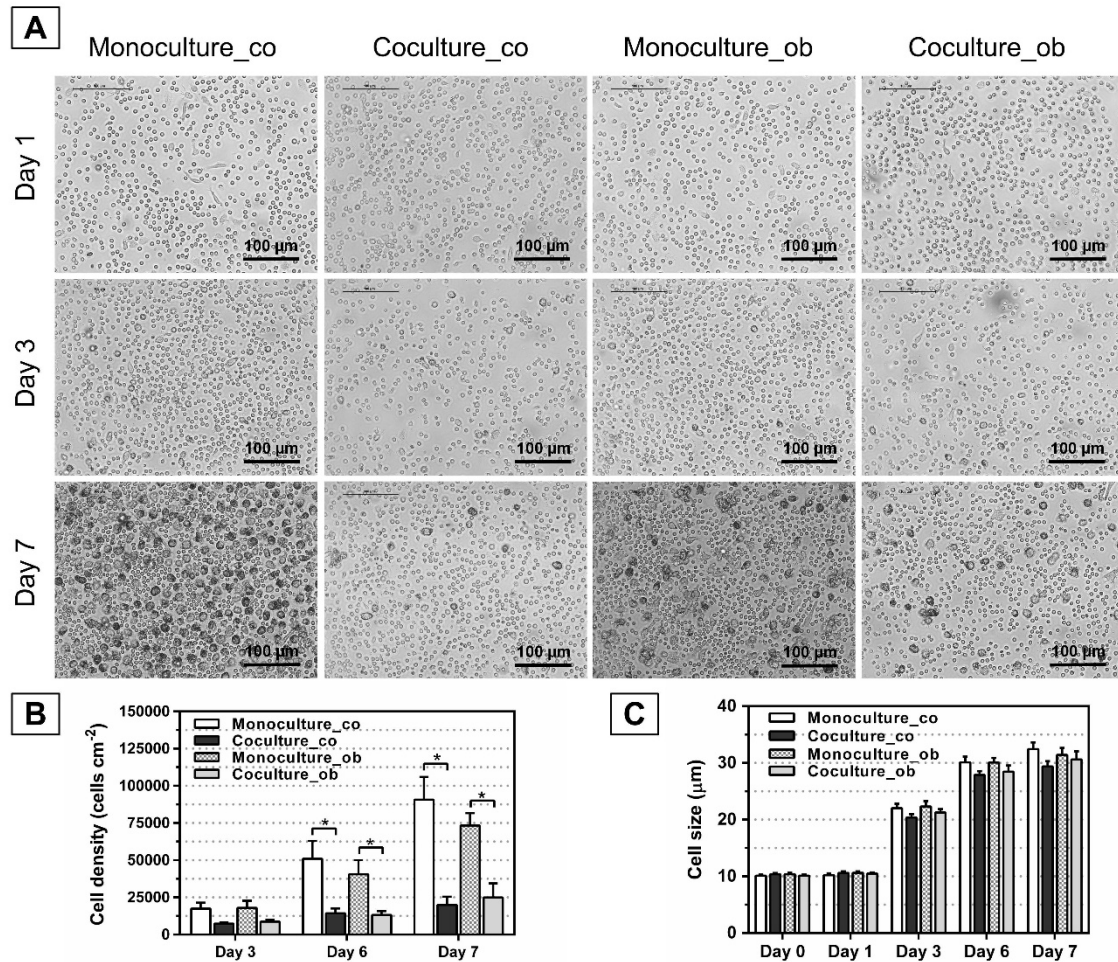


**Figure 2.4**. Morphology, cell numbers, and sizes of PBMCs during DC differentiation in monocultures or co-cultures with untreated (co) and osteogenically induced JPCs for 14 days (ob). Microscopic images of PBMCs during DC differentiation on day 1, day 3, and 7 are shown (part A); Resulting cell numbers (cells/cm$^2$, part B) and determination of cell sizes (µm, part C) in mono- and co-cultures were quantified using the ImageJ software. Results were averaged from 6 independent experiments. Scale bar, 100 µm.

**Figure 2.5.** Morphology, cell numbers, and sizes of PBMCs during DC differentiation in monocultures or co-cultures with untreated (co) and osteogenically differentiated JPCs for 21 days (ob). Microscopic images of PBMCs during DC differentiation on day 1, day 3, and 7 are shown (part A); Resulting cell numbers (cells/cm$^2$, part B) and determination of cell sizes (µm, part C) in mono- and co-cultures were quantified using the ImageJ software. Results were averaged from 6 independent experiments. Scale bar, 100 µm.
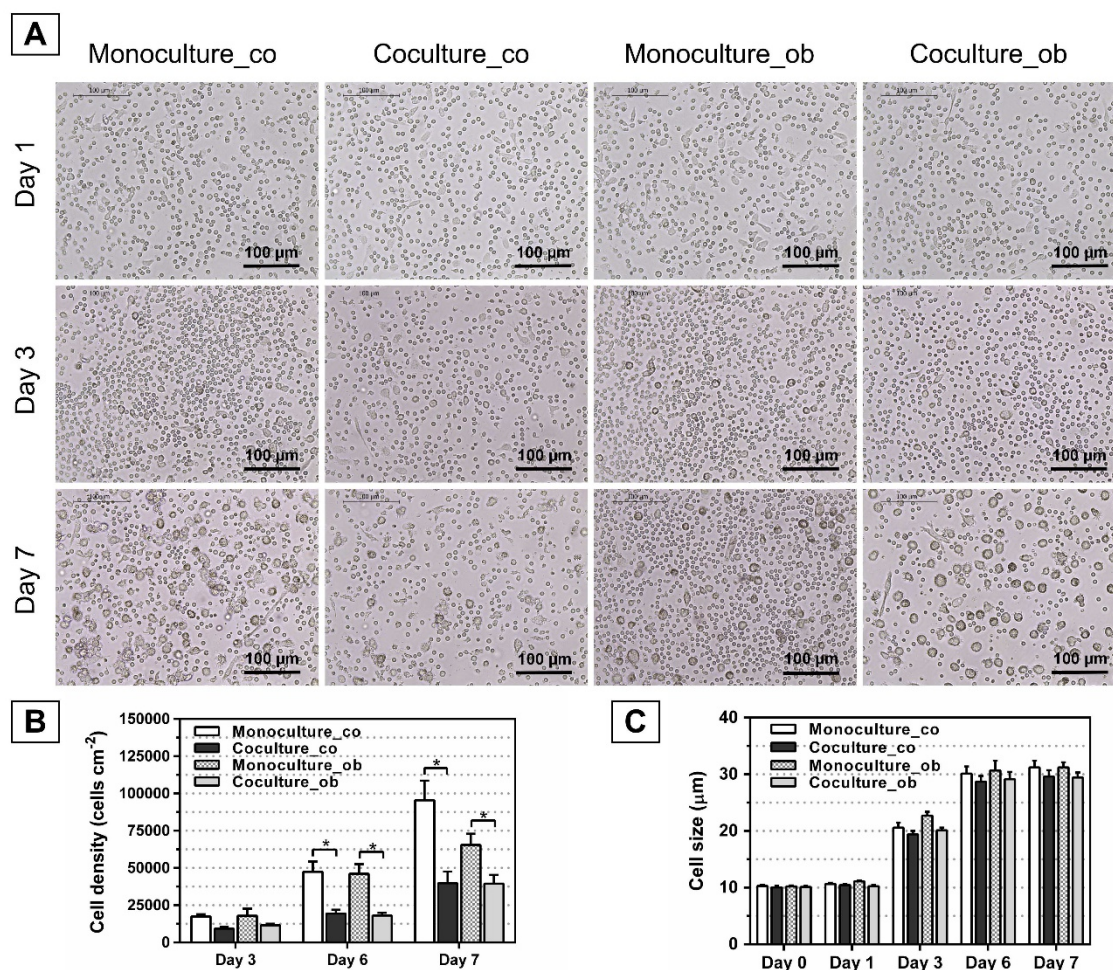
### 2.3.3. Effect of JPCs on DC Gene Expression

To evaluate the effect of JPCs on DC gene expression, monocytes were cultured with differentiation cocktails containing GM-CSF, IL-4, IL-6, IL-1β, TNF-α, and PGE2 for 7 days as monocultures together with control/osteogenic (co/ob) medium in the upper chamber, and as co-cultures with untreated/osteogenically induced JPCs in a transwell system. DCs cultivated in the presence of untreated JPCs showed significant down-

regulation of IL-12Rβ1 (0.79 ± 0.13-fold, p < 0.05) and up-regulation of three genes (TNF-α: 1.91 ± 0.55-fold, p < 0.05; IL-27: 1.52 ± 0.23-fold, p < 0.05; IL-10: 1.51 ± 0.22-fold, p < 0.05), compared to DC monocultures with control medium (set as 1) (Figure 2.6). However, DCs cultivated in the presence of osteogenically induced JPCs showed significant down-regulation of IL-8 (0.84 ± 0.12-fold, p < 0.05) and up-regulation of four genes (IL-12p40: 24.09 ± 6.57-fold, p < 0.05; IL-12Rβ1: 1.38 ± 0.34-fold, p < 0.05; IL-12Rβ2: 1.33 ± 0.18-fold, p < 0.05; IL-10: 1.68 ± 0.32-fold, p < 0.05), compared to DC monocultures with osteogenic (ob) medium. After exposure to osteogenic (ob) medium, gene expression by DCs showed a different pattern. This was further demonstrated by comparing DCs cultured with control/osteogenic (co/ob) medium and untreated or osteogenically induced JPCs, which showed statistically significant differences in the gene expression levels (Figure 2.6). As shown in the figure, DC monocultures cultivated in the presence of osteogenic (ob) medium showed significant down-regulation of six genes (IL-12p35: 0.15 ± 0.04-fold, p < 0.05; IL-12p40: 0.13 ± 0.12-fold, p < 0.05; IL-12Rβ1: 0.32 ± 0.08-fold, p < 0.05; IL-12Rβ2: 0.06 ± 0.01-fold, p < 0.05; IFN-γ: 0.0019 ± 0.0006-fold, p < 0.05; TNF-α: 0.30 ± 0.04-fold, p < 0.05) and significant up-regulation of two genes (IL-8: 3.16 ± 0.72-fold, p < 0.05; IL-10: 52.51 ± 4.48-fold, p < 0.05), compared to the control (co) medium (set as 1). Most importantly, co-cultures DCs cultivated in the presence of osteogenically induced JPCs showed significant down-regulation of six genes (IL-12p35: ob 0.17 ± 0.05-fold versus co 1.02 ± 0.22-fold, p < 0.05; IL-12Rβ1: ob 0.35 ± 0.07-fold versus co 0.79 ± 0.13-fold, p < 0.05; IL-12Rβ2: ob 0.09 ± 0.02-fold versus co 1.19 ± 0.26-fold, p < 0.05; IFN-γ: ob 0.005 ± 0.003-fold versus co 1.61 ± 0.65-fold, p < 0.05; TNF-α: ob 0.27 ± 0.03-fold versus co 1.91 ± 0.55-fold, p < 0.05; IL-27: ob 0.84 ± 0.12-fold versus co 1.52 ± 0.23-fold, p < 0.05) and significant up-regulation of two genes (IL-8: ob 2.41 ± 0.52-fold versus co 0.86 ± 0.11-fold, p < 0.05; IL-10: ob 83.30 ± 12.40-fold versus co 1.51 ± 0.22-fold, p < 0.05), compared to DC co-cultures with undifferentiated JPCs, as illustrated in Figure 2.6. These nine gene expression patterns showed a similar tendency in the groups of osteogenically differentiated JPCs for 7 days (as shown in Figure 2.7) and for 14 days (as shown in Figure 2.8).

**Figure 2.6.** Quantitative gene expression in DCs (day 7 of differentiation) cultivated as monocultures or co-cultures with undifferentiated (co) and osteogenically induced JPCs for 21 days (ob). IL-12p35, IL-12p40, IL-12Rβ1, IL-12Rβ2, IFN-γ, TNF-a, IL-27, IL-8, and IL-10 gene expressions were quantified by the Light Cycler system, and ratios of listed genes in relation to the housekeeping gene GAPDH were calculated. Gene levels in DC monocultures (with control (co) medium) were set as 1, and induction indices (x-fold) in relation to this control were calculated. Results were averaged from 6 independent experiments.
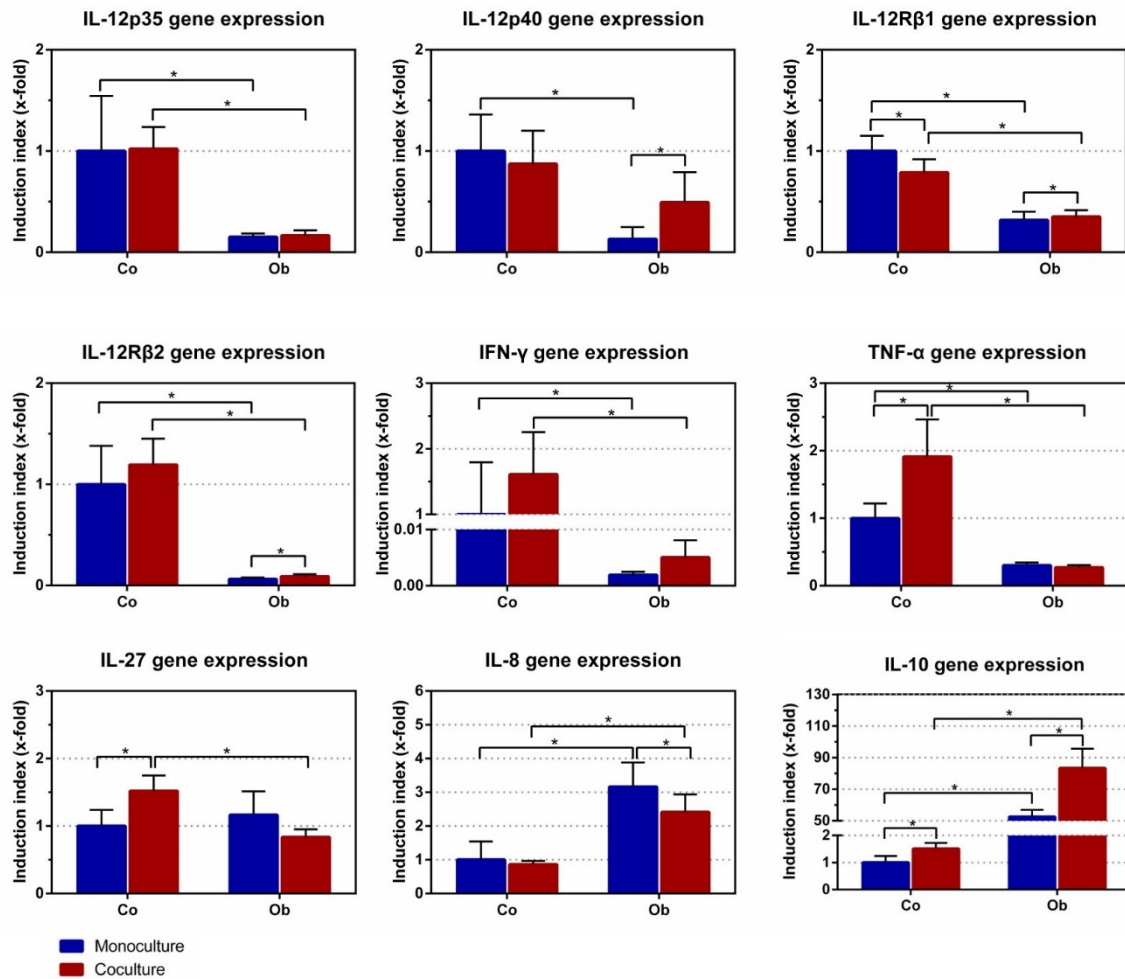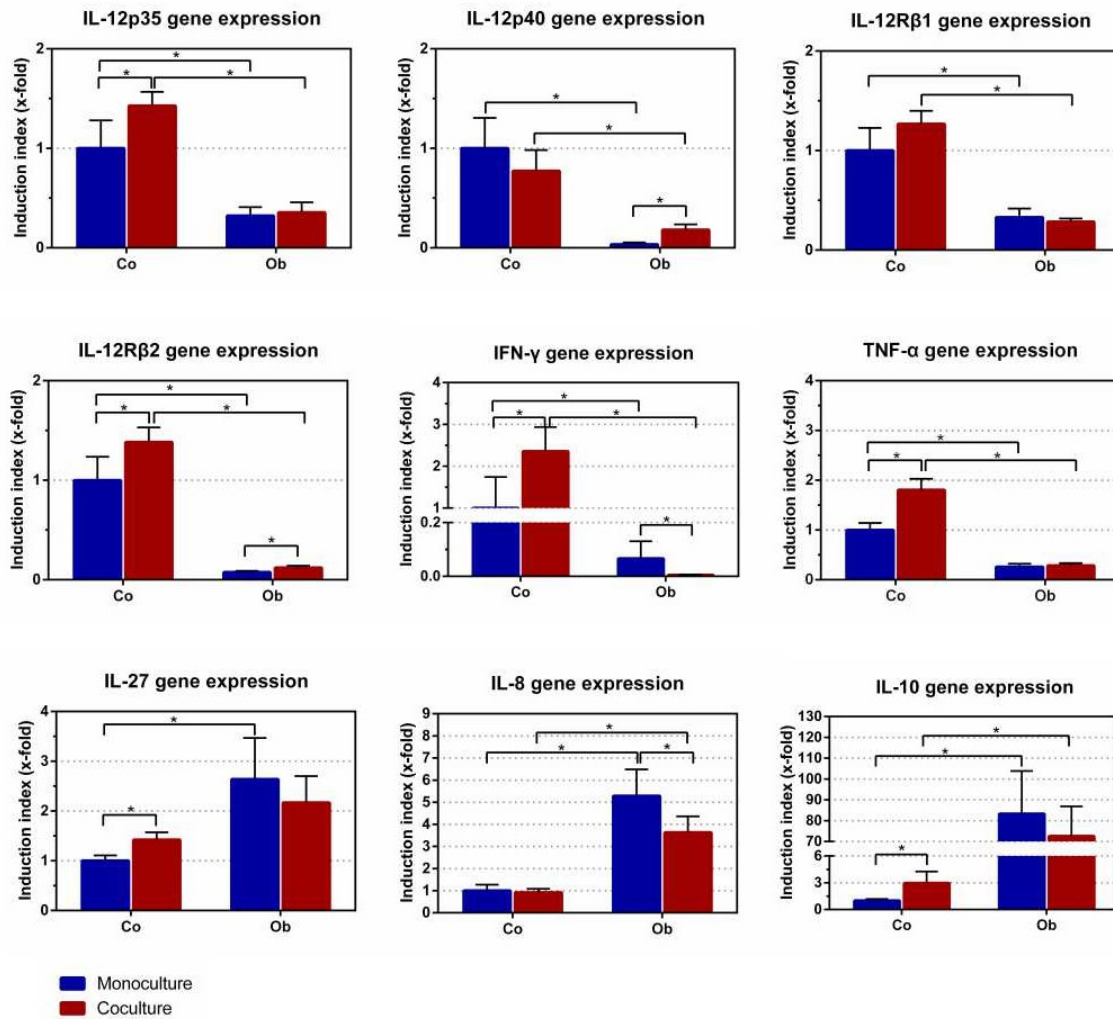
**Figure 2.7.** Quantitative gene expression in DCs (day 7 of differentiation) cultivated as monocultures or co-cultures with undifferentiated (co) and osteogenically induced JPCs for 7 days (ob). IL-12p35, IL-12p40, IL-12Rβ1, IL-12Rβ2, IFN-γ, TNF-a, IL-27, IL-8 and IL-10 gene expressions were quantified by the Light Cycler system and ratios of listed genes in relation to the housekeeping gene GAPDH were calculated. Gene levels in DC monocultures (with control (co) medium) were set as 1 and induction indices (x-fold) in relation to this control were calculated. Results were averaged from 6 independent experiments.
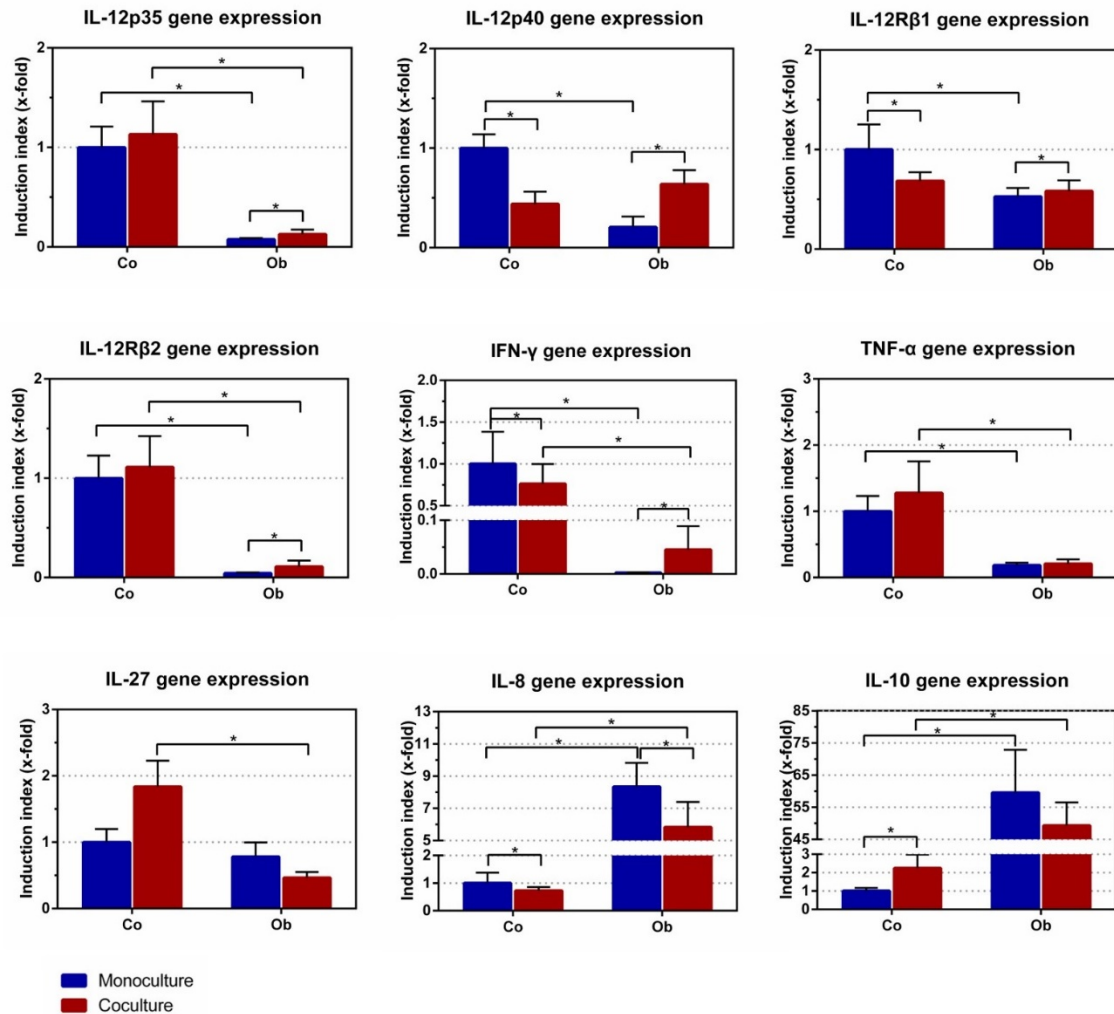
**Figure 2.8.** Quantitative gene expression in DCs (day 7 of differentiation) cultivated as monocultures with osteogenic medium in the upper chamber or as co-cultures with osteogenically induced JPCs for 14 days (ob). The same genes as illustrated in Figure 2.7 were analyzed. Gene levels of DC monocultures (with JPC osteogenic (ob) medium) were set as 1 and induction indices (x-fold) in relation to this control were calculated. Results were averaged from 6 independent experiments.

### 2.3.4.  Effect of JPCs on IL-8 Secretion of DC

Monocytes were cultured with DC differentiation cocktails in the presence and absence of JPCs for 7 days, supernatants from these cells were collected for cytokine quantification via ELISA. The amounts of IL-8 secretion were analyzed, as illustrated in Figure 2.9. After culturing of JPCs for 14 days, the largest amounts of IL-8 were secreted by untreated JPCs (90.51 ± 5.39

ng/mL), while significantly lower levels of IL-8 were released by osteogenically differentiated JPCs (69.16 ± 2.46 ng/mL, p < 0.05) (Figure 2.9B). Levels of IL-8 released by JPCs cultured for 24 h were below the detection limit of the test, however, after co-cultures with PBMCs for 7 days, the IL-8 concentration in co-cultures was strongly increased (co: 54.22 ± 9.43 ng/mL; ob: 54.14 ± 6.88 ng/mL) (Figure 2.9A). The same tendency was observed in Figure 2.9B (co: day 7 90.51 ± 5.39 ng/mL versus day 1 0.04 ± 0.007ng/mL, p < 0.05; ob: day 7 69.16 ± 2.46 ng/mL versus day 1 0.21 ± 0.03 ng/mL, p < 0.05) and Figure 2.9C (co: day 7 66.54 ± 9.77 ng/mL versus day 1 0.42 ± 0.07 ng/mL, p < 0.05; ob: day 7 49.69 ± 8.94 ng/mL versus day 1 0.69 ± 0.05 ng/mL, p < 0.05), after co-cultures with PBMCs, the IL-8 expression levels were significantly higher. It should be noticed that after co-cultures with PBMCs, IL-8 production in osteogenically induced JPCs was significantly down-regulated compared to untreated JPCs in Figure 2.9B (ob 69.16 ± 2.46 ng/mL versus co 90.51 ± 5.39 ng/mL, p < 0.05) and Figure 2.9C (ob 49.69 ± 8.94 ng/mL versus co 66.54 ± 9.77 ng/mL, p < 0.05). However, this tendency was not observed in Figure 2.9A. In addition, after co-cultivation experiments, IL-8 secretion by untreated or osteogenically induced JPCs was significantly increased, compared to monocultures with control (co) or osteogenic (ob) medium in the upper chamber, respectively (Figure 2.9A–C).

Similarly, supernatants from the lower chamber were collected and analyzed using ELISA. IL-8 production was significantly decreased in monocultures with control (co) or osteogenic (ob) medium at day 7, compared to day 1 in Figure 2.9D (co: 1.43 ± 0.31 ng/mL versus 6.69 ± 1.84 ng/mL, p < 0.05), Figure 2.9E (co: 3.16 ± 0.46 ng/mL versus 14.22 ± 2.45 ng/mL, p < 0.05; ob: 5.76 ± 0.33 ng/mL versus 14.17 ± 2.48 ng/mL, p < 0.05), and Figure 2.9F (co: 1.04 ± 0.02 ng/mL versus 14.65 ± 6.48 ng/mL, p < 0.05; ob: 4.79 ± 2.47 ng/mL versus 15.23 ± 5.53 ng/mL, p < 0.05), with the exception from the monoculture_ob group in Figure 2.9D (7.55 ± 2.03 ng/mL versus 7.40 ± 1.95 ng/mL, n.s.). However, IL-8 concentration was significantly up-regulated in co-cultures with untreated (co) or osteogenically induced JPCs at day 7 compared to day 1, as shown in Figure 2.9D (co: 49.88 ± 3.75 ng/mL versus 6.64 ± 1.90 ng/mL, p < 0.05; ob: 28.58 ± 1.94 ng/mL versus 7.12 ± 1.93

ng/mL, p < 0.05), Figure 2.9E (co: 72.89 ± 2.32 ng/mL versus 14.37 ± 2.39 ng/mL, p < 0.05; ob: 50.76 ± 1.63 ng/mL versus 15.24 ± 2.29 ng/mL, p < 0.05) and Figure 2.9F (co: 88.64 ± 6.27 ng/mL versus 11.36 ± 4.49 ng/mL, p < 0.05; ob: 67.19 ± 6.27 ng/mL versus 11.97 ± 4.03 ng/mL, p < 0.05). Notably, at day 7, significantly higher amounts of IL-8 were secreted by monoculture DCs with osteogenic (ob) medium, compared to monoculture with control (co) medium in the upper chamber; whilst significantly lower amounts were detected in DCs co-cultures with osteogenically induced JPCs, compared to DCs co-cultures with undifferentiated JPCs, as shown in Figure 2.9D–F. In the presence of untreated or osteogenically induced JPCs, IL-8 secretion by DCs was significantly increased at day 7, compared to monoculture with control (co) or osteogenic medium, respectively (Figure 2.9D–F).
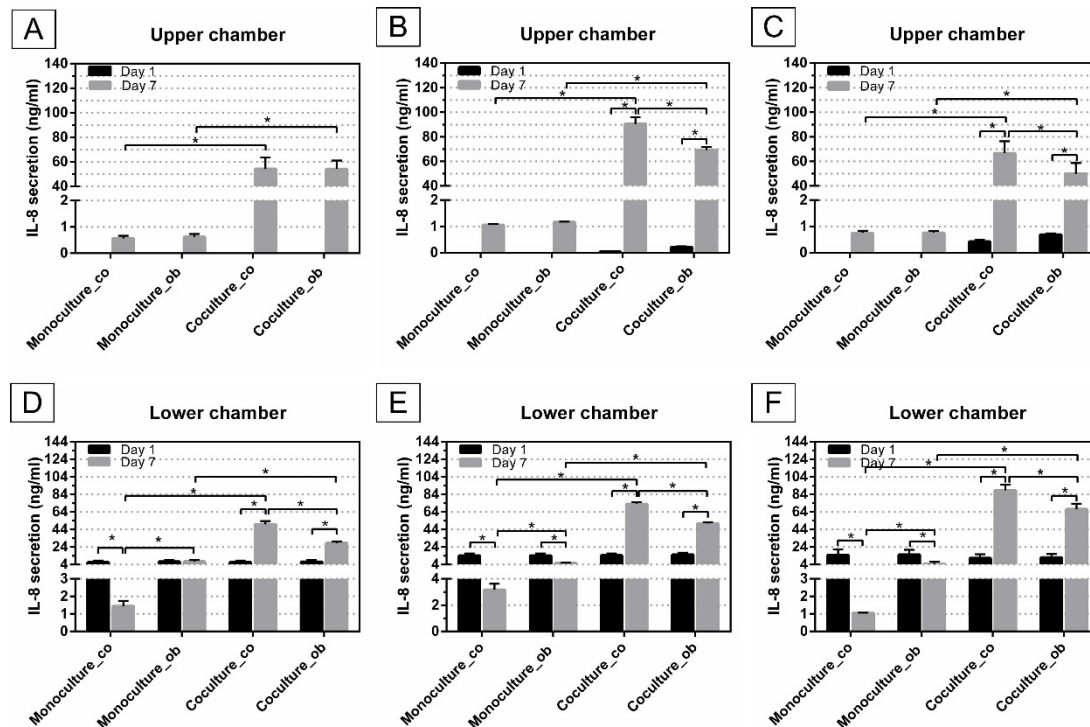


**Figure 2.9.** Analysis of IL-8 secretion in supernatants from upper and lower chamber of mono- and co-cultures, before and after DC differentiation (at day 1 and day 7). PBMCs/DCs were cultured in mono- and co-cultures with JPCs (untreated—co or osteogenically induced for 7 (A,D); 14 (B,E); and 21 (C,F) days) and IL-8 levels in supernatants from upper chambers of co-culture plates (upper panel) and lower chambers of co-culture plates (lower panel) were quantified by ELISA. Results were averaged from 6 independents.

## 2.4. Discussion

In our study, we could demonstrate for the first time an immunosuppressive effect eliciting from jaw periosteal cells.

After the addition of IL-4 and GM-CSF at day 1, immature monocyte-derived DCs differentiate. The induction of terminal differentiated DCs requires the addition of the second cocktail at day 6, and at day 7 mature DCs were generated [59]. After stimulation, DCs upregulate surface expression of co-stimulatory factors CD80, CD83, and CD86, as well as expression of HLA-DR [60]. We could successfully demonstrate the generation of mature DCs by flow cytometric measurements of DC surface marker, as shown in Figure 2.2.

The quantification of dendritic cell densities during DC maturation (day 3, 6, and 7) resulted in significant decreases when DCs were co-cultured with JPCs, whereby higher differences were observed in the tendency in co-cultures with undifferentiated JPCs, as shown in Figures 2.3–2.5 (day 6 and 7). However, significantly reduced dendritic cell numbers were counted likewise in co-cultures with osteogenically differentiated JPCs for 14 and 21 days, compared to monocultures cultivated with the respective media. Concerning the dendritic cell size, no significant differences were obtained; however, a tendency of diminished cell size in co-cultures with JPCs was evident. These results indicated clearly an inhibiting effect of JPCs on DC maturation, both in the undifferentiated and differentiated state.

Effects of JPCs on DC gene expression were much more complex. Figure 2.6 shows the overall effects of the osteogenic culture conditions on gene expression of DCs. Compared to monocultures with control medium in the upper chamber, addition of osteogenic medium led to overall lower gene expression of IL-12p35, IL-12p40, the two subunits of the IL-12 receptor, as well as pro-inflammatory cytokine (IFN-γ and TNF-α) expression. On the other site, we detected significantly higher IL-8 and extremely high up-regulated IL-10 expression levels under osteogenic conditions. These results indicated an overall suppression of pro-inflammatory cytokines, except IL-8, and a strong induction of the anti-inflammatory cytokine IL-10 by osteogenic culture conditions. Compared to monocultures with osteogenic medium in the upper

chamber, the effects emanating from osteogenically differentiated JPCs became evident. In these co-cultures, we detected significantly higher IL-12p40 expression levels and slightly higher IL-12Rβ1 and -β2 levels. At the same time, significantly lower IL-8 and significantly higher IL-10 expression levels were measured in co-cultures with osteogenically differentiated JPCs (for 21 days), in comparison to the respective monocultures. Although it might seem surprising at first sight because interleukin-10 is a physiologically relevant inhibitor of IL-12 secretion [61], it should be taken into consideration that we analyzed gene expression of the subunits p40 and p35. Natural killer stimulatory factor or interleukin 12 represents a major player in triggering T-helper 1 (Th1) responses [62, 63]. It is a 70 kD heterodimeric pro-inflammatory cytokine composed of two covalently linked chains, p35 and p40, and is produced by antigen presenting cells [64]. The main physiological producers for IL-12 are phagocytes (monocytes/macrophages and neutrophils) and dendritic cells [65].

In mice, it has been proposed that the so-called biologically inert p40 homodimer represents a natural inhibitor of IL-12 due to its similar affinity to the IL-12Rβ1 chain competing with the biologically active p70 heterodimer [66]. However, other studies report of biological functions of the mouse p40 homodimer [67]. Kalinski and co-authors could demonstrate that prostaglandin E2, with the known Th2-driving function, selectively enhanced IL-12p40 gene and protein expression in human TNF-α activated immature DCs, and suppressed IL-12p70 production [68, 69]. These results suggest that the IL-12p40 homodimer can inhibit IL-12p70 secretion, and consequently signal transduction. Unfortunately, we have not succeeded in measuring IL-12p70 protein levels in our co-cultures, limiting the examination of this hypothesis.

A recent study reports that MSCs secrete Galectin-1 and the authors postulate that this factor is able to inhibit dendritic cell function [70]. Furthermore, they detected increased Gal-1, IL-10, and IL-12 concentrations in supernatants from the co-culture system. Coinciding with the results from this study, we detected significantly higher IL-12p40 and IL-10 gene expression levels at the same time in DCs cultivated in co-cultures with

osteogenically differentiated JPCs. We also detected elevated levels of Galectin-1 and -3 at the end of osteogenic differentiation of JPCs (unpublished data from our lab).

IL-27 is a member of the IL-12/IL-23 heterodimeric family of cytokines, capable of both enhancement or suppression of immune responses [71]. IL-27 induces expansion of Th1 and on the other hand, IL-27 suppresses immune responses through inhibition of the development of T helper 17 cells and induction of IL-10 production. In our study, osteogenically differentiated JPCs seemed to have no relevant influence on IL-27 gene expression.

Indoleamine 2,3-dioxygenase (IDO) and prostaglandin E2 (PGE2) are key regulators of MSC immunosuppressive activities. Meisel and co-authors demonstrated that MSCs can limit T cell responses via IDO-mediated tryptophan degradation [72]. Additionally, inhibitors of PGE2 synthesis mitigated the overall suppressive effects of MSCs [73]. We did not perform measurements of PGE2 levels in our co-cultures, since this hormone is a component of the DC differentiation cocktail. However, JPCs express high levels of IDO in both undifferentiated and osteogenically differentiated states (data not shown).

Mature type 1 polarizing DCs produce pro-inflammatory cytokines IL-1β, IL-12, IL-8, and TNF-α.  Summarizing our results, we measured an overall induction of IL-8 gene expression (Figure 2.6) in mature DCs under osteogenic conditions, and also a significant reduction by co-culturing with osteogenically differentiated JPCs in comparison to the respective DC monocultures. The subsequent measurements of IL-8 protein levels showed very similar results: the osteogenic medium led to a significant upregulation of IL-8 release in DCs (Figure 2.9D–F monoculture_ob versus monoculture_co, day 7). Co-culturing with undifferentiated JPCs resulted in significant upregulation of IL-8 levels. We assume that this is probably the sum of IL-8 release from both cell types DCs and JPCs. However, we were not able to prove this hypothesis since JPC monoculture control was lacking in our experiments. IL-8 protein could also pass over the lower chamber into the upper chamber by diffusion. What is certain is that osteogenically differentiated JPCs were able to reduce significant maximal IL-8 levels

achieved in co-cultures with undifferentiated JPCs. It seems on the one hand, that our used osteogenic medium triggers IL-8 release in mature DCs in contrast to findings from other publications concerning the effects of dexamethasone on different cell types [74-76]. On the other hand, significant reduction of IL-8 levels by osteogenically differentiated JPCs was remarkable, since IL-8 expression strongly increased during JPC osteogenesis (data not shown). The significantly reduced IL-8 levels in DCs at day 7 compared to that of PBMCs at day 1, could be because additional IL-8 producing cells were present in the cell suspension at this time point.

## 2.5. Conclusions

Taken together, our data revealed an overall immunosuppressive effect of undifferentiated and osteogenically induced and differentiated JPCs on monocyte-derived DC maturation. This finding is based on the detection of significantly lower numbers of differentiated DCs in the presence of inactivated or activated JPCs. The underlaying mechanism might involve overall repression of pro-inflammatory cytokines and high induction of the anti-inflammatory IL-10. Since this is the first study examining JPCs effects on immune cells, further studies should follow to clarify JPC mode of action more profoundly.

## 3. Study II: Jaw Periosteal Cells Seeded in Beta-Tricalcium Phosphate Inhibit Dendritic Cell Maturation

***The part is a reprint of the following publication:***

**Abstract:**

Mesenchymal stem cells (MSCs) have gained attraction not only in the field of regenerative medicine but also in the field of autoimmune disease therapies or organ transplantation due to their immunoregulatory and/or immunosuppressive features. Dendritic cells (DCs) play a crucial role in initiating and regulating immune reactions by promoting antigen-specific T cell activation. In this study, we investigated the effect of human jaw periosteal progenitor cells (JPCs) seeded in beta-tricalcium phosphate (β-TCP) scaffolds on monocyte-derived DC differentiation. Significantly lower numbers of differentiated DCs were observed in the presence of normal (Co) and osteogenically induced (Ob) JPCs-seeded β-TCP constructs. Gene expression analysis revealed significantly lower interleukin-12 subunit p35 (IL-12p35) and interleukin-12 receptor beta 2 (IL-12Rβ2) and pro-inflammatory cytokine interferon-gamma (IFN-γ) levels in DCs under Ob conditions, while interleukin-8 (IL-8) gene levels were significantly increased. Furthermore, in the presence of JPCs-seeded β-TCP constructs, interleukin-10 (IL-10) gene expression was significantly induced in DCs, particularly under Ob conditions. Analysis of DC protein levels shows that granulocyte-colony stimulating factor (G-CSF) was significantly upregulated in coculture groups. Our results indicate that undifferentiated and osteogenically induced JPCs-seeded β-TCP constructs have an overall inhibitory effect on monocyte-derived DC maturation.

## 3.1. Introduction

Stem cell-based tissue engineering (TE) is a promising strategy for bone tissue regeneration, overcoming drawbacks associated with bone autografting such as complex surgical procedures, limited availability, and high costs [77, 78]. In bone TE, MSCs isolated from bone marrow and other tissues not only possess the ability of multipotent differentiation capacity but also promote tissue homeostasis, metabolism, growth, and repair. Notably, periosteum-derived cells can be a source of stem cells with great potential for bone and cartilage repair [79-83]. Compared to other skeletal stem cells, human jaw periosteal cells (JPCs) could represent the most suitable stem cell source in the field of oral bone regeneration. The advantages of JPCs are simple tissue harvesting and cell isolation. In our previous studies, we optimized cell culture conditions, biomaterials, and detection methods for the mineralization potential of JPCs in order to move further step by step towards bone regenerative clinical applications [12-16, 84].

The scaffold type plays a critical role in bone TE, possessing not only structural function for the colonializing cells but also providing mechanical stability, particularly in the masticatory region. β-TCP has been widely used in clinical applications because of its excellent biocompatibility and osteoconductive ability [14-17]. Additionally, β-TCP has moderate biodegradability in physiological environments. The β-TCP scaffold can be degraded by acidic products released by surrounding cells such as osteoclasts or macrophages, and substantially replaced by newly formed bone [85, 86]. Previously, cocultures of MSCs and MSC-derived endothelial cells seeded in porous β-TCP scaffolds resulted in successful repair of large segmental bone defects in a rabbit model [87]. Regarding periosteal cells, Vacanti et al. firstly reported a successful clinical case using periosteal cells combined with hydrogel and a calcium phosphate scaffold for bone regeneration [88]. Our group previously demonstrated that JPCs seeded into biofunctionalized β-TCP scaffolds could represent a suitable strategy for the development of bone TE constructs [19, 41].

DCs have been recognized as the most potent antigen-presenting cells

(APCs) widely distributed in the human body [25]. DCs can be derived from human peripheral blood monocytes (PBMCs) through culturing with granulocyte-macrophage colony-stimulating factor (GM-CSF) and interleukin-4 (IL-4) [89-91]. DCs play a critical role in the initiation of primary immune responses and tolerance induction [92]. In fact, DCs can be divided into two major types: an immature and a mature stage, respectively [62, 92] The mature stage of DCs is related to a high expression of costimulatory molecules involved in antigen presentation (i.e., CD80, CD86, and MHC-II). Undoubtedly, DC maturation is a fundamental prerequisite for the induction of immunogenic T cell responses [25]. Numerous studies have proven that MSCs not only can inhibit DC maturation [34, 35] but also can inhibit T cells proliferation [30, 93] due to their low immunogenicity and immunoregulatory properties. Previously, we reported that JPCs exhibit an overall inhibiting effect on DC maturation in a 2D Transwell system [94].

In the present study, we investigated the effects of JPCs seeded within β-TCP constructs on human DC maturation. Therefore, gene expression, phenotype, and differentiation of DCs were investigated under cocultivation with untreated or osteogenically induced JPCs cultured within β-TCP constructs.

**3.2. Materials and Methods**

3.2.1. Isolation of JPCs and PBMCs

Samples from three donors were included in the study, with the approval number 194/2008BO2 from the local ethics committee. After obtaining written informed consent from these three donors, human JPCs were isolated and cultured, as mentioned previously [19, 94]. JPCs were cultured in Dulbecco's Modified Eagle Medium/Nutrient Mixture F-12 (DMEM/F-12, Invitrogen/Thermo Fisher Scientific, Waltham, USA) containing 10% fetal calf serum (FCS) (Sigma-Aldrich, Darmstadt, Germany), 1% penicillin/streptomycin (Lonza, Basel, Switzerland), and 1% fungicides (Biochrom AG, Berlin, Germany) under standard cell culture conditions. Pooled JPCs of these three donors from the sixth passage were used for all coculture experiments, and cell culture medium was replaced every other day. The osteogenic differentiation potential of the used JPCs was evaluated as reported before [94].

The human peripheral blood was collected and diluted with Dulbecco's phosphate-buffered saline (DPBS, Sigma-Aldrich, Darmstadt, Germany), and layered over 12 mL of 1.077 g/mL Ficoll-Paque PLUS (GE Healthcare Europe GmbH, Freiburg, Germany). Plasma and red blood cells were separated from PBMCs by density gradient centrifugation (no break, 810× $g$, 20 °C) for 20 min. PBMCs were harvested and pipetted into another fresh 50 mL tube. The cells were washed 3 times with DPBS, and then a cell density of 1 × $10^6$ cells/well was cultivated in x-vivo serum-free medium (Biozym, Hessisch-Oldendorf, Germany) with 3% autologous plasma and 1% penicillin/streptomycin for 24 h.

3.2.2. Cell Seeding of β-TCP Constructs

JPCs in culture flasks were trypsinized (Trypsin-Versene EDTA, Lonza, Basel, Switzerland) and pooled JPCs of these three donors were seeded in β-TCP constructs (Curasan AG, Kleinostheim, Germany). The constructs were preincubated in 96-well polypropylene culture plates containing DMEM/F-12 media for 1 h. A starting density of 1 × $10^5$ cells/scaffold was seeded into β-TCP constructs in 50 μL volume; the JPCs-seeded β-TCP scaffolds were incubated for 2 h at 37°C. After 2 h of incubation, additional 150 μL medium

were subsequently pipetted to overlay JPCs-seeded β-TCP constructs.

For osteogenic differentiation of JPCs-seeded constructs before coculture experiments, the constructs were cultured in a 96-well plate under osteogenic (Ob) conditions (DMEM/F-12 complete medium containing 4 µM dexamethasone, 100 µM L-ascorbic acid 2-phosphate, and 10 mM β-glycerophosphate, Sigma-Aldrich, Germany) for 7 days. JPCs-seeded β-TCP scaffolds cultured with Co (untreated) medium for the same time period served as undifferentiated controls. The medium was replaced every 2 days. The osteogenesis-relevant genes by JPCs cultured within β-TCP constructs and cocultured with DCs were quantified. Figure 3.1 shows gene expression levels of ALP and RUNX2 after 14 days (7 days monoculture and 7 days coculture) of osteogenic differentiation.
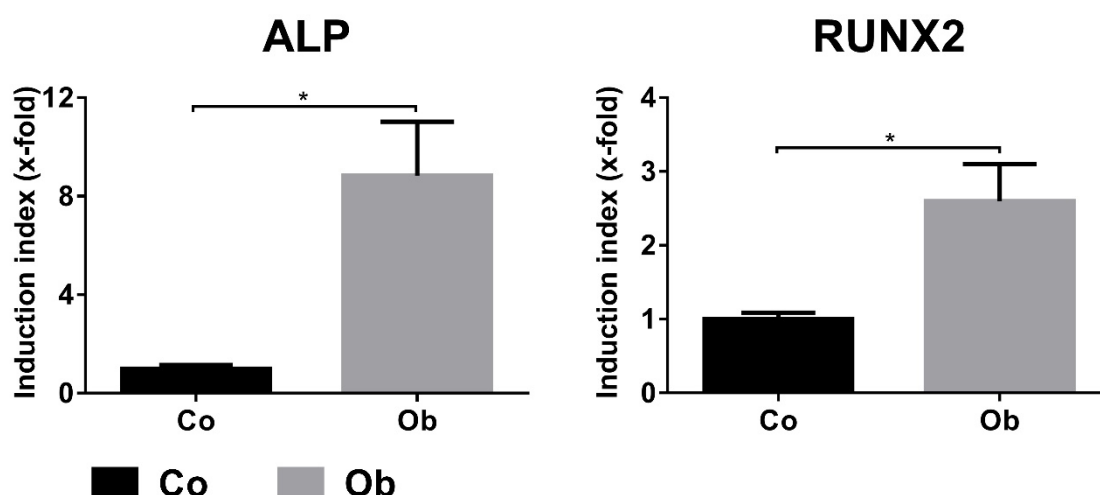


**Figure 3.1.** Quantitative gene expression of JPCs seeded within β-TCP constructs and co-cultured with DCs under Co and Ob conditions for 14 days. Tested gene expressions were quantified by the LightCycler System, and ratios of genes in relation to the housekeeping gene glyceraldehyde 3-phosphate dehydrogenase (GAPDH) were calculated. Gene levels in JPCs seeded within β-TCP constructs co-cultured with DCs under normal conditions (Co) was set as 1 (control), and induction indices (x-fold) in relation to the control were calculated. Data were collected from three independent experiments (* $p < 0.05$).

3.2.3. Coculture of JPCs-Seeded Constructs and Monocytes

For cocultivation experiments, 6-well Transwell coculture plates (0.4 µm pore size membrane, Corning, Wiesbaden, Germany) were chosen. PBMCs were incubated for 24 h after cell seeding in the lower compartment, and medium change was performed using autologous plasma-x-vivo medium containing 40 ng/mL IL-4 and 100 ng/mL GM-CSF (Sigma-Aldrich, Darmstadt, Germany) in order to begin DC differentiation. Coculture experiments were performed in the absence or presence of JPCs-seeded or cell-free constructs. Therefore, four scaffolds were placed per upper compartment under undifferentiated or osteogenic media. Four different groups were included into the upper compartment: 1. JPCs-free constructs cultured under undifferentiated DMEM/F-12 media conditions (β-TCP/Co), 2. JPCs-free constructs cultured under osteogenic medium (β-TCP/Ob), 3. JPCs-seeded constructs cultured under undifferentiated DMEM/F-12 media conditions (JPCs + β-TCP/Co), and 4. JPCs-seeded constructs cultured under osteogenic conditions (JPCs + β-TCP/Ob). At day 3, media change in the upper compartment was performed. At day 6, the second DC differentiation cocktail containing 40 ng/mL IL-4, 100 ng/mL GM-CSF, 10 ng/mL TNF-α, 10 ng/mL IL-1β, 10 ng/mL IL-6 (Tebu Bio, Offenbach, Germany), and 1 µg/mL PGE2 (Bio Trend, Köln, Germany) was added to the x-vivo medium containing autologous plasma for another 24 h to stimulate DCs maturation.

## 3.2.4. Analysis of Cell Viability Using Propidium Iodide

After 7 days of coculture, the suspension (mature DCs) and adherent (monocytes/immature DCs) cells of the lower compartment were harvested into separated 50 mL tubes and centrifugated for 7 min (1400 rpm, 8 °C). The cell pellet was resuspended in 1 mL DMEM/F-12 medium, and 100 µL of cell suspension was added into a FACS tube containing 100 µL DPBS. Then, 1 µL of 1 mg/mL propidium iodide (PI) staining solution was added to the sample, mixed gently, and incubated on ice in dark for 1 min. Following this method, the suspension and adherent cells were counted and analyzed by flow cytometry, respectively. The ratios of suspension/adherent cells under different culture conditions were calculated.

## 3.2.5. Flow Cytometric Analyses of Dendritic Marker Expression

Monocytes before coculture (day 1) and DCs after coculture (day 7) were collected for flow cytometric analysis and served as controls. After centrifugation for 7 min (1400 rpm, 8 °C), cell pellets were resuspended in 10% Gamunex (human immune globulin solution, Talecris Biotherapeutics, Germany), and incubated for 15 min on ice. After this incubation period time, the cell density was adjusted to $2 \times 10^6$ cells/mL with FACS buffer (DPBS, 0.1% BSA, and 0.1% sodium azide). Cells were incubated on ice with the specific phycoerythrin (PE)-labeled mouse antihuman HLA-DR (MACS Miltenyi Biotec, Bergisch Gladbach, Germany), and allophycocyanin (APC)-labeled mouse antihuman CD14, CD83, and CD209 (BioLegend, San Diego, USA) antibodies for 15 min in dark. Subsequently, labeled cells were washed two times with FACS buffer and centrifuged for 7 min (1400 rpm, 8 °C). Cell pellets were resuspended in 200 µL FACS buffer and analyzed by flow cytometry using the Guava easyCyte 6HT-2L Instrument (Merck Millipore, Darmstadt, Germany). For data evaluation, the guavaSoft 2.2.3 (InCyte 2.2.2, Luminex Corporation, Chicago, USA software was used.

### 3.2.6. RNA Isolation and Quantitative Gene Expression Analyses in DCs

RNA was isolated from DCs (after 7 days of differentiation) using the NucleoSpin RNA XS kit (Macherey-Nagel, Hoerd, France) as recommended by the manufacturer and photometrically measured and quantified using the Qubit RNA Broad-Range (BR) Assay Kit and a corresponding 3.0 fluorometer (Invitrogen/Thermo Fisher Scientific, Waltham, USA). Subsequently, cDNA synthesis was performed using 200 ng of RNA and the SuperScript VILO Kit (Invitrogen/Thermo Fisher Scientific, Waltham, USA), as recommended by the manufacturer. To quantify mRNA expression levels, the real-time LightCycler System (Roche Diagnostics, Mannheim, Germany) was used. For the PCR reactions, DEPC-treated water, DNA Master SYBR Green I kit (Roche, Mannheim, Germany), and commercial primer kits (IL-12p35, IL-12p40, IL-12Rβ1, IL-12Rβ2, IFN-γ, TNF-α, IL-4, IL-8, IL-10, MIP-1α, MIP-1β, and G-CSF) from Search LC (Heidelberg, Germany) were used for 40 amplification cycles of the target DNA. The target gene transcript levels were normalized to those of the housekeeping gene GAPDH (Search LC, Heidelberg, Germany). Finally, the ratio of the β-TCP/Co group was set as 1 (control), and x-fold

induction indices in relation to this control were calculated.

### 3.2.7. Proteome Profiler Array

To measure the expression of different proteins in DCs (lower chamber) or JPCs (upper chamber) supernatants at day 1 and 7 of DC differentiation and G-CSF levels in supernatants from JPCs (cultivation in the absence of DCs) cultured with human platelet lysate (hPL) under Co/Ob conditions (with or without dexamethasone) at day 15, proteome profiler array kits (Human Cytokine Array Kit, Human Soluble Receptor Array Kit, and Non-Hematopoietic Panel; R&D Systems, Germany) were used, following the manufacturer's instructions. Briefly, the membranes were blocked with respective array buffer for 1 h at room temperature (RT) and then incubated with 1.5 mL of sample/array buffer/detection antibody mixtures overnight at 4 °C. After washing three times, the membranes were incubated with 2 mL of diluted streptavidin–HRP at RT for 30 min. After three washing steps again, the membranes were exposed to 1 mL of the chemiluminescent reagent mixture and the radiographic films for 10 min. The developed films were scanned, and data analysis of positive signals was carried out using the ImageJ software.

### 3.2.8. Statistical Analysis

The statistical values for all measurements are expressed as means ± standard error of means (SEM). Student's t-tests or one-way analysis of variance (ANOVA) for repeated measurements followed by Tukey's multiple comparisons tests were used. All statistical analyses were carried out using the SPSS V22.0 software (IBM Corp., New York, NY, USA). A value of $p < 0.05$ (two-tailed) was considered as statistically significant.

## 3.3. Results

### 3.3.1. Cell Morphology of DCs

To investigate the effects of JPCs-seeded β-TCP constructs on DC maturation, cell-seeded scaffolds were cultured under untreated (Co) and osteogenic conditions (Ob) for 14 days. Representative microscopic images indicated the morphologic appearance of monocytes and DCs. The monocytes were observed as small round cells among all groups at day 1, whereas differentiating monocytes were found to be getting bigger at day 7, as shown in Figure 3.2. No obvious larger cell morphologies were observed in the presence of JPCs-seeded β-TCP constructs under both culture conditions, implying relatively less differentiated DCs.



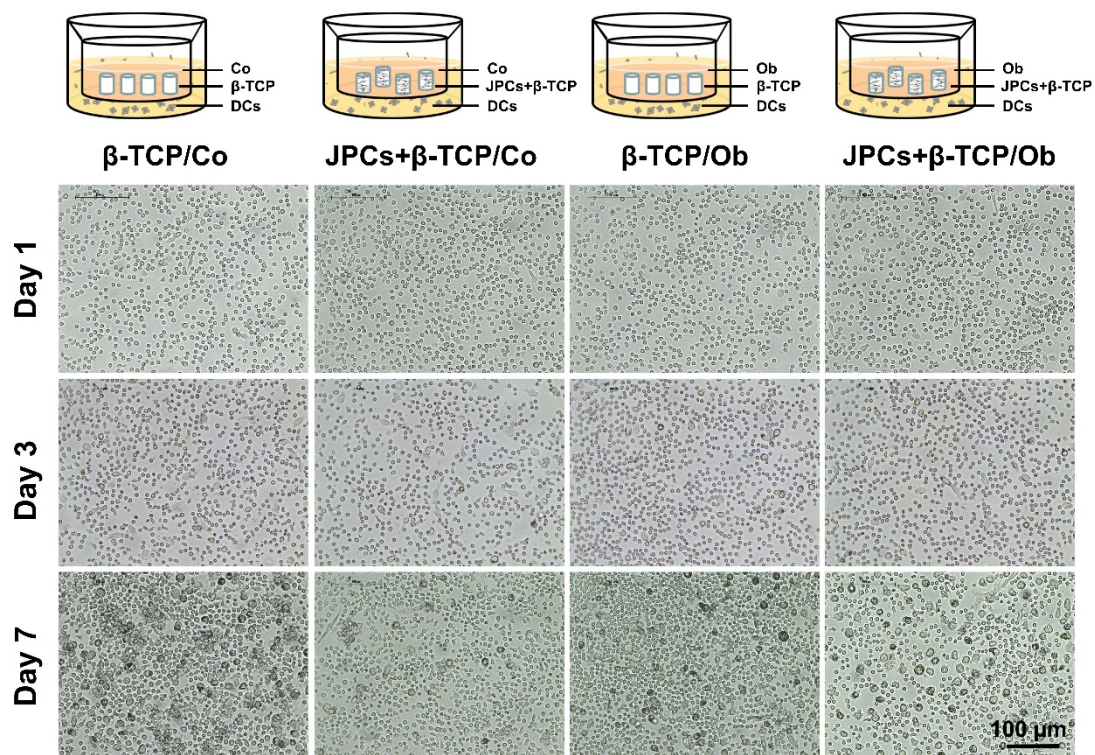**Figure 3.2.** Representative microscopic images showing the morphologic characteristics of monocytes and dendritic cells (DCs) in unseeded (beta-tricalcium phosphate, β-TCP) and jaw periosteal progenitor cells (JPC)-seeded constructs (JPCs + β-TCP) under untreated (Co) or osteogenic (Ob) conditions at day 1, 3, and 7 of DC differentiation, respectively.

### 3.3.2. DC Densities in Mono- (β-TCP/Co and β-TCP/Ob) and Cocultures

(JPCs + β-TCP/Co and Ob)

DC densities (adherent cells within the lower compartment) and the ratio of suspension/adherent cells were investigated in mono- (cocultivation with cell-free scaffolds) and cocultures (with JPCs-seeded β-TCP constructs). Compared to monocultures (β-TCP/Co), DC densities were significantly lower in untreated cocultures (JPCs + β-TCP/Co) at day 6 (JPCs + β-TCP/Co 27.76 ± 2.40 versus β-TCP/Co 50.90 ± 7.26, $p < 0.05$), as shown in Figure 3.3A. Similarly, at day 7, DC densities in cocultures (JPCs + β-TCP) were shown to be significantly lower than the counterparts of monocultures under both conditions (JPCs + β-TCP/Co 29.19 ± 1.19 versus β-TCP/Co 75.34 ± 2.47, $p < 0.05$ and JPCs + β-TCP/Ob 37.09 ± 2.76 versus β-TCP/Ob 59.07 ± 10.06, $p < 0.05$, respectively). As illustrated in Figure 3.3B, compared to the β-TCP monoculture groups, the significantly lower ratios of suspension to adherent DCs were detected in the coculture (JPCs + β-TCP) groups under both culture conditions (Co/Ob). (JPCs + β-TCP/Co 1.69 ± 0.56 versus β-TCP/Co 2. 84 ± 1.07, $p < 0.05$ and JPCs + β-TCP/Ob 1.26 ± 0.34 versus β-TCP/Ob 2.12 ± 0.57, $p < 0.05$, respectively).
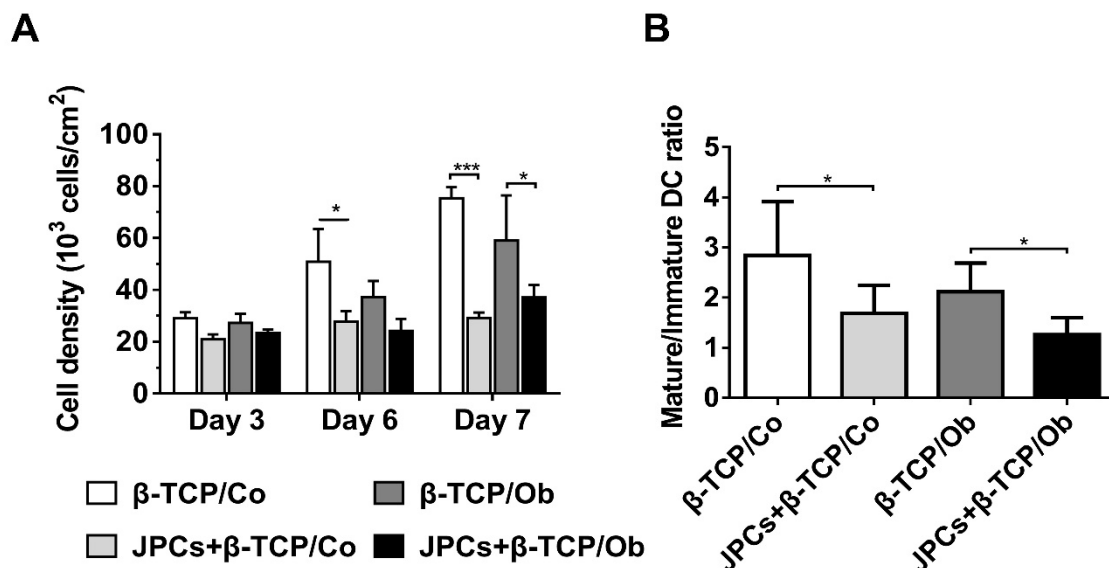
**A**

**B**



**Figure 3.3.** DC densities and mature/immature DC ratios in monocultures (β-TCP-groups) and cocultures (JPCs + β-TCP) preincubated under untreated (Co) and osteogenic (Ob) conditions for 7 days. (A) DC densities (103 cells/cm2) were quantified using ImageJ software. (B) The ratio of suspension (mature)/adherent

(immature) cells in the lower chamber was determined by flow cytometry using propidium iodide (PI) staining after DC differentiation at day 7. Data were collected from five independent experiments (* p < 0.05, *** p < 0.001).

### 3.3.3. Flow Cytometric DC Characterization

To compare the monocyte phenotype before and after cocultures, surface marker expression was detected in five independent experiments. Figure 3.4 shows significantly down-regulated expression (MFI) of CD14 on DCs in β-TCP (Co/Ob) groups compared to undifferentiated monocyte control. More importantly, CD14 protein expression was found to be significantly lower in monocultures (β-TCP) compared with cocultures with JPCs-seeded β-TCP constructs under normal conditions. In addition, MFIs for CD83, CD209, and HLA-DR expressions on differentiated DCs were significantly increased in monocultures (β-TCP-group) and cocultures (JPCs + β-TCP) under Ob compared to Co conditions. Similarly, MFIs of CD209 and HLA-DR were significantly upregulated in monocultures (β-TCP-group) and cocultures (JPCs + β-TCP) under Ob conditions compared to the undifferentiated monocyte control.
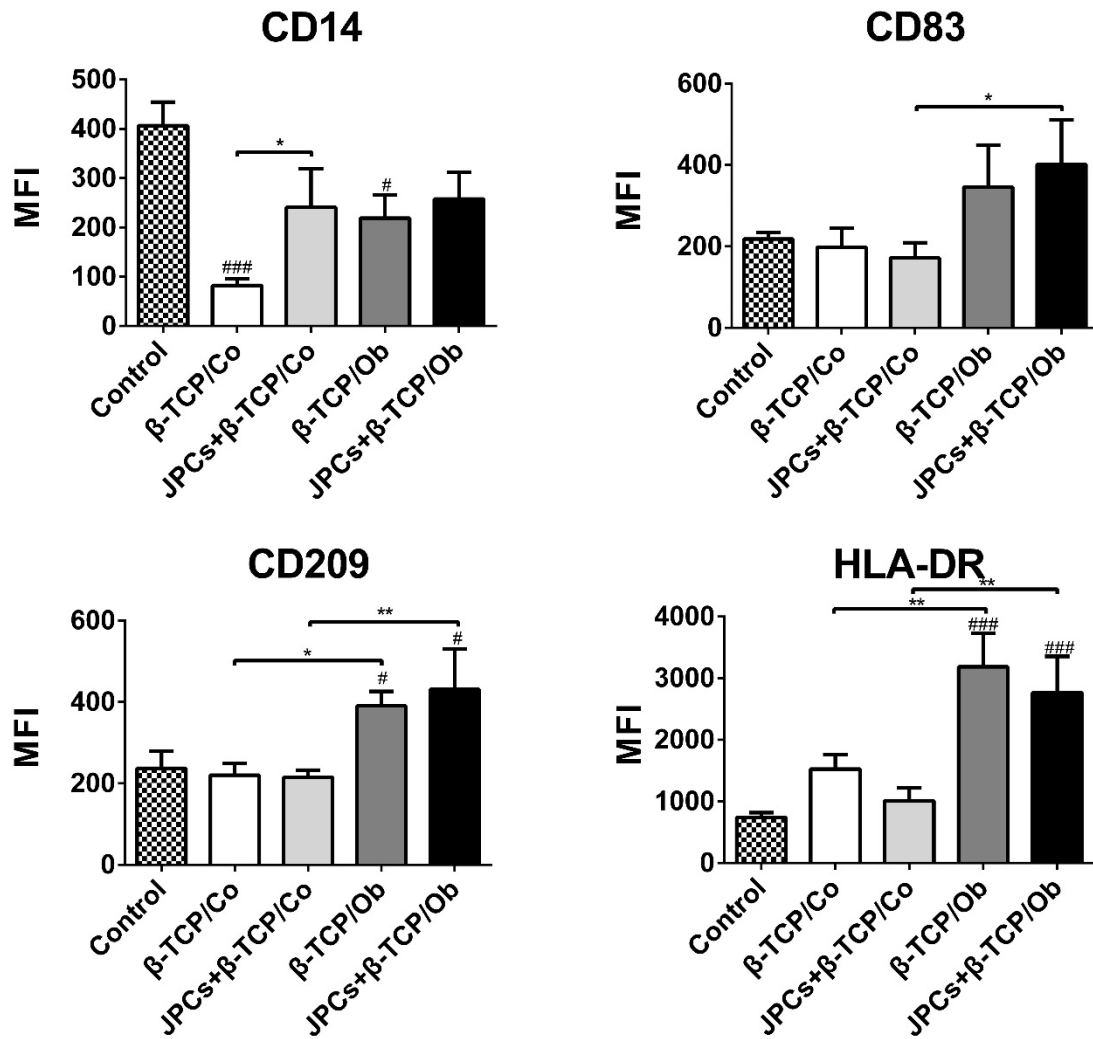
**Figure 3.4.** Flow cytometric analysis of DC surface marker expression in the undifferentiated state (monocyte control) and after 7 days DC differentiation in monocultures (β-TCP) and cocultures (JPCs + β-TCP) preincubated under Co and Ob conditions for initial 7 days (constructs were cultivated for 14 days in total). The mean fluorescence intensity (MFI) of positive cells is shown for the indicated markers CD14, CD83, CD209, and HLA-DR. Data were collected from five independent experiments (* $p < 0.05$, ** $p < 0.01$ # and ### represent $p < 0.05$ and $p < 0.001$ when compared to the undifferentiated monocyte control, respectively).

The percentages of positive cells for the four surface markers are listed in Table 3.1. DCs cocultured with cell-free β-TCP or JPCs-seeded β-TCP constructs under Ob conditions revealed significant higher percentages of CD14-positive cells compared to control and Co conditions. In addition, a

similar trend could be found between the results of CD209 and CD14, whereas DCs cocultured with JPCs-seeded β-TCP constructs exhibited no statistically significant differences under Ob conditions in comparison to Co conditions. Additionally, HLA-DR was significantly upregulated in the groups cocultured with β-TCP and JPCs-seeded β-TCP constructs under both Co/Ob conditions compared to undifferentiated monocyte controls.

**Table 3.1.** Percentages of positive monocytes (control) and dendritic cells (DCs) cocultured with cell-free beta-tricalcium phosphate (β-TCP) or jaw periosteal progenitor cells (JPCs)-seeded β-TCP constructs under normal/osteogenically induced (Co/Ob) conditions for 14 days (β-TCP constructs for 7 days monocultures followed by 7 days cocultures with DCs) for the listed surface antigens.

| Surface Markers | Control | Experimental Groups | | | |
| --- | --- | --- | --- | --- | --- |
| | | β-TCP/Co | β-TCP/Ob | JPCs + β-TCP/Co | JPCs + β-TCP/Ob |
| CD14 | 11.06 ± 6.39 | 20.85 ± 10.68 [a] | 72.45 ± 3.44 [a]* | 14.27 ± 2.37 [A] | 66.67 ± 1.39 [A]* |
| CD83 | 9.21 ± 4.76 | 40.85 ± 21.36 | 38.64 ± 26.19 | 48.48 ± 9.91 | 41.38 ± 15.69 |
| CD209 | 1.03 ± 0.59 | 14.35 ± 7.32 [a] | 69.50 ± 13.02 [a]* | 28.56 ± 6.19 | 62.77 ± 13.54 * |
| HLA-DR | 26.74 ± 5.68 | 91.55 ± 5.86 * | 95.83 ± 1.57 * | 87.85 ± 6.25 * | 93.73 ± 3.59 * |

The data of five independent experiments are shown as mean ± SEM. [a] Significant differences observed between β-TCP/Co and β-TCP/Ob ($p < 0.05$). [A] Significant differences observed between JPCs + β-TCP/Co and JPCs + β-TCP/Ob ($p < 0.05$). Superscript asterisks represent statistical significance differences compared to the control ($p < 0.05$).

### 3.3.4. DC Gene Expression Analysis

To evaluate the effect of cell-free or JPCs-seeded β-TCP constructs on DC gene expression, monocytes were differentiated in mono- and cocultures for 7 days after precultivation of JPCs under untreated and osteogenic conditions for 1 week. As shown in Figure 3.5, cocultured DCs (JPCs + β-TCP/Co) showed significant downregulation of four genes (IL-12p35,

interleukin 12 receptor beta 1 (IL-12Rβ1), IL-12Rβ2, and IFN-γ) and upregulation of IL-4 and G-CSF compared with the expression of DCs cultured in monocultures (β-TCP/Co). In addition, DCs cultivated in coculture with osteogenically induced constructs (JPCs + β-TCP/Ob) showed significant downregulation of IL-8 and upregulation of interleukin-12 subunit p40 (IL-12p40) as well as of the anti-inflammatory IL-10 compared to DC expression in monocultures (β-TCP/Ob). Nevertheless, DCs exposed to cell-free β-TCP constructs under Ob conditions revealed a different gene expression pattern. Compared to DC expression in coculture with cell-free β-TCP constructs under untreated conditions, significant downregulation of the genes IL-12p35, IL-12p40, IL-12Rβ1, IL-12Rβ2, IFN-γ, TNF-α, and IL-4 and an upregulation of the genes IL-8, IL-10, macrophage inflammatory proteins-1α (MIP-1α), and macrophage inflammatory proteins-1β (MIP-1β) were detected, indicating that this gene regulation is only due to the effects of the osteogenic medium. Additionally, DCs cultured with JPCs + β-TCP constructs under Ob conditions showed a significantly downregulated gene expression of IL-12Rβ2, IFN-γ, and IL-4 and an upregulated gene expression of IL-8, IL-10, and MIP-1β compared to JPCs + β-TCP/Co.

In summary, when the effects of the osteogenic medium are deducted, JPCs seem to partially suppress IL-12p35, IL-12Rβ1, IL-12Rβ2, IFN-γ, and IL-8 gene expression, whereas JPCs as well as osteogenic medium seem to induce IL-4, IL-10, and G-CSF transcript levels.
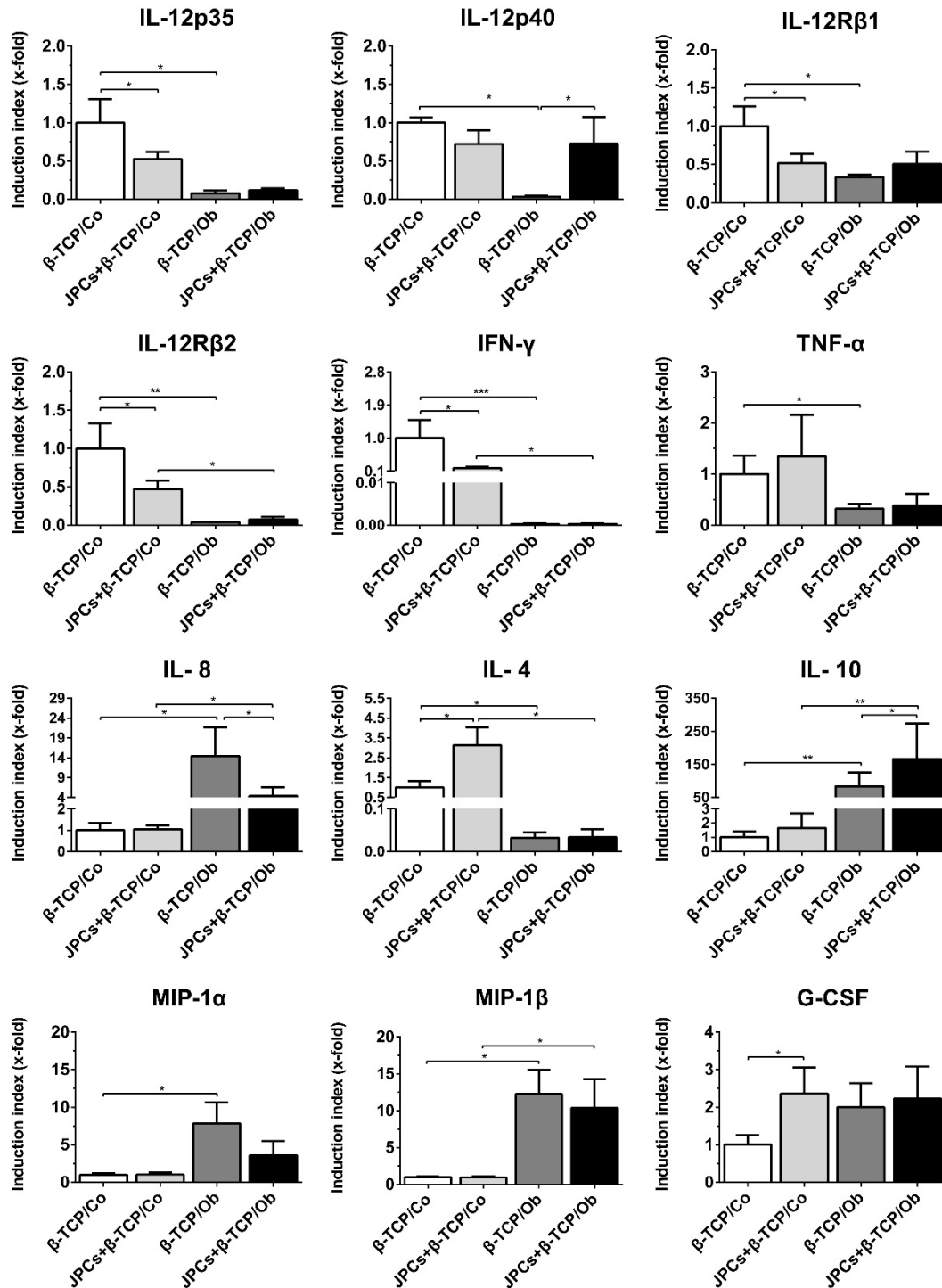
**Figure 3.5.** Quantitative gene expression of DCs cocultured with cell-free β-TCP and JPCs-seeded β-TCP constructs for 7 days after their preincubation under Co and Ob conditions for initial 7 days (constructs were cultivated for 14 days in total). Analyzed gene expressions were quantified by the LightCycler System, and ratios of genes of interest in relation to the housekeeping gene glyceraldehyde 3-phosphate dehydrogenase (GAPDH) were calculated. Gene levels

in DCs cultured with cell-free β-TCP constructs under normal conditions (Co) was set as 1 (control), and induction indices (x-fold) in relation to the control were calculated. Data were collected from three independent experiments (* $p < 0.05$, ** $p < 0.01$, *** $p < 0.001$).

### 3.3.5. DC Protein Expression Analysis

To identify the protein expression patterns in DCs, we used a human cytokine array comprising 36 human cytokines. Supernatants of DCs in coculture after 7 days of dendritic differentiation were collected and used for secretome analysis. The used cell-free and cell-seeded constructs were cultured under Co and Ob conditions for 7 days before cocultures with DCs were started and for additional 7 days in cocultures. As shown in Figure 3.6A, expression of MIP-1α/β and IFN-γ were decreased under Ob condition. Notably, the expression of G-CSF was increased in JPCs + β-TCP under both culture conditions. Figure 3.6B shows that the pro-inflammatory proteins MIP-1α/β and IFN-γ were significantly decreased in the β-TCP/Ob and JPCs + β-TCP/Ob groups compared to the corresponding Co groups, respectively. In the JPCs + β-TCP/Co group, the expression of IL-8 was significantly suppressed compared to the JPC-free β-TCP/Co group. Moreover, JPCs-seeded β-TCP constructs significantly induced the expression levels of G-CSF compared to cell-free β-TCP constructs under both culture conditions. Unfortunately, we were not able to detect IL12p70 levels. IL-4, IL-6, and GM-CSF were compounds of the DC maturation cocktail. Therefore, we performed no quantification of these cytokines.
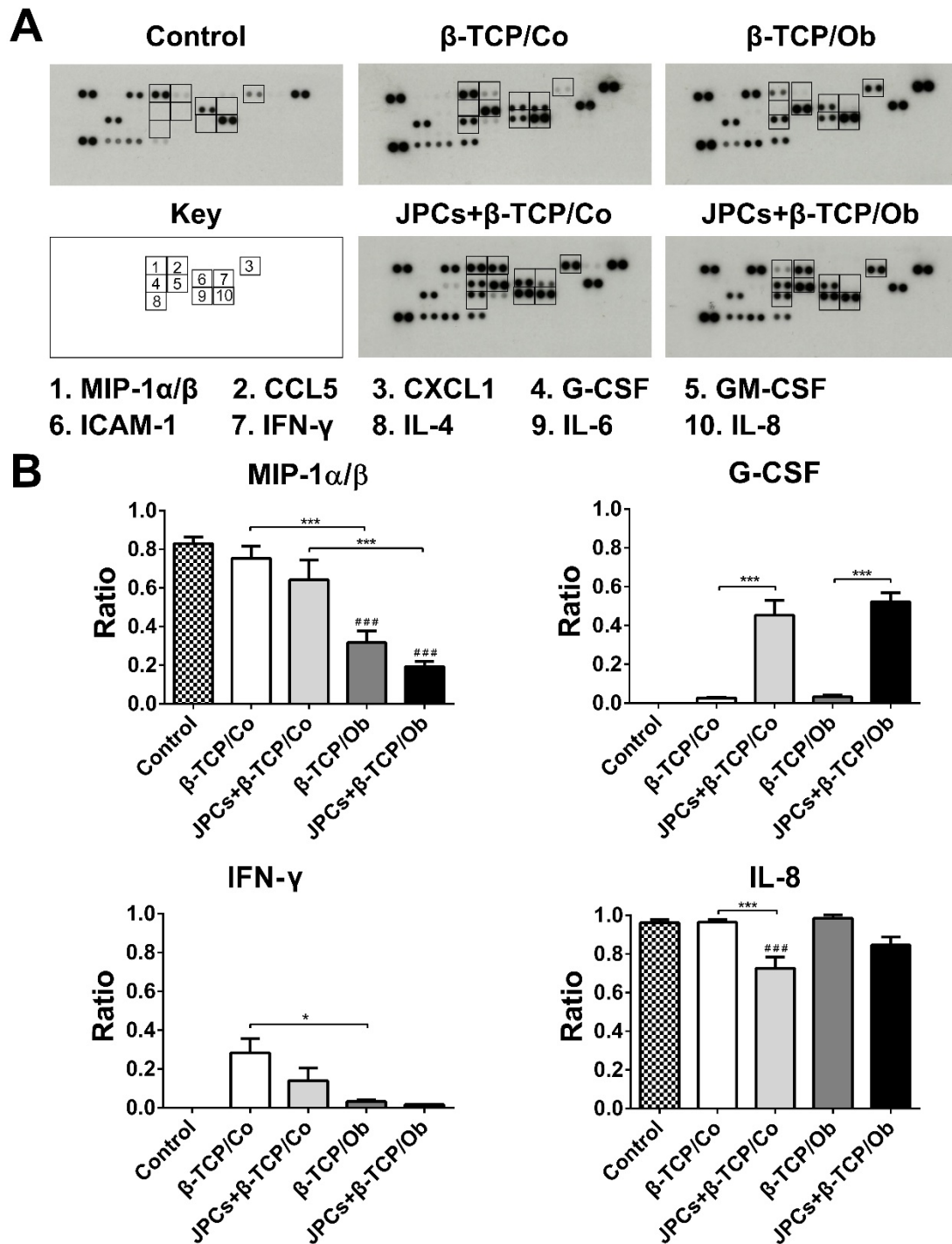
**Figure 3.6.** Protein expression of macrophage inflammatory proteins-1α/β (MIP-1α/β), interferon-gamma (IFN-γ), interleukin-8 (IL-8), and granulocyte-colony stimulating factor (G-CSF) in supernatants from peripheral blood monocytes (PBMCs) (control) and differentiated DCs (for 7 days) cocultured with cell-free β-TCP and JPCs-seeded β-TCP constructs after their precultivation under Co and Ob conditions for initial 7 days (constructs were cultivated for 14 days in total). (A)

Representative images of proteome profiler arrays (Human Cytokine Array Kit) and (B) quantification analysis of the protein expression of the 4 marked proteins (MIP-1 α/β, G-CSF, IFN-γ, and IL-8) by ImageJ software. Data were collected from three independent experiments (* $p < 0.05$, *** $p < 0.001$; ### represents $p < 0.001$ when compared to the PBMCs control).

## 3.4. Discussion

For bone regeneration, an ideal bone substitute should safely biodegrade *in vivo* and should be replaced by new bone tissue at the same time. It has been shown that β-TCP is a promising biomaterial, showing a balance between scaffold degradation and new bone formation in physiological environments [95, 96]. Numerous studies have demonstrated that β-TCP possesses excellent biocompatibility and low immunogenicity [97, 98]. Despite of the abovementioned advantages, the β-TCP material shows low osteoinductive abilities. Our previous studies reported that biofunctionalized β-TCP scaffolds improved functions of the colonializing cells [19, 41]. Dendritic cells and macrophages are specialized antigen-presenting cells that initiate and orchestrate immune responses. In order to exclude rejection of our *in vitro* engineered constructs after implantation into the defect site, we decided to investigate the interactions between JPCs-seeded β-TCP scaffolds and DCs in the present study.

Dendritic cell maturation is mainly determined by stromal microenvironment [99, 100]. Human bone marrow-derived MSCs possess the ability to inhibit human monocytic-derived DC differentiation [101]. In our previous study, we could demonstrate that undifferentiated and osteogenically differentiated two-dimensionally cultivated JPCs are potentially capable of suppressing DC maturation in the coculture [94]. In the present study, three-dimensionally cultured JPCs within β-TCP scaffolds significantly decreased DC numbers during DC maturation, as shown in Figure 3.2 and Figure 3.3A. Additionally, Figure 3.3B shows that the ratio of suspension cells (corresponding to mature DCs) to adherent cells (corresponding to immature DCs) was significantly lower when DCs were cocultured with JPCs-seeded β-TCP constructs compared to that of monocultures of the respective media. Therefore, we can assume that a higher number of monocytes might differentiate into DCs in monocultures (in the presence of β-TCP constructs) than in cocultures with JPCs-seeded constructs. For our experiments, we used the "standard" cytokine cocktail to induce final DC maturation. A more specific cocktail containing IL-1β, TNF-α, IFN-α, IFN-γ, and

polyinosinic:polycytidylic acid can give rise to an α-type 1-polarized DC type expressing substantially higher levels of costimulatory molecules, as reported in several studies [102]. Since derived αDC1 cells display stronger immunostimulatory functions, we did not consider this aspect showing a limitation of our study.

Concerning the CD14 expression on differentiated DCs in the coculture with cell-free β-TCP scaffolds, we detected a significant decrease compared with the undifferentiated monocyte control, as shown in Figure 3.4. Notably, JPCs growing within β-TCP scaffolds could significantly upregulate CD14 expression compared to that in the presence of cell-free β-TCP constructs, under normal culture conditions, indicating that 3D-cultured JPCs inhibited monocytes differentiation into DCs. CD14 has been considered as a useful marker of monocytes. In addition, CD14+ monocytes in human peripheral blood play an important role in both innate and adaptive immunity. In that, CD14+ monocytes can recognize pathogens, do phagocytosis, and secrete cytokines, such as IL-1β, IL-10, and IL-6 [103]. Specifically, CD14+ monocytes can promote umbilical cord matrix stem cell-induced suppression of T cell proliferation probably through the IL-1β–PGE2 axis [104]. Our Figure 3.4 shows an increased expression of the markers CD83, CD209, and HLA-DR probably related to the osteogenic medium, especially by induction with the corticoid dexamethasone. Notably, a similar tendency was observed between the results of percentage of CD14-positive DCs (Table 3.1) and MFIs of HLA-DR expression (Figure 3.4). Hawrylowicz and coauthors reported in a previous work that dexamethasone can promote GM-CSF-induced HLA-DR antigen expression on monocytes [105]. In our experiment, DC differentiation cocktail contains IL-4, GM-CSF, and TNF-α, which can effectively upregulate CD83 of myeloid lineage cells as previously reported [106].

To further analyze the effects of JPCs, we investigated the gene expression of DCs cultured in the presence of β-TCP with or without cells. Figure 3.5 presents the overall inhibitory effects of JPCs-seeded β-TCP scaffolds on the gene expression of DCs. For the normal culture conditions, JPCs + β-TCP led to overall lower gene expression of IL-12p35, IL-12Rβ1, IL-12Rβ2, and the pro-inflammatory cytokine IFN-γ. We also detected

significantly higher anti-inflammatory cytokine expression of IL-4 and G-CSF, whereas osteogenic conditions led to decreased pro-inflammatory IL-8 and increased anti-inflammatory IL-10 transcript levels. These data indicated that JPCs-seeded β-TCP scaffolds not only inhibit pro-inflammatory cytokine expression but also induce anti-inflammatory cytokine expression. It is well known that IL-10 is a relevant inhibitor of the IL-12 secretion [61]. Previous studies demonstrated that mature DCs express specifically natural killer stimulatory factor or IL-12, which plays a key role in triggering T-helper 1 responses [62, 63]. In our experiments, we found significantly higher IL-10 and IL-12p40 but not IL-12p35 gene expression levels of DCs cultured in the presence of osteogenically induced JPCs-seeded β-TCP scaffolds. A previous study reported that galectin-1 secreted by MSCs inhibit the function of DCs through downregulation of mitogen-activated protein kinase (MAPK) signaling pathway, whereas high levels of IL-12 and IL-10 were detected in the supernatants [70]. As shown in Figure 3.7, we also detected high concentrations of galectin-1 and -3 in JPCs at the end of coculture with DCs, suggesting a similar underlaying mechanisms whereby we did not analyze the MAPK pathway. In addition, our results showed increased gene levels of the anti-inflammatory cytokine G-CSF in DCs cultured in the presence of JPCs-seeded β-TCP scaffolds under normal culture conditions (Figure 3.5). It is reported that G-CSF is considered as an activator of signal transducer and activator of transcription 3 (STAT3) [107]. Activation of the STAT3 pathway was shown to suppress antitumor immunity, specifically by the inhibition of DC differentiation [108, 109].

**A**



**B**
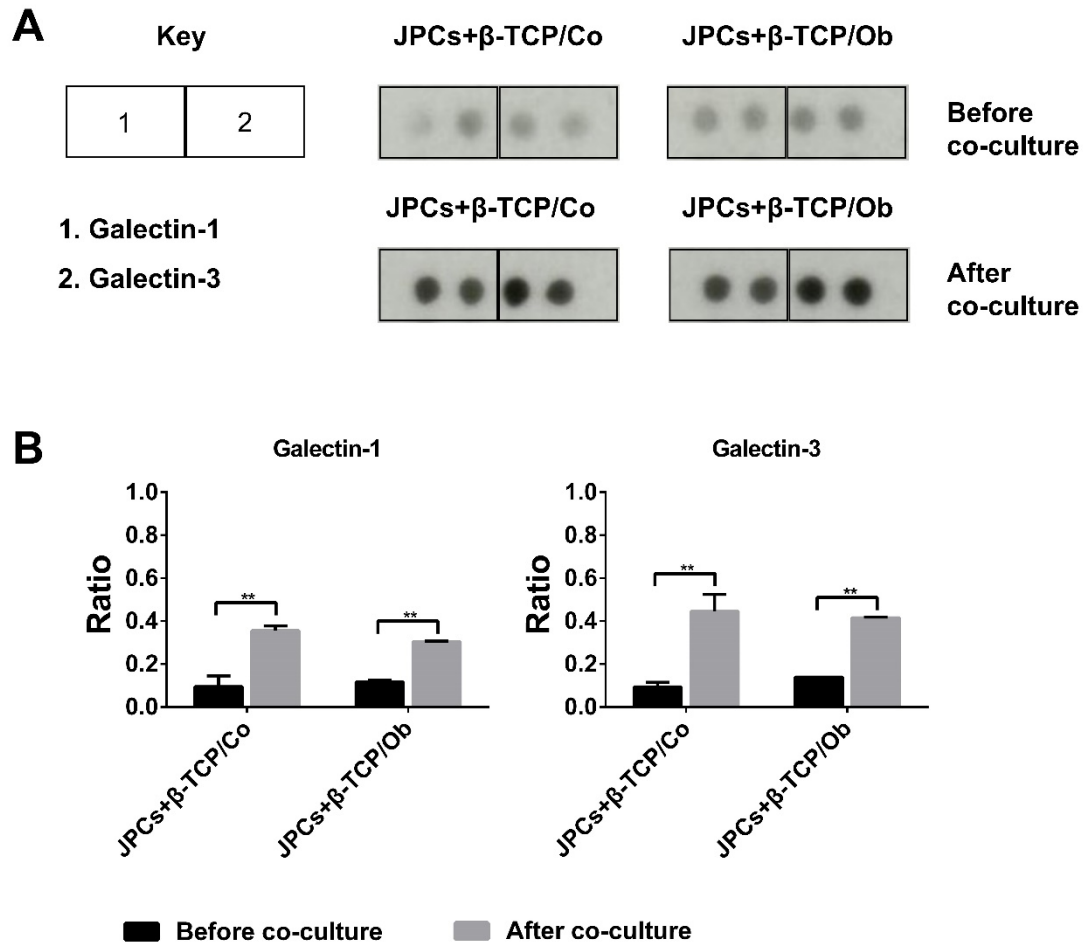


**Figure 3.7.** Protein expression of Galectin-1 and Galectin-3 in supernatants from JPCs cultured within β-TCP constructs before and after co-culture with DCs under Co (untreated) and Ob (osteogenic) conditions for 14 days (7 days monocultures followed by 7 days co-culture). (A) Representative images of proteome profiler arrays (human soluble receptor array kit); (B) Quantification analysis of the protein expression by ImageJ software. Data were collected from three independent experiments (**p < 0.01).

Effects triggered by the addition of osteogenic medium only, in the present study, have to be taken into consideration. We detected an overall suppression of IL-12p35, IL-12p40, both subunits of the IL-12 receptor, and pro-inflammatory cytokine IFN-γ as well as increased chemokine expression levels of MIP-1α/β and the anti-inflammatory cytokine IL-10 (Figure 3.5). These effects are probably caused by the presence of dexamethasone in the osteogenic medium. Xia and coauthors have proven that dexamethasone promotes the generation of IL-10-producing, immature DCs with little IL-12

production [110]. An additional important aspect is the influence of the DMEM medium in the absence or presence of osteogenic stimuli on the degradation behavior of β-TCP material. This could have an impact on the response of monocultured DCs. In our study, DCs cultured in the presence of β-TCP scaffolds under normal DMEM conditions revealed highest gene expression levels of IL-12 and its receptor subunits as well as highest IFN-γ transcript and protein levels. DCs cultivated in the presence of β-TCP scaffolds under osteogenic conditions showed highly reduced levels of the mentioned cytokines. Lange et al. previously reported that β-TCP particles increased the production of IL-1β, IL-8, TNF-α, and GM-CSF in DCs [111]. The comparison to our results is difficult, while in Lange's work DCs were generated only by the addition of GM-CSF for 5 days and the β-TCP material was added to the cells in form of a fine particle solution containing particles of a diameter of 0.1–150 μm for 24 h. Further, only RPMI medium was used. On the other hand, Dong et al. demonstrated that BMMSC-seeded β-TCP scaffolds slowed down the degradation of the β-TCP material under osteogenic medium [112]. This result is not unexpected, considering the fact that the scaffold surface is not in direct contact with the medium due to the cell layer covering the surface. However, β-TCP particles phenotypically and functionally stimulated DCs, including upregulated costimulatory molecules CD40, CD80, and CD86, and MHC class II and increased cytokines and chemokines M-CSF, CCL2, and CCL3 [113].

We further investigated cytokine protein production released by DCs. However, a limitation of our study is the lack of validation by other approaches such as ELISA or Western blot. As shown in Figure 3.6B, G-CSF expression, as an anti-inflammatory immunomodulatory factor, increased significantly by the coculture with JPCs under both culture conditions [114]. In studies examining phenotypical and functional characteristics of human MSCs, G-CSF release in MSC supernatants was almost undetectable [115-117]. Similarly, we detected low G-CSF concentrations in JPC supernatants when they were cultured under human platelet lysate (hPL) supplementation and normal unstimulated conditions (Figure 3.8). Therefore, we can assume that detected G-CSF protein levels in DC supernatants were released by DCs, and

not by cocultured JPCs. G-CSF was shown to decrease the expression of the costimulatory molecule CD86 and to inhibit TNF-α and IL-12 production by DCs [118, 119]. This mechanism could be also an explanation for IL-12p35 and IL-12p40 repression detected under osteogenic conditions in our study by gene expression analysis. Since IL-12p70 protein levels remained too low, we were not able to detect them by protein analysis. G-CSF as a potent hematopoietic factor can stimulate bone marrow production of granulocytes and hematopoietic stem cells (HSCs), mobilizing them into the bloodstream to replenish lymphoid and myeloid lineages [120, 121]. Therefore, G-CSF is used not only to accelerate the recovery of patients with neutropenia but also to increase HSC mobilization into the peripheral blood of the donor before isolation and transplantation of HSCs [120, 122]. Additionally, our results from proteome arrays show that in contrast to gene expression analysis, protein levels of the two closely related T cell chemoattractants, MIP-1α and MIP-1β, were significantly reduced under osteogenic culture conditions and, also to a higher extent, by JPCs-seeded constructs (Figure 3.6B). MIP-1α plays an important role in DCs migration into peripheral tissues [123]. Additionally, MIP-1α/β regulate T lymphocyte trafficking into lymph nodes during immune responses *in vivo* [124]. It is possible that the suppression of MIP-1α and MIP-1β secretion could be a part of the underlaying mechanism of immunomodulatory JPC functions under osteogenic culture conditions. We found that IFN-γ release showed a similar pattern as MIP-1α/β, and it was significantly suppressed by osteogenic conditions. This effect is probably mainly due to the presence of dexamethasone in the osteogenic medium, since this effect was also described for the human monocytic cell line (THP-1) [125].

**A** **Control**



**Ob+Dex**



**Ob-Dex**



**B**
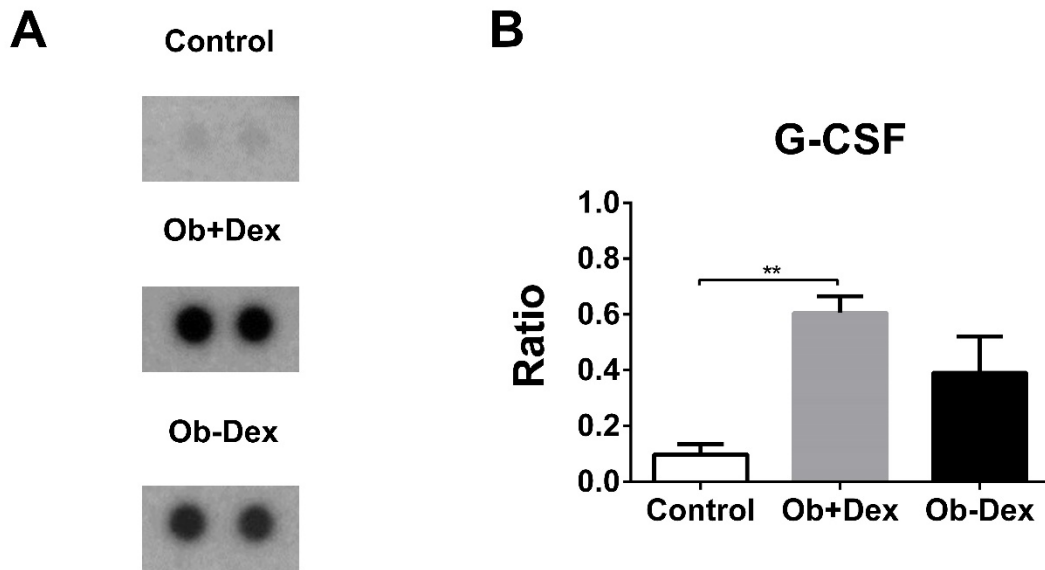


**Figure 3.8.** Protein expression of G-CSF in supernatants from JPCs (cultivation in the absence of DCs) cultured under human platelet lysate (hPL) supplementation and Co (untreated) and Ob (osteogenic) conditions for 15 days with or without dexamethasone. (A) Representative images of proteome profiler arrays (human cytokine array kit); (B) Quantification analysis of G-CSF protein expression by ImageJ software. Data were collected from three independent experiments ($**p < 0.01$).

## 3.5. Conclusions

In this study, we demonstrated that JPCs cultured within β-TCP scaffolds suppress monocyte-derived DC maturation *in vitro*. Our finding is based on detected lower cell densities and mature/immature DC ratios in the presence of JPCs-seeded β-TCP scaffolds, probably attributed to the overall inhibition of pro-inflammatory and induction of the anti-inflammatory cytokines such as IL-10 and G-CSF. Our findings lead to the speculation that JPCs represent a promising stem cell source for bone tissue regeneration. Nevertheless, the underlying mechanism for the suppressive effects of JPCs on DC differentiation should be further investigated.

## 4. Study III: Response of human periosteal cells to degradation products of zinc and its alloy

*The part is a reprint of the following manuscript:*

Ping Li, Jingtao Dai, Ernst Schweizer, Frank Rupp, Alexander Heiss, Andreas Richter, Ulrich E. Klotz, Jürgen Geis-Gerstorfer, Lutz Scheideler, Dorothea Alexander. Response of human periosteal cells to degradation products of zinc and its alloy. Materials Science and Engineering: C, 2020, 108: 110208. (Equally contributed first authors to this works).

**Abstract:**

Zinc (Zn) and its alloys are proposed as promising resorbable materials for osteosynthesis implants. Detailed studies should be undertaken to clarify their properties in terms of degradability, biocompatibility and osteoinductivity. Degradation products of Zn alloys might affect directly adjacent cellular and tissue responses. Periosteal stem cells are responsible for participating in intramembranous ossification during fracture healing. The present study aims at examining possible effects emanating from Zn or Zn-4Ag (wt%) alloy degradation products on cell viability and osteogenic differentiation of a human immortalized cranial periosteal cell line (TAg cells). Therefore, a modified extraction method was used to investigate the degradation behavior of Zn and Zn-4Ag alloys under cell culture conditions. Compared with pure Zn, Zn-4Ag alloy showed almost fourfold higher degradation rates under cell culture conditions, while the associated degradation products had no adverse effects on cell viability. Osteogenic induction of TAg cells revealed that high concentration extracts significantly reduced calcium deposition of TAg cells, while low concentration extracts enhanced calcium deposition, indicating a dose-dependent effect of Zn ions. Our results give evidence that the observed cytotoxicity effects were determined by the released degradation products of Zn and Zn-4Ag alloys, rather than by degradation rates calculated by weight loss. Extracellular Zn ion concentration was found to modulate osteogenic differentiation of TAg cells. These findings provide significant implications and guidance for the development of Zn-based alloys with an optimized degradation behavior for Zn-based osteosynthesis implants.

## 4.1. Introduction

Absorbable zinc (Zn) and its alloys have been considered as potential materials for osteosynthesis implants [126-130]. Indeed, Zn-based alloys can address main drawbacks of current osteosynthesis materials, such as non-degradability issues caused by bioinert implants [131], low strength of polymeric implants [132], and unsuitable degradation behavior of magnesium-based or iron-based implants [133]. Most notable is the fact that Zn-based materials possess biocompatible, biodegradable, osteoinductive and antibacterial properties [134-136]. The ionic zinc, as the main degradation product of Zn-containing chemical bonds or biomaterials, is one of the essential elements in the human body since it represents the metallic part of numerous proteins [135]. Moreover, the ionic zinc possesses superior osteoinduction and promotes new bone formation [137]. Nonetheless, pure Zn exhibits relatively low strength, insufficient for the most clinical requirements. By adding alloying elements, mainly including Mg, Cu, Ag, Ca, Sr, Al, Li and Mn, etc., to pure Zn mechanical strength can be enhanced substantially [128, 133].

Previous studies demonstrated that Zn-Ag alloys exhibit superior mechanical properties compared to those of pure Zn [138-141]. Increasing Ag content improved gradually the mechanical properties of Zn-Ag alloys, mainly due to the formation of ε-AgZn3 particles [140, 141]. The extensive localized corrosion of Zn-Ag alloys was observed when the alloying content reached 5 wt% and higher Ag, probably contributing to more pronounced micro-galvanic effects caused by the high-volume fraction of ε-AgZn3 [140]. Previously, we reported that Zn alloyed with 4 wt% Ag was characterized by excellent mechanical properties compared to those of most polymeric materials and pure Mg [128, 138]. It has been shown that Zn-Ag based stents implanted into porcine iliofemoral arteries showed excellent biocompatibility and constant degradation behavior [139]. Additionally, incorporation of Ag ions into implants is beneficial for antibacterial properties and does not interfere or even disturb the process of bone regeneration [137]. However, it is not trivial to investigate the correlation between the degradation behavior within specific physiological

environments and the impact of the resulting degradation products on biocompatibility.

As potential osteosynthesis materials, the degradation products of Zn and its alloys not only directly participate in the adjacent cellular reaction but affect bone tissue regeneration as well. In general, bone fracture healing consists of a complex series of physiological responses, and the exact mechanism of the respective cells mediating bone healing is still unknown [142]. Periosteal stem cells play an important role in callus formation and participate in intramembranous bone formation during the bone healing process [10, 11]. Compared to other skeletal stem cells, periosteal stem cells can directly form bone tissue via the intramembranous pathway, and are also capable to induce endochondral ossification after trauma [11]. For bone regeneration therapies in the oral and maxillofacial surgery, jaw periosteal cells could represent the most suitable stem cell source. In previous and present works, we characterized this cell type in detail and optimized culturing conditions to advance step by step towards clinical use [14, 15, 23, 94]. Notably, Zn-based alloys pins (Zn-1Mg, -1Ca, -1Sr) implanted into a non-fracture femora cavity induced new bone formation emanating from periosteum, indicating that zinc might induce periosteum-mediated new bone formation [143]. Although the osteoinductive properties of Zn ions and Zn-containing biomaterials have been reported previously, the effect of degradation products of Zn and its alloys on cellular response of periosteal osteoprogenitor cells remains obscure.

Biocompatibility of implant materials mainly depends on their degradation behavior in the body. Nevertheless, the suitability of current standardized *in vitro* cytocompatibility tests for absorbable metallic materials has been controversially discussed [144-146]. According to ISO 10993-5, a combination of direct contact- and extract tests is suggested to evaluate cell response. In previous studies, various cell types were used for cultivation on the initial dynamic interface of absorbable metals, such as Mg-based alloys [147, 148] and Zn-based alloys [143, 149]. Direct cultivation of cells on absorbable metals, however, might be hampered by the rapidly developing and partly shedding corrosion layers. Thus, extract tests are in some cases preferable

for an initial screening. In general, an extract test should investigate possible effects of degradation products of materials caused by the cell culture medium on cellular response [150, 151]. In most studies, performed tests cover only the initial degradation stage [151-153]. Previously, we reported about a developed extraction method which correlates between initial degradation behavior and cytotoxicity of Zn and its alloys. The results indicated that cytotoxicity of Zn and its alloys is influenced by released Zn ion concentrations [138, 150]. In fact, during the degradation process of Zn and its alloys, various Zn degradation products, soluble (i.e., $Zn^{2+}$ and $OH^{-}$) or complex insoluble products (i.e., zinc phosphate) are produced, synergistically participating to the physiological response *in vivo* [127, 129, 154]. Herein, the influence of the long-term degradation products of Zn and its alloys on cytocompatibility should be further investigated.

In our study, a modified extraction method was used to investigate the degradation behavior of pure Zn and Zn-4.0 wt% Ag alloy (Zn-4Ag) under cell culture conditions. The paper also focuses on the effect of associated degradation products on cellular function of human immortalized cranial periosteal cells (TAg cells). The use of TAg cells was chosen due to their genetic and phenotypic similarity to the primary cells from which they derive. The immortalized cells seem to possess a higher osteogenic capacity compared to the parental cells, as reported previously [155]. Thus, our study is a comprehensive investigation of (i) the *in vitro* degradation behavior of Zn and Zn-4Ag under cell culture conditions; (ii) the effects of associated degradation products on cell viability and osteogenic differentiation of TAg cells; (iii) the respective effects of pH and Zn ion concentrations on TAg cell response and (iv) the establishment of a modified extraction method to correlate *in vitro* long-term degradation behavior with the cellular response, offering a suitable screening method for the testing of absorbable Zn-based alloys.

## 4.2. Materials and Methods

4.2.1. Materials preparation

A Zn-4Ag (wt%) alloy was fabricated via conventional casting followed by a series of thermochemical treatments and pure Zn was prepared as a control, as described previously [138]. Subsequently, the ingots of Zn and Zn-4Ag were cut into 1.5 mm thick sheets. The as-produced pure Zn and Zn-4Ag sheets were cut into 23 mm × 8 mm × 1.5 mm in size. Prior to all tests, samples were ground with SiC abrasive paper up to grit 600 (CarbiMet P1200, Buehler, Germany), ultrasonically cleaned for 10 min in absolute ethanol, individually weighted with sensitivity of 0.1 mg, and immediately disinfected under ultraviolet radiation for 1 h each side (Lamin Air HB2472, Heraeus, Germany).

4.2.2. Experimental design

To correlate between *in vitro* degradation behavior and cytocompatibility, we modified an extraction method (as illustrated in Figure 4.1) based on previously established methods [138, 150, 156, 157]. In order to collect extract medium, Zn and Zn-4Ag sheets were incubated in pure Dulbecco's modified Eagle's medium/nutrient mixture F-12 (DMEM/F12; Life Technologies, Paisley, UK) for 28 days under continuous medium change. Every other day, extract medium was collected and added to TAg cells in different concentrations (100%, 50%, 25%, 10%, 5% and 2% extracts, respectively). Cytocompatibility was evaluated at different time points: cell metabolic activity at day 2, 6 and 12, gene expression pattern at day 14 and osteogenic potential at day 21 and 28. Additionally, Zn extracts were analyzed in terms of metallic ion concentration, pH values and insoluble products. At the end of the experiment (day 28), surface characterization after immersion test was analyzed and degradation rates were calculated by weight loss.
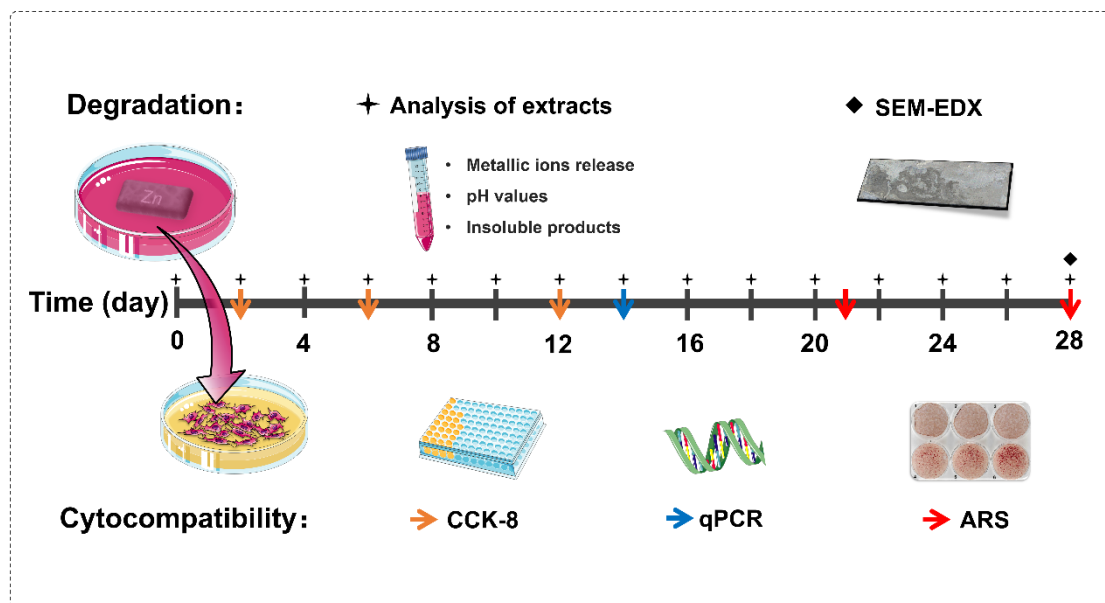
**Figure 4.1.** Draft of the experimental procedure with a time line (day) of performed experiments. Samples were incubated in DMEM/F-12 for 28 days. Sample media were exchanged every 48 h (plus signs) and the old ones were used for TAg cell cultivation at different concentrations. Extraction media were additionally used for the analysis of ion concentrations, pH values and the insoluble products. In order to visualize surface degradation of the samples, scanning electron microscopy (SEM) and element analysis (EDX) were performed at day 28. Cytocompatibility of Zn/Zn-4Ag alloys was assessed in terms of cell viability (cell counting kit-8 (CCK-8) at day 2, 6 and 12, orange arrows), gene expression (qPCR, at day 14, blue arrows) and osteogenic potential of TAg cells (Alizarin Red staining, ARS, at day 21 and 28, red arrows).

### 4.2.3. *In vitro* degradation test

All samples were immersed in pure DMEM/F12 and incubated under standard cell culture conditions (37 °C, 95% rel. humidity, 5% $CO_2$ and 20% $O_2$) for 28 days. The surface area to medium volume ratio was set to 1.25 $cm^2$/mL, according to ISO 10993-12: 2012 [158]. The media were refreshed every 48 h to simulate a semi-static immersion test. For analysis of sample extracts, pH values were recorded at each time point, and released metallic ion concentrations ($Zn^{2+}$ and $Ag^{2+}$) were detected by an inductively coupled plasma atomic emission spectroscopy (ICP-OES; Optima 4300DV, Germany).

To determine the insoluble products, the extracts at 28 days immersion were collected and centrifuged at 170 g for 5 min. The visible insoluble products were analyzed by using a scanning electron microscope (SEM) equipped with an energy dispersive X-ray (EDX) spectrometer at 10 kV (LEO 1430, Carl Zeiss GmbH, Germany). Additionally, phases of the corrosion products were identified by X-ray powder diffraction (XRD), using a diffractometer Bruker D8 Discover Da Vinci with Cu Kα radiation. Small amounts of the powdered samples were prepared on zero diffraction plate sample holders and measured with variable divergence slit to keep the sample area (6 mm), respectively the sample volume during the measurement constant. The measured reflections were compared with the Powder Diffraction File (PDF) database by the International Centre for Diffraction Data (ICDD).

At the end of the immersion period, the degradation products on the sample surfaces were removed by incubation in 250 g/L glycine ($NH_2CH_2COOH$) for 10 min, according to ISO 8407: 2009 [159]. Afterwards, the degradation rates were calculated by weight loss and expressed as µm/year, according to ASTM G31-12a [160]. Degradation rate (DR) was calculated as DR = $(8.76 \times 107 \times W) / (A \times D \times T)$, namely, W is the weight loss (g); A is the surface area ($cm^2$); D is the density ($g/cm^3$) and T is the immersion time (h). In addition, surface morphologies and chemical composition after immersion and removal of degradation products were analyzed by SEM-EDX.

### 4.2.4. Cytocompatibility test

### 4.2.4.1. Cell culture and extract preparation

A human SV40 T-antigen immortalized cranial periosteal cell line (TAg cells) as described previously was used for cytocompatibility evaluation [155]. TAg cells were cultured in complete DMEM/F-12 supplemented with 10% fetal bovine serum (FBS, Sigma-Aldrich, Germany), 1% penicillin/streptomycin (P/S, Lonza, Switzerland), 1% amphotericin B (Biochrom, Germany), 0.25 mg/mL immortalization maintenance dose of G418 (Biochrom, Germany). TAg cells were cultured in either normal (Co) or osteogenically induced conditions (Ob) throughout the experiments. Osteogenic medium of TAg cells contained

complete DMEM/F-12 medium supplemented with 100 μM L-ascorbic acid 2-phosphate, 4 μM dexamethasone and 10 mM β-glycerophosphate (Sigma-Aldrich, Germany).

To further correlate between degradation and cytocompatibility, the sample extracts collected every 48 h during the 28 days immersion time were used as cell culture media supplement in parallel, as described in section 4.2.3. Prior to transferring to cell culture, all extracts were further supplemented with 10% FBS, 1% P/S, 1% amphotericin B and 0.25 mg/mL G418-BC to adjust TAg cell culture conditions. For evaluation of the osteogenic potential, extracts were added to the normal and osteogenic medium, respectively. The original extracts under both conditions were diluted by the respective complete media to different concentrations (50%, 25%, 10%, 5% and 2% extracts, respectively).

### 4.2.4.2. Cell counting kit-8 assay

Cell counting kit-8 (CCK-8) assay was used to evaluate a potential inhibition of metabolic activities of TAg cells cultured under normal and osteogenic conditions containing sample extracts, according to ISO 10993-5: 2009 [161]. TAg cells were seeded in 96-well culture plates at a density of 3 × $10^3$ cells cm$^{-2}$. After 24 h, the medium was removed and replenished by gradient sample extracts containing normal and osteogenic medium, and respective normal and osteogenic media were used as the negative controls, respectively. After incubation for 2, 6, and 12 days, sample extracts were replaced by 100 μL fresh DMEM/F-12 and 10 μL CCK-8 reagent (Dojindo Laboratories, Japan) was added to each well. After incubation for 2 h, optical density was measured by a microplate reader (Tecan, Austria) at a wavelength of 450 nm and relative metabolic activities were calculated, as described before [150].

### 4.2.4.3. Alizarin red staining

TAg cells were seeded in 6-well culture plates at a density of 3 × $10^3$ cells cm$^{-2}$ and pre-cultivated overnight. TAg cells were induced osteogenically for 28 days in the presence of 48 h sample extracts. After osteogenic induction for 21 and 28 days, TAg cells were fixed with 4% formalin for 20 min. After

washing with DPBS, cell monolayers were stained with alizarin dye solution (40 mM, Sigma-Aldrich, Germany) for 20 min and washed 4 times with deionized water. A colorimetric assay was carried out to quantitate the calcium phosphate precipitates according to the instructions of the manufacturer (Osteogenesis Quantitation Kit, Merck Millipore, Germany). Briefly, Alizarin red dyes were dissolved from the monolayers over a period of 30 min by the addition of 10% acetic acid solution. The monolayers were detached from the well bottom by scraping. The samples were vortexed for 30 s and heated at 85 °C for 10 min, cooled on ice for 5 min, and then centrifuged at 20.000 g for 20 min. After neutralization of the supernatants by adding 10% ammonium hydroxide, quantification of calcium precipitates was performed using an ELx800 plate reader (BioTek Instruments GmbH, Germany) at a wavelength of 405 nm.

## 4.2.4.4. Gene expression analysis

RNA isolation from TAg cells was carried out at day 14 of osteogenic stimulation in the presence of Zn extracts, according to the manufacturer's instructions using the NucleoSpin RNA kit (Macherey-Nagel, Germany). The isolated RNA was photometrically measured and quantified (GE Healthcare, Germany). cDNA synthesis was performed using 200 ng of RNA and the SuperScript VILO kit (Invitrogen, USA), according to the manufacturer's instructions. The real-time LightCycler System (Roche Diagnostics, Germany) was used to quantify mRNA levels of Runt-related transcription factor-2 (RUNX2), alkaline phosphatase (ALP), osteocalcin (OCN) and the alpha-1 chain of type I collagen (COL1A1), respectively. The DNA Master Sybr Green 1 (Roche Diagnostics, Germany) and the commercial primer kits (Search LC, Germany) were used for 40 cycles of PCR amplification. Transcript levels of target genes were normalized to those of the housekeeping gene glyceraldehyde 3-phosphate dehydrogenase (GAPDH, Serach LC, Germany). Calculated ratios in control groups were set as 1 (control) and induction indices in relation to this control were calculated.

## 4.2.5. Effects of alkaline pH values and different Zn ion concentration on cell viability

To evaluate the effect of alkaline media conditions induced by Zn degradation on cell viability, TAg cells were seeded in 96-well culture plates at a density of $3 \times 10^3$ cells cm$^{-2}$ and pre-cultivated overnight. Subsequently, the medium was replaced by normal complete DMEM/F-12 (Co) and osteogenic complete medium DMEM/F-12 (Ob) of pH values intentionally adjusted to 8, 9, 10, 11 and 12, and the normal culture media as a negative control. After incubation for 24 h, the relative metabolic activities were determined by CCK-8 assay, as described above.

To identify which Zn ion concentration modulated cell viability and osteogenic differentiation of TAg cells, separate experiments evaluating the effects of different concentrations of extracellular Zn ions were carried out. The normal complete DMEM/F-12 (Co) and osteogenic complete DMEM/F-12 (Ob) were adjusted to the respective Zn ion concentration gradient (2-100 μM) using a ZnCl$_2$ solution (Sigma-Aldrich, Germany). Cell culture media without supplemented Zn solution was used as a negative control. TAg cells were seeded in 96-well plates at a density of $3 \times 10^3$ cells cm$^{-2}$ for 24 h. Subsequently, the medium was replaced by media containing various Zn ion concentrations and refreshed every other day. The relative cell metabolic activities were analyzed at day 2, 6, and 12, respectively, as described above. After initial testing of various Zn concentrations on cell vitalities, typical low (2 μM) and typical high (40 μM) Zn ion concentrations were further used to investigate a potential influence on the osteogenic differentiation of TAg cells. Mineral deposition and osteogenesis-related gene expression were analyzed using qPCR as described above.

### 4.2.6. Statistical analysis

All data were presented as mean and corresponding standard deviations. All assays were repeated at least three times to ensure reproducibility. Where applicable, all data sets were first analyzed concerning their normal distributions by the Shapiro-Wilk test. For comparisons between two groups, a Student's t-test was performed. Mann-Whitney U-tests were analyzed if normality tests failed. For comparisons of three or more groups, parametric data sets were analyzed by one-way analysis of variance (ANOVA), followed by Tukey's multiple comparisons test. Non-parametric data sets were

analyzed by the Kruskal-Wallis test followed by Dunn's multiple comparisons test. Statistical analyses were analyzed using GraphPad PRISM (vision 6.01, GraphPad Software, Inc., San Diego, US). A P-value < 0.05 was considered as statistically significant.

## 4.3. Results

### 4.3.1. *In vitro* degradation behavior of Zn and Zn-4Ag sheets

*In vitro* degradation behavior was evaluated in DMEM/F-12 under cell culture conditions for 28 days. The degradation rates of Zn and Zn-4Ag alloy calculated by weight loss were 4.80 ± 0.82 μm/year and 17.38 ± 0.78 μm/year, respectively. A Student's t-test was used to confirm the statistically significant difference between both groups (p < 0.001). As already macroscopically visible, all samples showed after the respective immersion period a dark blackish surface without obvious bulk degradation products. Furthermore, the surface morphology and chemical composition of Zn and Zn-4Ag sheets after immersion for 28 days are shown in Figure 4.2. The degradation precipitations dispersed on sample surfaces are visible under two different magnifications. Compared with Zn-4Ag surfaces, less structures of white appearance were formed on Zn surfaces. SEM images at higher magnification showed that some tiny degradation particles were distributed on the surfaces but no obvious thick degradation layers covering the whole surfaces were visible. As shown in Figure 4.2e, EDX analysis indicated that Zn, C, O and P were identified as elemental composition of degradation products on the surfaces. Additionally, Figure 4.3 illustrates sample surfaces after removal of the degradation products. The surfaces of Zn and Zn-4Ag showed a relatively uniform degradation morphology, without extensive localized corrosion spots.
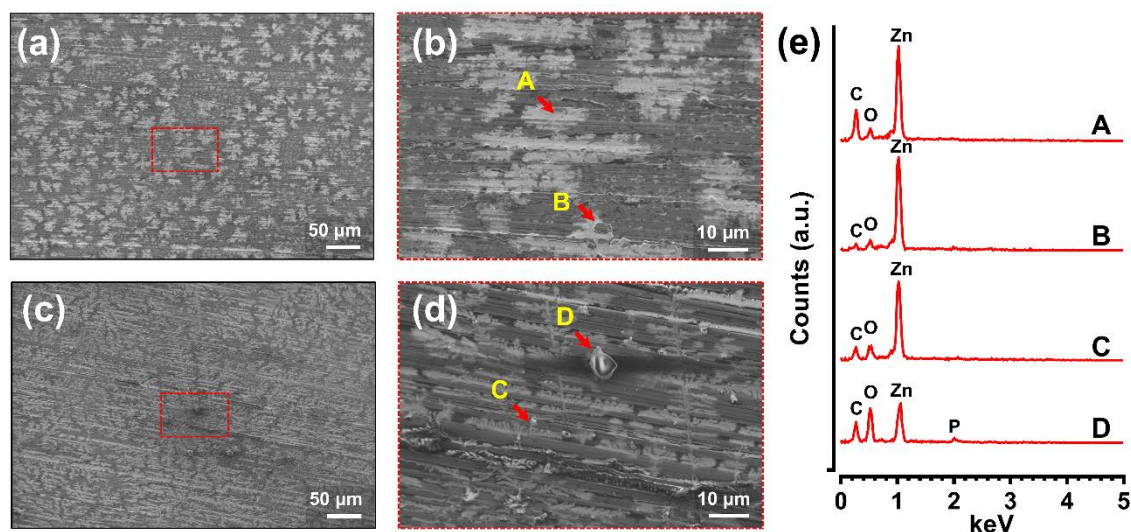


**Figure 4.2.** Representative SEM-EDX analysis of samples after

immersion in DMEM/F-12 for 28 days. SEM images showing (a,b) pure Zn and (c,d) Zn-4Ag alloy. The spots highlighted as red rectangles are shown in a higher magnification in b and d. (e) Representative EDX results from spots arrowed with yellow letters A/B and C/D in (b) and (d).
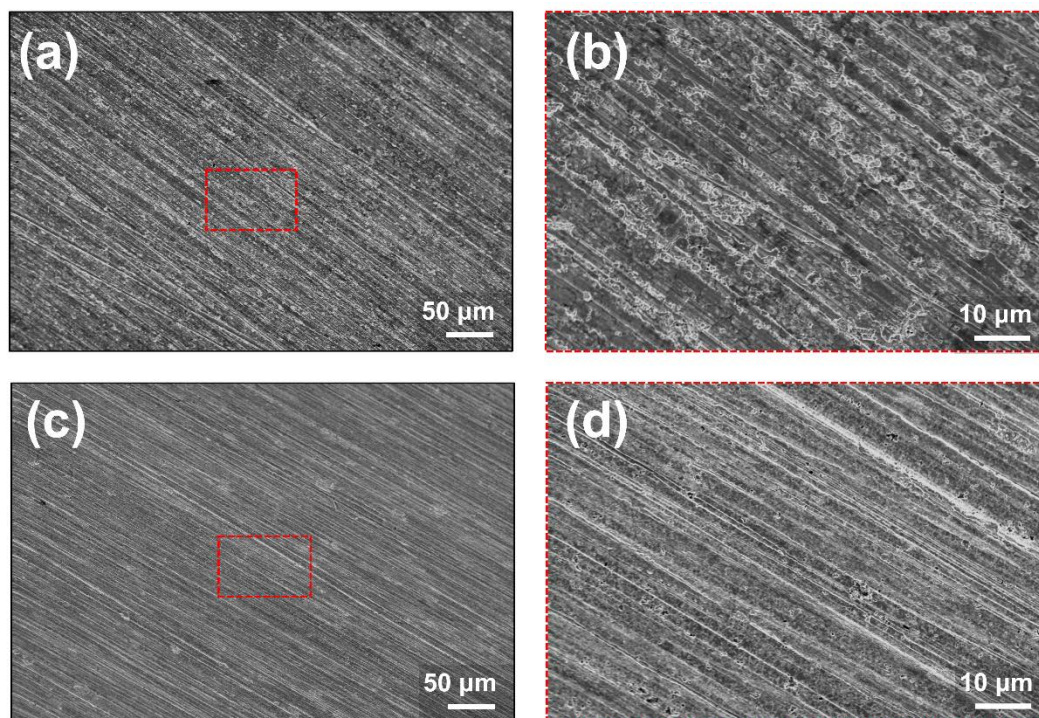


**Figure 4.3.** Representative SEM images of pure Zn and Zn-4Ag alloy after removal of degradation products. SEM images showing (a,b) pure Zn and (c,d) Zn-4Ag alloy. The red rectangles correspond to the magnified degradation morphologies of (b) pure Zn and (d) Zn-4Ag alloy.

4.3.2. Analysis of sample extracts during the 28-day period of immersion

Figure 4.4 shows the metallic ion release of pure Zn and Zn-4Ag alloy in DMEM/F-12 as well as the pH values of the respective extracts for the 28 day-period of immersion. According to ICP-OES measurements, only Zn ions released from the Zn-4Ag sheets could be detected in DMEM/F-12. Released Ag ion concentrations were shown to be under the detection limit (< 50 µg/L). At all analyzed time points, the mean Zn ion release from samples was below 6.5 µg/mL (approximately 100 µM). The tendency of Zn ion release was generally consistent between pure Zn and Zn-4Ag alloy (Figure 4.4a). The

cumulative Zn ion release amount of pure Zn (81.7 ± 1.87 µg/mL) was slightly, but significantly higher than that of Zn-4Ag (79.1 ± 0.99 µg/mL) for the 28 day-period of immersion (p = 0.015), independent of degradation rates calculated by weight loss. The evolution of pH values during immersion is illustrated in Figure 4.4b. Pure Zn and Zn-4Ag showed a similar trend of pH changes during immersion in DMEM/F-12. A rapid increase in pH values was detected at initial time points, thereafter constantly decreasing pH values were measured. All mean pH values measured were in the range from 8.4 to 8.9, so all pH changes were below 0.8 compared to the respective initial values. At the end of the 28-day period, mean pH values of 8.42 and of 8.47 were measured for Zn-4Ag and Zn sheets respectively.
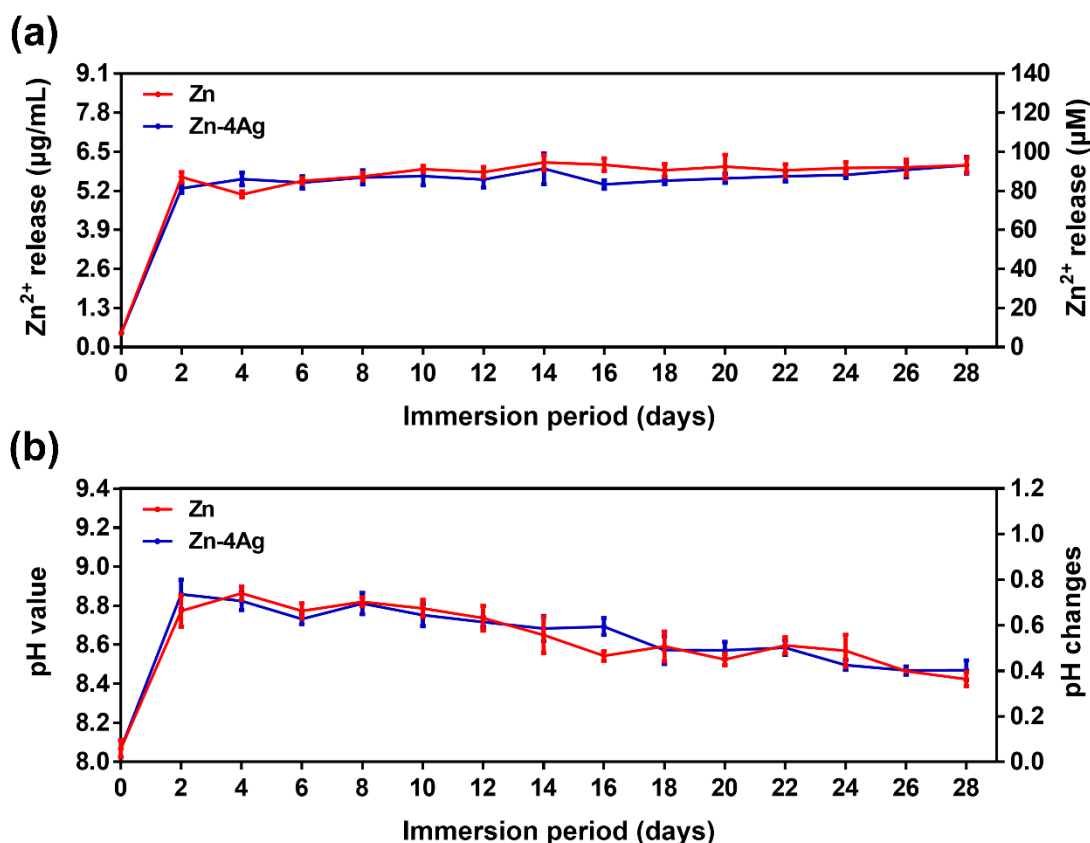


**Figure 4.4.** Analysis of sample extracts during the 28 day-period of immersion. (a) Zn ion release (µg/mL and µM respectively) of pure Zn and Zn-4Ag in DMEM/F-12. (b) Evaluation of pH values.

To further analyze the degradation products, the solid degradation particles in the extracts were analyzed by SEM-EDX. As shown in Figure 4.5a, a precipitation of insoluble degradation granules could be observed in Zn-4Ag extracts only after centrifugation. The SEM image shows that crystal-like

degradation granules are visible (Figure 4.5b). The corresponding EDX spectrum revealed that the degradation granules of Zn-4Ag were mainly composed of Zn, O, C and Cl (Figure 4.5c) All investigated degradation products showed similar diffraction patterns. A representative sample of obtained diffraction pattern is shown in Figure 4.5d. It was detected that the crystalline phases are consisting of zinc carbonate hydroxide $Zn_5(CO_3)_2(OH)_6$, hydrozincite (ICDD-PDF 72-1100), sodium chloride NaCl (IDDD-PDF 05-0628) and zinc carbonate hydroxide hydrate $Zn_4(CO_3)(OH)_6 \cdot H_2O$ (ICDD-PDF 11-0287), respectively.
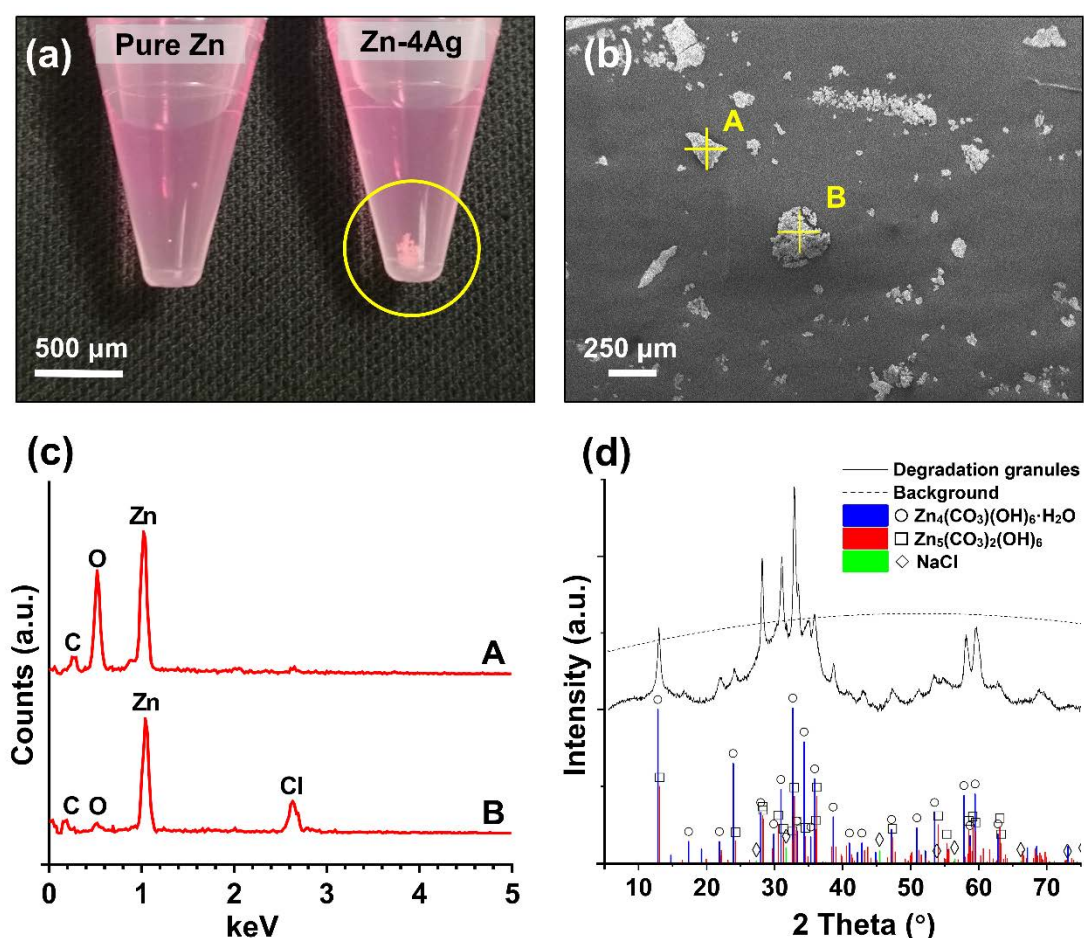


**Figure 4.5.** Analysis of degradation granules in Zn and Zn-4Ag alloys extracts after a 28 day-period of immersion. (a) Formation of degradation granules in Zn-4Ag extracts (indicated by the yellow circle) in comparison to plain Zn extracts, both after centrifugation. (b) Representative SEM image of insoluble degradation granules from Zn-4Ag extracts, marked with yellow letters. (c) The EDX spectrum indicates the elemental composition of spots marked with yellow

letters in b. (d) XRD pattern of representative insoluble degradation granules.

## 4.3.3. Examination of TAg cell functions after exposure to Zn and Zn-4Ag extracts

Figure 4.6 shows the relative metabolic activity of TAg cells after exposure to various concentrations of Zn and Zn-4Ag extracts under normal and osteogenic conditions for 12 days. An inhibition of cell metabolic activity below 70%, compared to the negative control, was regarded as a cytotoxic effect, according to ISO 10993-5: 2009 [42]. Herein, TAg cells exposed to Zn or Zn-4Ag extracts exhibited relative metabolic activities above 70%, indicating that no cytotoxic effects are emanating from Zn extracts in all concentrations tested. In contrast, in the presence of low concentrated Zn-4Ag extracts (i.e., 25%, 10% and 5%), a significant increase in metabolic activities of TAg cells under normal and osteogenic conditions was observed at day 2 compared to the controls ($p < 0.05$). With increased culture time, there were no significant increases or decreases in metabolic activities of TAg cells, independent of various Zn extract concentrations at day 12 ($p > 0.05$). Notably, significant differences were detected only in TAg cells cultured in the presence of Zn-4Ag extracts.
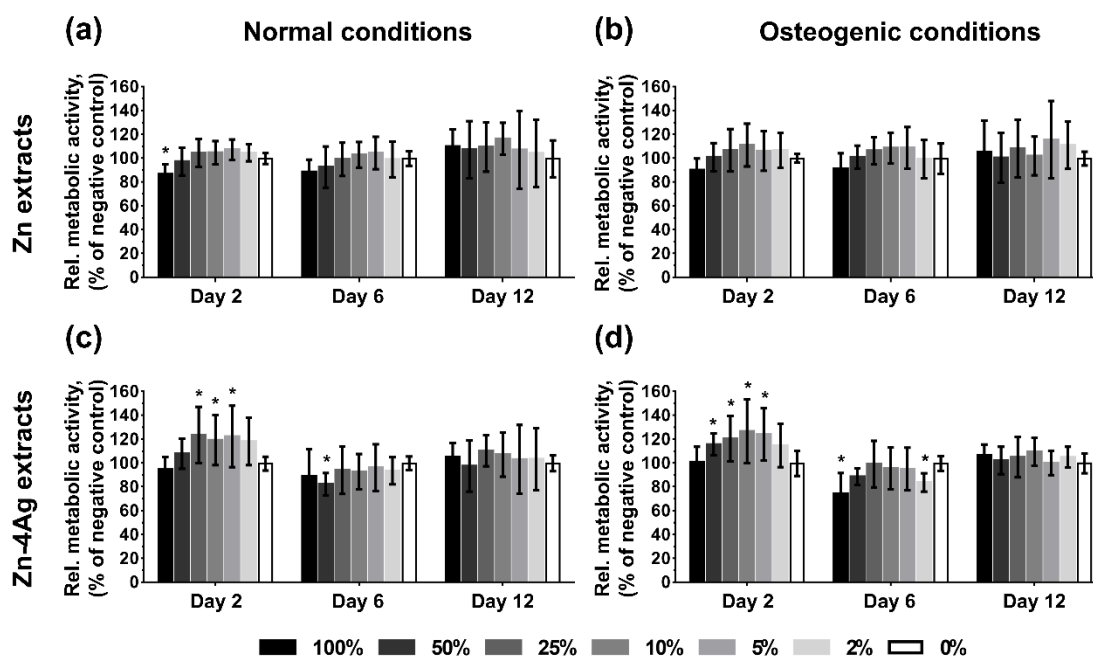


**Figure 4.6.** Relative metabolic activities of TAg cells cultured in the presence of Zn and Zn-4Ag extracts for up to 12 days, determined by

CCK-8 assay. (a, b) cell vitalities in the presence of pure Zn extracts of various concentration, (c,d) cell vitalities in the presence of Zn-4Ag extracts of various concentration under normal conditions (a, c) and under osteogenic conditions (b, d). The DMEM/F-12 complete media (normal and osteogenic) were considered as the negative controls and set to 100%. * represent $p < 0.05$ when compared to the negative control.

For the analysis of a potential influence of Zn/Zn-4Ag extracts on osteogenic differentiation of TAg cells, one typical low (2%) and one typical high (50%) concentration of sample extracts was used. Figure 4.7a displays Alizarin red staining of TAg cells cultured in the presence of sample extracts in order to evaluate their osteogenic potential. Only weak Alizarin red staining was observed in TAg cell monolayers treated with 50% of sample extracts at day 21 and 28. In contrast, TAg cells cultivated in the presence of low concentrated (2%) sample extracts exhibited much stronger Alizarin red staining, indicating pronounced formation of calcium phosphate nodules (Figure 4.7b). For quantification of TAg cell mineralization, the ratio of Ca concentration in the extract-treated cultures was related to that determined in the control (TAg cells cultivated in the absence of Zn extracts) as illustrated in Figure 4.7c and d. Significance tests were calculated by comparing Ca ratios of osteogenically induced TAg cells in the presence of extracts with those of cells in the absence of sample extracts. The Kruskal-Wallis test showed significant differences at day 21. Dunn's multiple comparisons tests showed significantly higher Ca concentrations in the osteogenic control (ratio of 2.39 ± 0.44) compared with those cells cultivated in the presence of 50% Zn extracts (ratio of 1.13 ± 0.58; $p < 0.001$) and 50% Zn-4Ag extracts (0.77 ± 0.27; $p < 0.001$). Nevertheless, no significant differences were detected when comparing the Ca ratio of osteogenic control (without Zn extracts) with those from cells cultivated in the presence of 2% Zn (ratio of 2.10 ± 0.29; $p > 0.05$) or 2% Zn-4Ag extracts (ratio of 1.96 ± 0.91; $p > 0.05$), respectively. By comparing Ca ratios in TAg cells cultivated under 2% and 50 % of sample extracts, significant differences were obtained ($p < 0.05$). In addition, ANOVA was used to confirm statistically significant differences of Ca ratios at day 28.

Notably, post hoc pairwise comparisons showed significantly higher Ca concentrations in TAg cells cultivated in the presence of 2% Zn-4Ag (ratio of 3.23 ± 0.77) and 2% Zn (ratio of 2.63 ± 0.65) extracts compared with those of osteogenic control (ratio of 1.59 ± 0.23). Similarly, as already shown for Ca quantification after 21 days, significantly higher Ca ratios in TAg cells cultivated in the presence of 2% sample extracts were detected compared to cells cultured in the presence of 50% sample extracts, respectively.
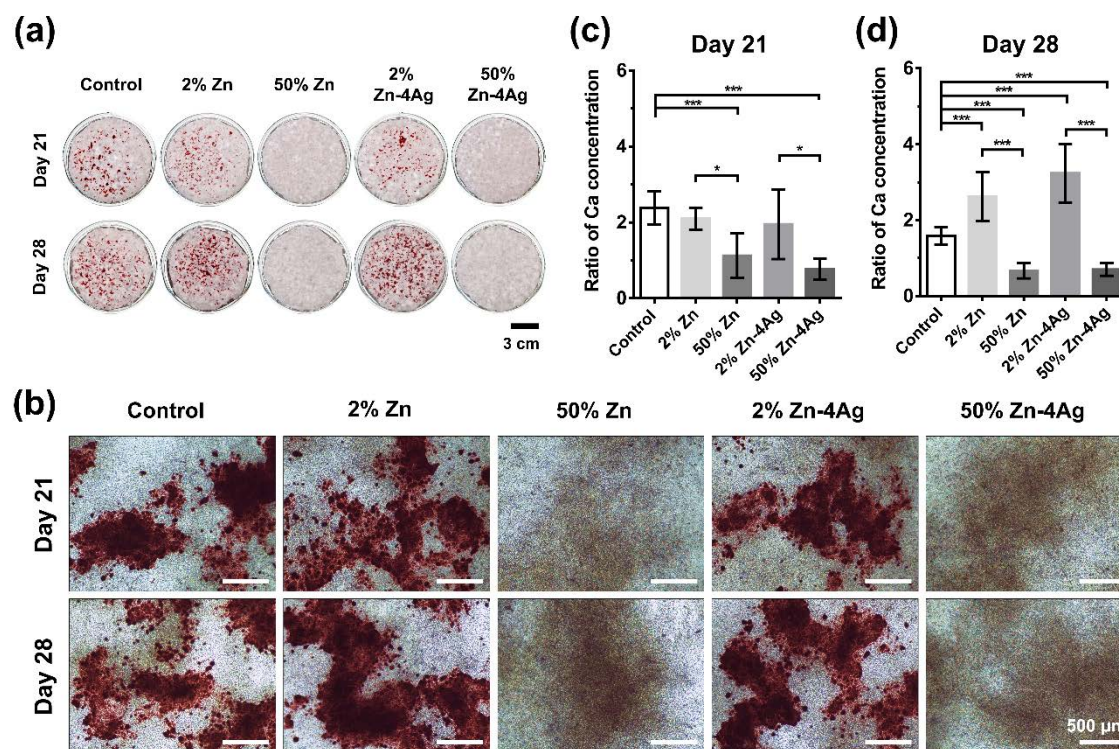


**Figure 4.7.** Detection of TAg cell mineralization exposed to Zn and Zn-4Ag extracts. (a) Alizarin red staining of TAg cells cultured in the presence of sample extracts under osteogenic conditions for 21 and 28 days. (b) Representative microscopic images of differentiated TAg cells cultured in the presence of sample extracts for 21 and 28 days (magnification 4×; scale bar = 500 μm). Quantification of calcium precipitates is shown at day 21 (c) and day 28 (d). The ratio of Ca concentration (osteogenic/normal culture condition) was quantitatively analyzed by dissolving the Alizarin dye from TAg cell monolayers. Statistical differences were calculated compared to the osteogenic control without extracts. * p < 0.05, *** p < 0.001.

Figure 4.8 shows gene expression levels of RUNX2, ALP, OCN and COL1A1 in osteogenically induced TAg cells at day 14 of immersion with or without Zn extracts. Statistically significant differences of COL1A1 expression were confirmed by ANOVA. Post hoc pairwise comparisons showed a significantly lower COL1A1 expression in osteogenically induced TAg cells in the presence of 50% Zn-4Ag ($p < 0.05$) and 50% Zn ($p < 0.05$) extracts compared to the osteogenic control (without extracts). By comparing COL1A1 expression in cells cultivated in the presence of 2% Zn ($1.03 \pm 0.14$) and 2% Zn-4Ag ($1.08 \pm 0.15$) extracts to that in cells cultured in the presence of 50% extracts of Zn ($0.59 \pm 0.11$, $p < 0.05$) and Zn-4Ag ($0.52 \pm 0.11$, $p = 0.014$), significant differences were obtained. In addition, RUNX2, ALP and OCN expression was shown to be significantly decreased in TAg cells cultured in the presence of 50% Zn and for ALP also in the presence of 50% Zn-4Ag extracts ($p < 0.05$). Herein, the above results coincide with the result that high concentrations of Zn and Zn-4Ag extracts (50%) significantly reduced calcium deposition of TAg cells.
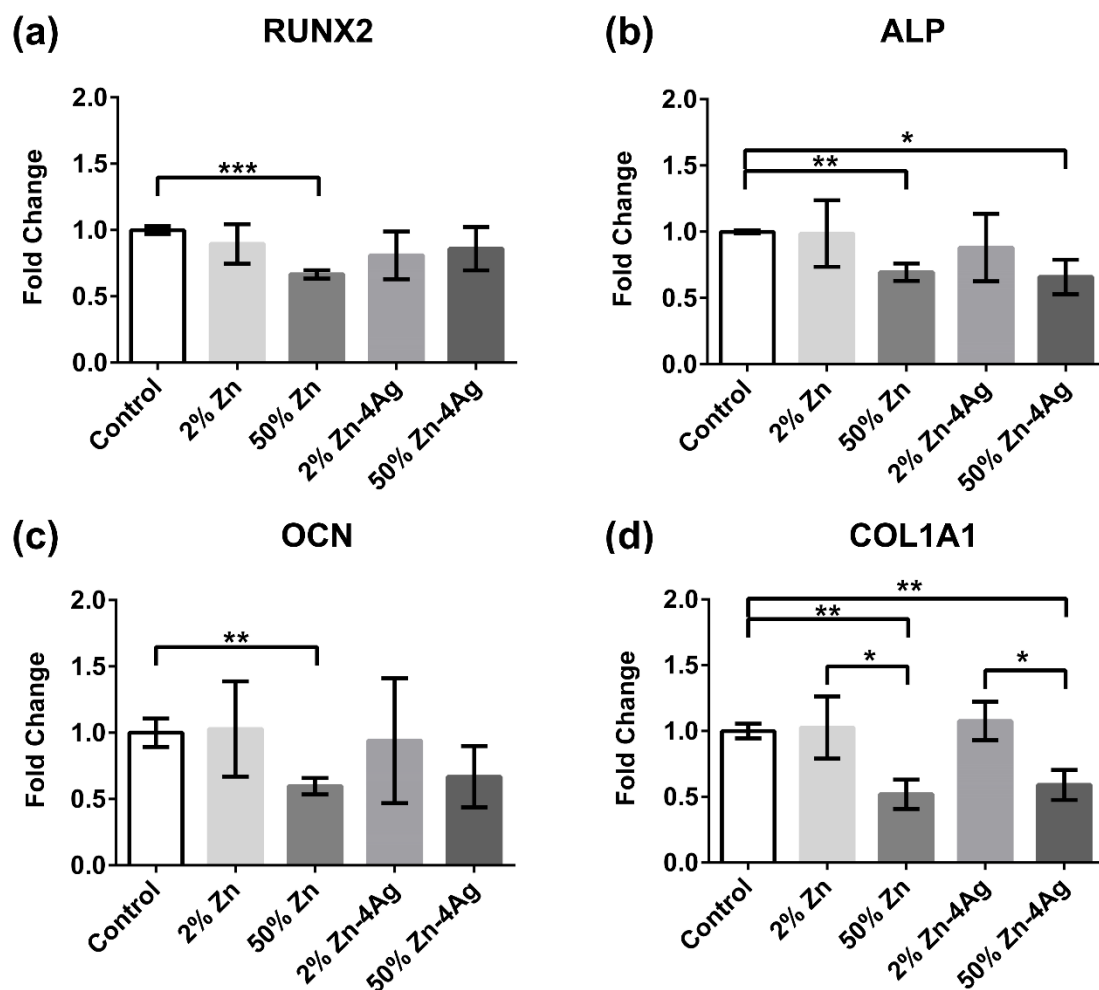
**Figure 4.8.** Quantitative gene expression of osteogenically induced TAg cells exposed to sample extracts for 14 days. Gene levels of osteogenically induced TAg cells in the absence of Zn extracts were set as 1 and induction indices in relation to this control were calculated. Relative expression of (a) Runt-related transcription factor-2 (RUNX2), (b) Alkaline phosphatase (ALP), (c) Osteocalcin (OCN) and (d) Alpha-1 chain of type I collagen (COL1A1) are illustrated. * $p < 0.05$, ** $p < 0.01$ and *** $p < 0.001$.

## 4.3.4. Effects of different pH values and Zn ion concentrations on TAg cell viability

Figure 4.9 shows the results of the relative metabolic activities of TAg cells after 24 h incubation with the normal and osteogenic media adjusted to different pH values. For pH values below 9, no impact on TAg cell viabilities was detected ($p > 0.05$). In contrast, when pH values reached 10, for both media conditions the relative metabolic cell activities were significantly

decreased compared to the control ($p < 0.05$).
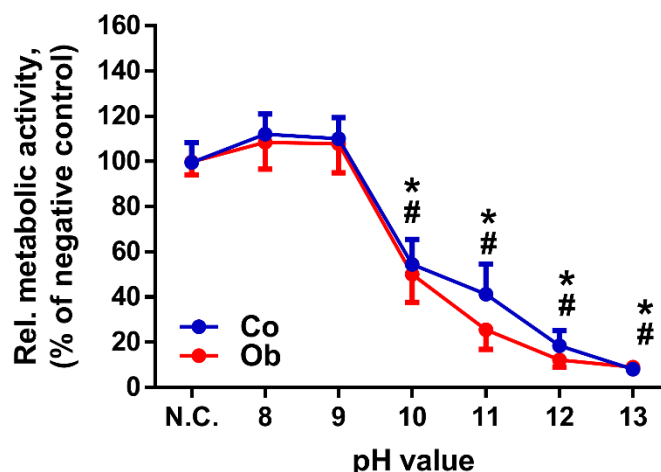


**Figure 4.9.** Relative metabolic activities of TAg cells after a 24 h incubation period in normal and osteogenic media of various alkaline pH values. The original media were used as negative controls (N.C.). Undifferentiated TAg cells were denoted as Co, and osteogenically induced cells as Ob. * and # represent $p < 0.05$ when compared to the respective negative controls cultured under normal and osteogenic medium, respectively.

In Figure 4.10, metabolic activities of TAg cells are plotted as a function of Zn ion concentration (2-100 µM) under normal and osteogenic conditions. At day 2 of incubation (Fig. 9a), low Zn ion concentrations (5-20 µM) significantly increased relative metabolic activities of TAg cells ($p < 0.05$) under both culture conditions. Zinc concentrations of 40-60 µM led to significantly higher cell activities only under normal conditions. If a Zn concentration of 100 µM was chosen, for both media conditions cell activities were significantly decreased compared to the control ($p < 0.05$). At day 6 of incubation, only Zn concentrations of 40 µM under normal conditions increased metabolic activity. At day 12 of incubation, TAg cell viabilities were almost comparable under normal and osteogenic conditions ($p > 0.05$). As already observed for day 2 and 6, Zn concentrations of 100 µM showed clearly cytotoxic effects.
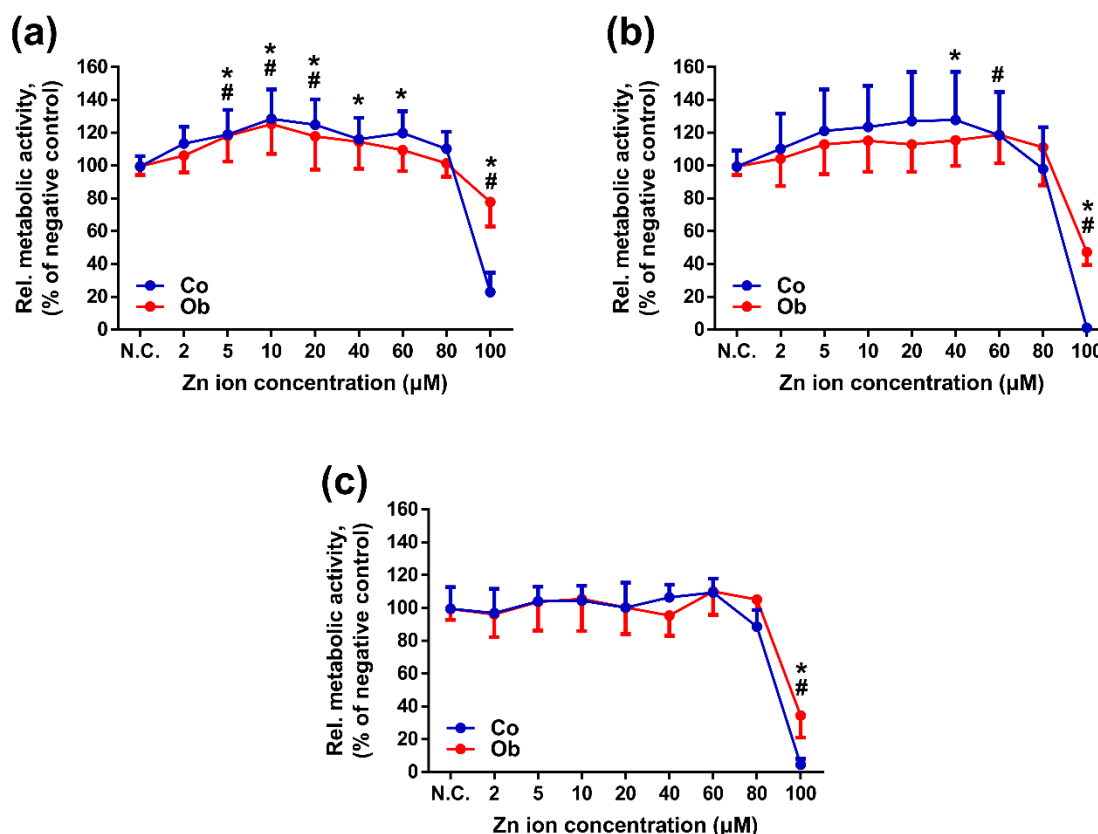
**Figure 4.10.** Relative metabolic activities of TAg cells treated with different Zn ion concentrations determined by CCK-8 assay. (a) 2 days of incubation, (b) 6 days of incubation and (c) 12 days of incubation. The original media served as negative controls (N.C.). * and # represent p < 0.05 when compared to the respective negative controls cultured under normal and osteogenic medium, respectively. Undifferentiated TAg cells were denoted as Co, and osteogenically induced cells as Ob.

To identify whether Zn ions in the medium influence the osteogenic differentiation of TAg cells, one typical low (2 µM) and one typical high (40 µM) Zn ion concentration were used. As shown in Figure 4.11a, the effect of Zn ion concentration on osteogenic differentiation was assessed by Alizarin red staining. A Zn concentration of 2 µM led to a clearly stronger Alizarin red staining compared to the staining of TAg monolayers which were incubated constantly with 40 µM Zn ions for 21 and 28 days. Almost no staining was observed at this Zn concentration. After 28 days, TAg cells cultured in 2 µM Zn ion media showed significantly higher Ca concentration than those in control and 40 µM Zn ion media (p < 0.001). In addition, TAg cells cultured in

2 µM Zn ion was statistically higher mineralization than that in control media at day 28 (p < 0.001).

**(a)**



**(b)**
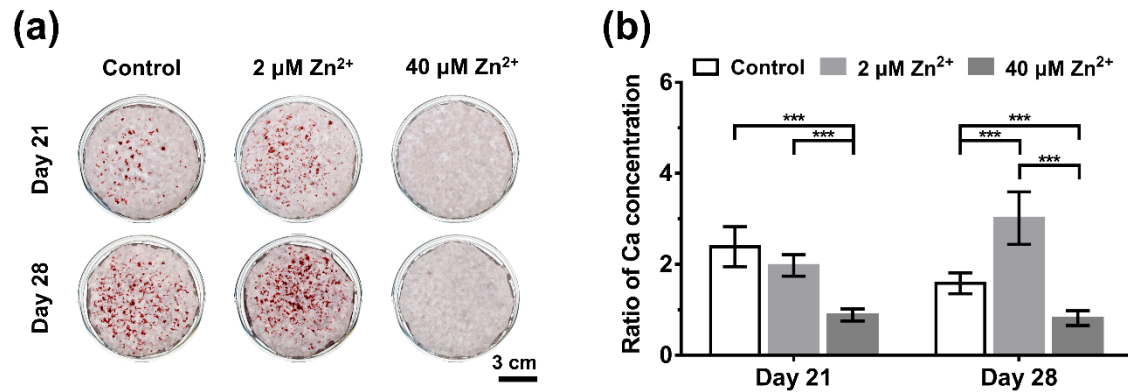
**Figure 4.11.** Mineralization of TAg cells treated with 2 µM and 40 µM Zn ion concentration. (a) Alizarin red staining of TAg cells under osteogenic conditions for 21 and 28 days. (b) Quantification of calcium precipitates after osteogenic induction for 21 and 28 days. The ratio of Ca concentration (osteogenically induced: untreated cells) was quantitatively analyzed by dissolving the Alizarin dye from cell monolayers, *** p < 0.001.

## 4.4. Discussion

4.4.1. *In vitro* assays for testing of absorbable metals for implants

The ideal *in vitro* tests should simulate *in vivo* conditions to the utmost, in order to accurately predict the *in vivo* performance of implants. To date, *in vitro* assays for the evaluation of degradation behavior and cytocompatibility of absorbable metals have been controversially discussed, since both aspects were considered independently [133, 162, 163]. To overcome this shortcoming, the aim of our work was to develop a modified test design in order to be able to consider and analyze *in vitro* degradation behavior and cytocompatibility at the same time.

The aspect of the *in vitro* degradation behavior under cell culture conditions was performed based on previously published methods [164, 165]. It has been shown that the composition of cell culture medium is close to that of human extracellular fluids [164-166]. Additionally, DMEM was recommended as appropriate fluid to obtain a comparable *in vivo* degradation behavior of Zn [167]. Herein, DMEM/F-12 has been selected, whose main constituents were compared with human extracellular fluids (Table 4.1). Previous studies on the degradation behavior of Mg alloys under cell culture conditions (37 °C, 95% rel. humidity, 5% $CO_2$ and 20% $O_2$) reported on comparable conditions to physiological environments [163, 168]. The main reason was attributed to the fact that the bicarbonate buffer system in the medium requires triggering by active $CO_2$, regulating pH values of the degradation medium, which is similar to the physiological conditions [169].

**Table 4.1.** Main composition of human extracellular fluids and the used medium.

| | Human extracellular fluid | | |
|---|---|---|---|
| | Blood plasma [101, 125] | Interstitial fluid [125] | DMEM/F-12 [167] |
| Inorganic ions (mM) | | | |
| $Na^+$ | 142.0 | 139.0 | 150.6 |
| $K^+$ | 4.2 | 4.0 | 4.2 |
| $Mg^{2+}$ | 0.8 | 0.7 | 0.7 |
| $Ca^{2+}$ | 1.3 | 1.2 | 1.1 |

| | | | |
|---|---|---|---|
| Cl$^-$ | 106.0 | 108.0 | 126.1 |
| SO$_4^{2-}$ | 0.5 | 0.5 | 0.4 |
| HPO$_4^{2-}$ | 2.0 | 2.0 | 0.5 |
| HCO$_3^-$ | 24.0 | 28.3 | 29.0 |
| Organic components | | | |
| Protein | 1.2 (mM) | 0.2 (mM) | - |
| Glucose (mM) | 5.6 | 5.6 | 17.5 |
| Amino acids | 2.0 (mM) | 2.0 (mM) | 1.3 (g/L) |
| Concentrations of buffering agents (mM) | | | |
| HCO$_3^-$ | 24.0 | 28.3 | 29.0 |
| HPO$_4^{2-}$ | 2.0 | 2.0 | 0.5 |
| Tris-HCl | - | - | - |
| Human protein | 16.0-18.0 [101] | - | - |
| Total | 42.0-44.0 | 30.3 | 29.5 |

Standardized cytocompatibility evaluation tests for absorbable metals based on the ISO 10993-5 and -12 standards are not satisfactory based on the fact that they were developed for intentionally bioinert materials, neglecting the properties of absorbable materials [133, 151]. Attempts to improve the efficacy of *in vitro* evaluation methods for absorbable Mg-based and Zn-based metals, including the dilution of extracts [170, 171], the selection of extraction medium [150, 172], and the surface pretreatment [157, 173], have been reported. Considering the degradation properties of Zn and its alloys, various degradation products during long-term degradation process all participate in tissue healing *in vivo* [127, 129, 154]. Thus, in our test model, sample extracts were repeatedly collected during the degradation process and given to cultivated cells for cytocompatibility evaluation.

### 4.4.2. Degradation behavior under cell culture conditions

The *in vitro* degradation behavior of pure Zn and Zn-4Ag alloys in DMEM/F-12 was analyzed under common cell culture conditions. According to our results, the following degradation mechanism in DMEM/F-12 can be proposed. Immersion in DMEM/F-12 (slightly alkaline solutions, pH value: 8.06) leads to anodic and cathodic reactions as described by Eq (1) and Eq (2), respectively [133]. With the dissolution of Zn, a rapid increase in Zn ion concentration and pH value can be detected in DMEM/F-12 (Figure 4.4).

According to the Pourbaix diagram, Zn trends to be passivated in slightly alkaline solutions, while the chemical reactions as described in Eq (3) and Eq (4) take place. The accumulation of zincite (ZnO) and zinc hydroxide ($Zn(OH)_2$) on the surfaces tends to form the passivation layers [150, 167]. Figure 4.4 shows constantly decreasing pH values with immersion time probably related to the passivation layers formed on the surface and to the buffering effect of the DMEM/F-12 medium (Figure 4.4b). On the other hand, the released Zn ions can spontaneously react with phosphate ions and carbonate ions contained in DMEM/F-12 to form Zn phosphate ($Zn_3(PO_4)_2 \cdot 4H_2O$) and Zn carbonate ($ZnCO_3$) [133, 167]. According to our EDX analysis, we detected the elements Zn, O, C and P on sample surfaces, as expected (Figure 4.2e). Additionally, more degradation products were observed on Zn-4Ag surfaces compared with those on Zn surfaces (Figure 4.2a and c). This might be linked to higher degradation rates of Zn-4Ag resulting in higher amounts of degradation precipitates on their surface.

Anodic reaction: $Zn\ (s) \rightarrow Zn^{2+}\ (aq) + 2e^-$         (Eq1)

Cathodic reaction: $2H2O + O2 + 4e^- \rightarrow 4OH^-$       (Eq2)

$Zn(OH)2$ formation reaction: $Zn^{2+} + 2OH^- \rightarrow Zn(OH)2$    (Eq3)

ZnO formation reaction: $Zn^{2+} + 2OH^- \rightarrow ZnO + H2O$    (Eq4)
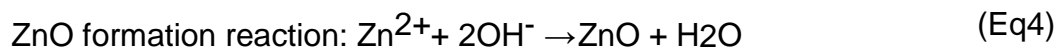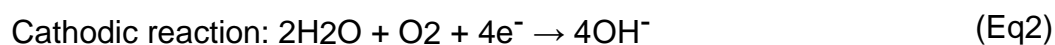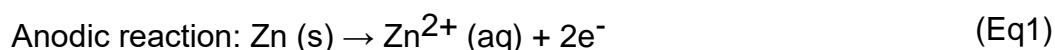
Generally, the formation of Zn degradation layers can retard the degradation process [133, 174]. However, no obvious decrease in Zn ion release could be detected by ICP-OES measurements (Figure 4.4a). It can be assumed that some organic components contained in DMEM/F-12 can interfere with the surface passivation, probably similar to the effect of protein adsorption on Zn surfaces [175]. Further on, more complex degradation products, such as hydrozincite ($Zn_5(CO_3)_2(OH)_6$) and simonkolleite ($Zn_5(OH)_8Cl_2 \cdot H_2O$) may be formed on the surfaces, as previously reported [133, 136]. The formed degradation layers can be dissolved by chloride ion attack and subsequently be transformed into zinc chloride salts. Regarding our results, the phases of the crystalline fraction of the degradation granules could be identified as zinc carbonate hydroxide $Zn_5(CO_3)_2(OH)_6$, hydrozincite (ICDD-PDF 72-1100) and a small amount of sodium chloride NaCl (IDDD-

PDF 05-0628), as shown in Figure 4.5d. Some reflections like the (311) of hydrozincite are missing, suggesting substitutions in the crystal structure with $H_2O$, $OH^-$ or $Cl^-$. Further, obtained diffraction pattern also matches zinc carbonate hydroxide hydrate $Zn_4(CO_3)(OH)_6 \cdot H_2O$ (ICDD-PDF 11-0287). The structure of zinc carbonate hydroxide hydrate has not been fully resolved and therefore is marked as a low-quality pattern in the ICDD database. A previous crystallographic investigation of Zn corrosion products encountered this problem as well [176]. Thus, we believe that the corrosion product is a mixture of both phases or the structure of hydrozincite is slightly modified, e.g. by substitution or attached water. The identified phase content corresponds to the elemental composition qualitatively assessed by EDX (Figure 4.5c). In addition, zinc carbonate hydroxide ($Zn_5(CO_3)_2(OH)_6$) is described as a typical corrosion product of zinc alloys under atmospheric conditions [177]. Simulations of *in vitro* corrosion of Zn alloys also suggested the formation of zinc carbonate hydroxide $Zn_5(CO_3)_2(OH)_6$ as a specific corrosion product [178]. The general reflection shape with a broad full width at half maximum indicates small crystallite sizes, i.e. a poor crystallinity respectively.

The degradation rates of Zn and Zn-4Ag alloys in DMEM/F-12 medium were 4.80 ± 0.82 μm/year and 17.38 ± 0.78 μm/year, respectively. These values are obviously lower than the degradation rates of Zn alloys in standard salt solutions such as simulated body fluids (SBF), namely 0.107 mm/year for Zn-4Ag alloy [141] and 0.14 mm/year for Zn-2Al alloy [179]. Apart from the different alloys and manufacturing processes, these discrepancies might be attributed to the fact that the Zn degradation process is retarded in DMEM medium compared to that in SBF [167]. In addition, our results revealed significantly higher degradation rates of Zn-4Ag alloys compared to those of pure Zn, probably due to the occurrence of a secondary phase (ε-$AgZn_3$) within the microstructure [138]. A recent study reported on micro-galvanic effect between the Zn matrix and the secondary ε-$AgZn_3$ phase, leading to high degradation rates [140]. Notably, the cumulative Zn ion release of pure Zn was significantly higher than that of Zn-4Ag alloy, which is inconsistent with our obtained degradation rates. We postulate that a fraction of free Zn ions released from Zn-4Ag surfaces rapidly binds to zinc degradation granules,

which is not the case with those of pure Zn. This is probably attributed to a higher number of degradation precipitates on Zn-4Ag compared to Zn surfaces (Figure 4.2). As a consequence, a higher formation of degradation granules was observed in Zn-4Ag extracts (Figure 4.5a). Thus, released Zn ion concentration in the sample extracts is not directly related to the degradation rates determined in our test.

### 4.4.3. Assessment of cytocompatibility of Zn and Zn-4Ag alloys using immortalized periosteal cells

Viabilities of TAg cells cultured in the presence of Zn and Zn-4Ag alloy extracts for up to 12 days were shown to be unaffected, indicating no obvious cell cytotoxic effects (Figure 4.6). Zn ion concentrations analyzed in all extracts were below 90 µM after supplementation with 10% FBS (Figure 4.4a), indicating cell tolerance for this concentration. This is in accordance with the tolerance level determined for TAg cells in this study by testing different extracellular Zn ion concentration between 2-100 µM, adjusted by the addition of a $ZnCl_2$ solution (Figure 4.10). A significant improvement of TAg cell viabilities was achieved by low concentrations of either Zn-4Ag extracts or Zn ions at day 2 of examination (Figure 4.6 and Figure 4.10). This result coincides with findings from previous studies describing the activation of vascular muscle or endothelial cell viabilities in the presence of low Zn ion concentrations [180, 181]. Ag ion concentration in the extracts from Zn-4Ag alloys was under the detection limit of ICP-OES (< 0.5 µM). This Ag ion concentration remained under the previously reported cell tolerance limit (approx. 4.25 µM), indicating that limited Ag ion release does not cause the toxic effects [182]. Due to the buffering effect of the DMEM/F-12 medium, pH values in all extracts were below 8.9 (Figure 4.4b). Under pH 9, we did not detect any significant decrease of metabolic activities of TAg cells (Figure 4.9).

In our study, we detected fourfold higher degradation rates of Zn-4Ag alloys, but no higher cytotoxic effects emerged from them as compared to those of pure Zn. This finding contradicts the conclusion that cytotoxicity of Zn and its alloys is consistent with the variation of degradation rates [183, 184]. We postulate that during degradation of Zn-4Ag, free Zn ions were bound to degradation granules, leading to relatively low Zn ion concentrations in the

analyzed extracts (Figure 4.4). Therefore, we conclude that cytotoxicity of Zn and its alloys is mainly determined by available Zn ions. Previously, studies have reported on obvious cytotoxicity of undiluted extracts of Zn and its alloys towards bone-related cells [129, 138, 185]. DMEM/F-12 medium without FBS was chosen for the generation of Zn extracts. The presence of FBS in the extraction medium can increase Zn ion release, leading to additional cytotoxicity [150].

Periosteum derived mesenchymal stromal cells can differentiate into multiple cell lineages and play a critical role in bone regeneration [11, 15, 186]. We explored potential effects of long-term Zn degradation products on the mineralization potential of TAg cells considering the potential application of Zn-based alloys as suitable osteosynthesis materials. Our results showed that extracts of low concentrations promote the osteogenic differentiation of TAg cells, in contrast to high concentrated extracts, indicating a dose-dependent effect (Figure 4.7). Similar effects on the mineralization potential of TAg cells were detected by using Zn ion concentrations of 2 µM and 40 µM in osteogenic media (Figure 4.11). In coincidence, other studies reported on osteogenic induction caused by Zn ion release from Zn-containing biomaterials [187, 188]. Zn-mediated cellular response seems to involve GPR39/ZnR and TRPM7 receptors for Zn-entry into MSCs, thus triggering the intracellular cAMP and PKA pathway, leading to the activation of MAPK [46]. Our qPCR data revealed no obvious increase in RUNX2, ALP and OCN gene expression at day 14, when TAg cells were cultured in the presence of low concentrated extracts (Figure 4.8) in comparison to TAg cells without extract supplementation. On the other hand, we observed a significant decrease in gene expression of the osteogenesis-relevant genes in the presence of high concentrated Zn extracts. A delayed osseointegration of pure Zn, characterized by less new bone formation directly on Zn surfaces, was observed in *in vivo* studies, which might be caused by the local accumulation of excessive Zn ion concentrations [129, 134]. Our data also verify the *in vivo* performances of Zn-based implants, indicating that the Zn ion concentration should be controlled in order to not disturb the bone tissue healing process. Nevertheless, the mechanisms of Zn modulated osteogenesis are still not fully

understood and should be further investigated.

## 4.5. Conclusions

A modified extraction method was established for better correlation of Zn/Zn-4Ag alloy degradation behavior and cytocompatibility. Both Zn and Zn-4Ag exhibited predictable *in vitro* degradation behavior under cell culture conditions. Compared with pure Zn, a Zn-4Ag alloy with higher degradation rates seemed to exhibit no adverse cytotoxic effects on TAg cells. Concerning the degradation behavior, Zn ion concentrations in the extracts were not related to the calculated degradation rates of samples. This discrepancy is probably caused by formation of insoluble precipitates of degradation products, leading to a decreased concentration of free Zn ions in the extracts. This implies that cytotoxicity cannot be predicted by calculated degradation rates, determined by e. g. sample weight loss, since it is correlated with released free ions rather than with degradation rates. In addition, osteogenic differentiation of TAg cells was significantly induced in the presence of low concentrated Zn extracts and significantly inhibited after supplementation of medium with high concentrated Zn extracts. Therefore, optimized Zn-based implants should produce low Zn ion concentrations in the local tissue to avoid interference with new bone formation.

## 5. Discussion

In this cumulative thesis, the first goal was to assess the influence of 2D-cultivated jaw periosteal cells on monocyte-derived dendritic cell differentiation in a co-culture system. In the second part, the effects of JPCs seeded within β-TCP constructs on human DC maturation was investigated. In the third part of the present thesis, the effects of extracellular Zn ion concentrations on cell viabilities and osteogenic differentiation of immortalized periosteal (TAg 58) cells was evaluated. In the following, the overall results are comprehensively discussed.

### 5.1. Immunosuppressive effects of JPCs on DC maturation

MSCs are considered to play a key role in bone tissue regeneration due to their capacity for self-renewal and differentiation. Notably, MSCs have been proven to elicit potent immunosuppressive effects on cells of the innate (monocytes, neutrophils, macrophages, natural killer (NK), and dendritic cells (DCs)) and adaptive (B lymphocyte and T lymphocyte) immune system through cell-to-cell interactions and several immunomodulatory factors, as shown in Figure 5.1 [26, 27].
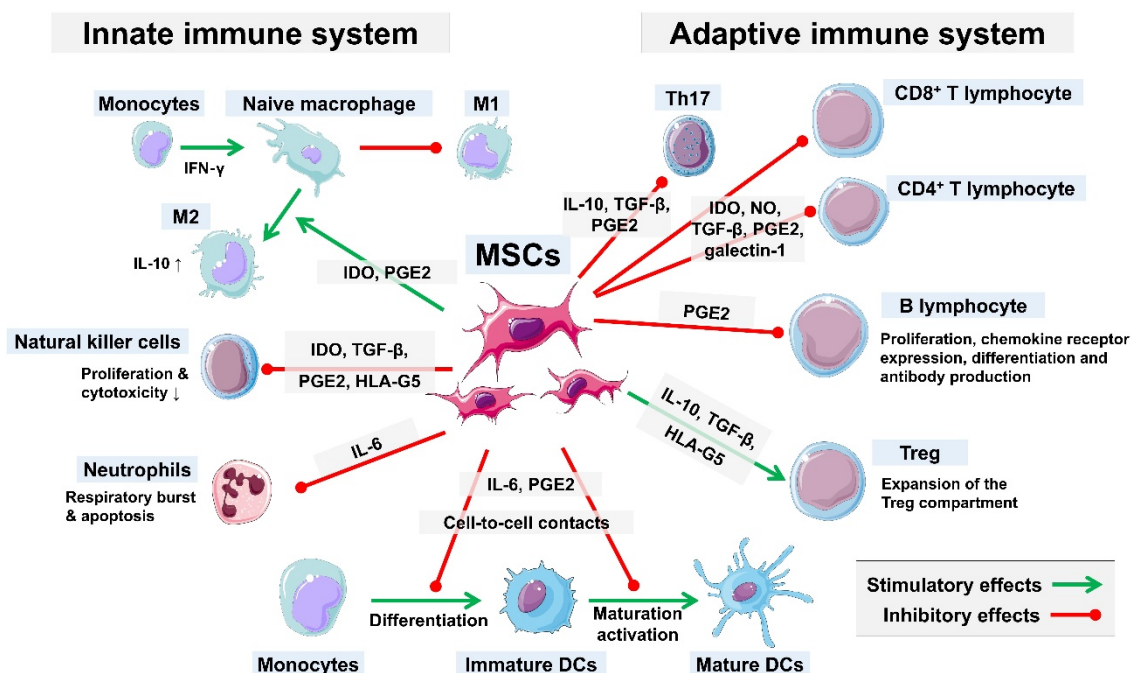


**Figure 5.1.** The schematic summarizing immunomodulation effects of

94

mesenchymal stem cells [26, 27].

The basic mechanisms mediating immunomodulation of MSCs can be summarized as follows. MSCs and their derived extracellular vesicles (EVs) influence mechanisms of the adaptive immune system, including the regulation of B and T lymphocytes. MSCs produced chemokine (C-X-C motif) ligand 9 (CXCL9) and CXCL10 under inflammatory conditions to attract activated T-cells and the close contact to MSCs might increase their immunosuppressive function [189]. Furthermore, it is known that the proliferation of pro-inflammatory IL-17 producing Th17 cells can be inhibited by transforming growth factor-beta (TGF-β), the lipid mediator prostaglandin E2 (PGE2) and Interleukin- (IL-) 10 secretion by MSCs [190, 191]. Furthermore, MSCs can suppress B cell proliferation, inhibit the production of different immunoglobulins (IgA, IgG, and IgM) [192]. In context of macrophages, the switch from an inflammatory M1 into an anti-inflammatory M2 state is partially mediated by PGE2 produced by MSCs [193]. NK cells are a subset of lymphocytes, whose effector functions, and cytotoxic production can be inhibited by immunomodulatory factors such as PGE2, IDO, and HLA-G5 produced by MSCs [194, 195].

In fact, DCs are key regulators for understanding the impact of MSCs on both parts, the innate and adaptive immune system [92]. DCs can be derived from CD34+ hematopoietic stem cells (monocytes) in the presence of granulocyte-macrophage colony-stimulating factor (GM-CSF) and interleukin-4 (IL-4) [196]. The initiation of primary immune responses or the tolerance induction can be affected by the different phenotypes of DCs, which can be divided into an immature and a mature type, respectively [92]. Mature DCs are involved in the upregulation of costimulatory molecules of antigen presentation, such as CD80, CD86, and MHC-II. Thereby, DC maturation is considered as the most important step towards the induction of immunogenic T cell responses [25]. As shown in Table 5.1, previous numerous studies showed that MSCs isolated from different tissues not only can influence the differentiation and maturation of DCs but also can modulate T cell proliferation based on their low immunogenicity and immunoregulatory properties [34, 197-204].

**Table 5.1.** Summary of the effects of MSCs on monocyte-derived DC differentiation and maturation. The results are indicated as follows: -: inhibition, +: activation, n.s.: not significant and /: not analyzed.

| MSC origin | Monocyte-derived DC phenotype | | | Induction of T cell proliferation | Production of IL-12 |
|---|---|---|---|---|---|
| | CD1a | CD14 | Co-stimulators | | |
| Bone marrow | - [34, 197-199] | + [34, 197, 199]<br>n.s. [198] | - [197, 198] | + [199]<br>- [197, 198] | + [199]<br>- [198] |
| Cord blood | / | + [201]<br>n.s. [200] | - [202]<br>n.s. [200, 201] | / | + [200] |
| Deciduous teeth pulp | / | + [203] | / | - [203] | / |
| Periapical lesions | / | + [204] | / | - [204] | / |

In study I, the effects of JPCs on monocyte-derived DC maturation were investigated by using a two dimensional (2D) co-culture sytem. When DCs were co-cultured with JPCs for 3, 6, and 7 days, respectively, DC cell sizes and densities were significantly decreased. Although DCs' gene expression induced by 2D-cultivated JPCs is much more complex, the overall tendency clearly indicated the repression of pro-inflammatory cytokines. Furthermore, an overall induction of IL-10 gene expression in the present mature DCs. Thereby, the results indicated that 2D-cultivated JPCs could overall inhibit DC maturation, which is in agreement with the immunosuppressive effects of MSCs. Nevertheless, the exact mechanism of 2D-cultivated JPCs on DCs is not completely understood but probably related to the inhibition of pro-inflammatory cytokines (IFN-γ and TNF-α) and induction of anti-inflammatory factor IL-10.

## 5.2. JPCs-seeded β-TCP constructs inhibit DC maturation

Scaffold materials play a crucial role in bone tissue regeneration, which not only provide mechanical support but also possess excellent biocompatibility and even biofuntionality [2, 24]. Even though most scaffolds exhibit no obvious systemic toxicity, foreign body reactions occured after implantation of scaffold materials [205, 206]. Undoubtedly, the biological performance of a scaffold material is determined by the host response and its interaction with the immune system [207]. Generally, the foreign body response to implant materials can be summarized as in the following [205-208]: Firstly, a layer of body fluid proteins is adsorbed on implant surfaces after the initial implantation. In the next step, adsorbed and non-adsorbed proteins can activate platelet activation, coagulation and the upregulation of complement system components, leading to the recruitment of monocytes which differentiate into macrophages and dendritic cells. Afterwards, polymorphonuclear leukocytes, as phagocytes, infiltrate tissues environment and produce reactive oxygen species (ROS) and proteolytic enzymes to foster "pathogen" killing. Additionally, they secrete chemokines which attract further monocytes and dendritic cells. During this activation phase, stimulated tissue fibroblasts participate to the process of excessive fibrosis and biomaterial encapsulation. At the end, regulatory DCs recruit regulatory T-cells and inhibit macrophage activation and an immunological equilibrium is restored.

Based on the aforementioned aspects, DCs are considered to be the most potent antigen-presenting cells, bridging innate and adaptive immunity. Due to the fact that DCs are involved in the host immune repose to biomaterials, they influence indirectly the biofunationality of implant materials [205, 209]. Regarding tissue engineering scaffolds, numerous investigations demonstrated that the phenotype and function of DCs are determined by the physicochemical properties of the implant materials. These properties mainly include material composition, surface chemistry, hydrophobicity and topography (surface roughness). Regarding the material composition, J. Park et al. demonstrated that DC maturation can be affected by different material types [210]. The activation and maturation of DCs can be triggered by lactic-

coglycolic acid, alginate and chitosan while hyaluronic acid exerts suppressive effects on DC functions. Additionally, DC maturation is also influenced by self−assembled monolayers (SAMs) of alkanethiols on titanium or gold-plated surfaces. The surface treated with −CH₃ SAMs showed the least mature DCs while treatment with −OH, −COOH, or −NH₂ SAMs caused moderate DC maturation [211]. Furthermore, polylactic Acid (PLA) microparticles with a hydrophobic surface significantly promoted antigen internalization into dendritic cells compared to poly(lactic-*co*-glycolic acid) (PLGA) and polyethylene oxide (PEO)/PLA (PELA)-based microparticles [212]. Relatively rough Ti-based surfaces (modSLA) maintained an immature phenotype while pretreatment of the surface promoted a mature DC phenotype [213]. Moreover, Tai et al. reported that β-TCP particles induced murine bone marrow-derived DC maturation through up-regulating DC surface molecules (CD86, CD80, CD40, MHC class II, and class I molecules), soluble cytokines and chemokines (chemokine (C-C motif) ligand 2 (CCL2), CCL3, and macrophage colony-stimulating factor (M-CSF)) [113]. Taken together, these investigations show that material properties exert a key role in the activation and maturation of DCs.

In study II, we evaluated the effect of JPCs-β-TCP scaffolds on monocyte-derived DC differentiation. JPCs-β-TCP scaffolds could significantly decrease the numbers of differentiated DCs. Monocultured/co-cultured DCs under osteogenic conditions showed the decreased gene expressions of IL-12Rβ2 and IFN-γ and increased IL-8 levels. Furthermore, the analysis of the protein levels in co-cultured DCs indicate that G-CSF expression was significantly upregulated. Thereby, JPCs-seeded β-TCP constructs exhibited an overall inhibitory effect on DC maturation. Notably, to elucidate the effects of JPCs, the gene expression in DCs was measured in the presence of cell-free or cell-seeded β-TCP constructs. Regarding JPCs-seeded β-TCP constructs under untreated conditions, lower gene expression levels of IL-12p35, IL-12Rβ1, IL-12Rβ2 were detected. Also, JPCs-seeded β-TCP constructs under untreated conditions led to higher gene expression of the anti-inflammatory IL-4 and G-CSF. These results demonstrated that JPCs possess the ability to inhibit pro-inflammatory cytokine expression and induce

anti-inflammatory cytokine expression. In fact, the modulatory effect of JPCs-seeded β-TCP constructs on DC maturation is in line with previous findings published for MSCs-seeded PLGA scaffolds [99]. The potential mechanism of DC function inhibition by MSCs might be mediated by the suppression of p38/MAPK and ERK/MAPK pathways. Taken together, JPCs-seeded β-TCP constructs provide an accessible strategy not only to improve osteoinductive abilities of the material but also to inhibit DC maturation.

## 5.3. Effects of Zn ions on the osteogenic potential of immortalized periosteal cells

As one of the regulatory signals for bone formation, Zn ions are counted as essential cofactors of enzymes involved in bone formation and resorption [214]. As listed in Table 5.2, numerous previous studies demonstrated that Zn ions or Zn-containing biomaterials can induce the osteogenic differentiation of MSCs, probably mediated by a mechanism involving the MAPK/ERK signalling pathway [215]. Nonetheless, to our knowledge, there are no published studies investigating the effect of extracellular Zn ions on the osteogenic differentiation of immortalized periosteal (Tag 58) cells. In the framework of my first joint authorship and the third study presented in this cumulative thesis, we investigated the effect of Zn ions on the mineral deposition and osteogenesis-related gene expression of a human immortalized cranial periosteal cell line (Tag 58).

**Table 5.2.** Summary of osteoinductive effects of Zn ions and Zn-containing biomaterials.

| Materials | Cells | Key findings | Ref. |
|---|---|---|---|
| Zn sulfate | Mouse monocytic cell line (RAW264.7)<br><br>Mouse preosteoblastic cell line (MC3T3-E1) | Zn suppressed osteoclast differentiation and promoted osteoblast mineralization.<br><br>Zn might involve in the antagonism of NF-κB activation. | [216] |
| ZnCl2 | Mouse preosteoblastic cell line (MC3T3-E1) | Zn ion can increase osteogenic differentiation of MC3T3-E1 probably through the stimulation of the cell proliferation, ALP activity and collagen synthesis in osteoblastic cells. | [217] |
| $ZnSO_4$ | Rat bone marrow mesenchymal stem cells (rBMSCs) | The double-edged effects of Zn ion microenvironments on the osteogenic properties of rBMSCs, probably probably mediated by the activation the MAPK/ERK signaling pathway | [215] |
| ZnCl2 | Mouse preosteoblastic cell line (MC3T3-E1) | Zn ions can activate ATP activity and regulates the transcription of osteoblastic differentiation genes (COL I, ALP, OP and OCN) | [218] |
| Zn-modified titanium | Dental pulp stem cells (DPSC) | Eluted zinc ions stimulated gene expression of osteoblast markers (Type I collagen, ALP, OCN, Runx2 and VEGF-A).<br><br>Eluted zinc ions induced ALP expression and calcium deposition in DPSC. | [219] |
| Zn-modified titanium | Human bone marrow-derived mesenchymal cells (hBMCs) | Zn ions released from the implant promoted cell viability, osteoblast marker gene (type I collagen, OCN, ALP and BSP) expressions and calcium deposition in hBMCs. | [187] |

| Zn-implanted titanium surfaces | Mouse preosteoblastic cell line (MC3T3-E1) | Zn-implanted titanium could significantly stimulate proliferation of osteoblastic MC3T3-E1 cells. | [220] |
|---|---|---|---|
| | Rat bone marrow mesenchymal stem cells (rBMSCs) | The initial adhesion, spreading activity, ALP activity, collagen secretion and extracellular matrix mineralization of rMSCs could be significantly stimulated. | |
| Titania nanotubes incorporated with Zn (NT-Zn) | Rat bone marrow mesenchymal stem cells (rBMSCs) | NT-Zn modification of titanium surfaces led to a significant increase in osteogenic MSC differentiation, which seemed to be related to the activation of the ERK1/2 signaling pathway. | [221] |
| Zinc-substituted hydroxaapatite (HA, ZnHA) | Human adipose-derived MSCs | ZnHA biomaterial enhanced the cell growth and osteogenesis-related differentiation markers (OCN and COL). | [222] |
| Zn-incorporated $TiO_2$ coatings | Rat bone marrow mesenchymal stem cells (rBMSCs) | Zn-implanted coatings led to higher ALP activities and up-regulated osteogenic-related genes (OCN, Col-I, ALP, Runx2) in rMSCs. | [223] |
| Zn-containing bioactive glass scaffolds | Human adipose stem cells (hASCs) | Zn-containing bioactive glass scaffolds resulted in increased proliferation and differentiation of hASCs. | [224] |

Thereby, we demonstrated that the effects of Zn ions on the osteogenic differentiation of immortalized periosteal cells is dose-dependent. In particular, our results showed that a low concentration (2 µM) of Zn ions elicits inductive, whereas high Zn ion concentrations (40 µM) show inhibitive effects on osteogenesis (Figure 4.11), which is in agreement with previous studies reporting on similar effects on BMSCs [46, 215]. In fact, previous studies reported that appropriate Zn ions released from Zn-containing biomaterials can not only stimulate ALP activity and collagen secretion of MSCs but can also induce its extracellular matrix mineralization [220, 223]. A possible mechanism of this effect might be that extracellular Zn ions enter into MSCs through specific receptors (GPR39/ZnR and TRPM7), and then activate the intracellular MAPK signalling pathway [46]. Similarly, a recent study revealed double-edged effects of Zn ion microenvironments on osteogenic differentiation of BMSCs and the related underlaying mechanism [215]. Appropriate Zn ion concentrations in microenvironments can moderately increase intracellular Zn ion concentrations via the activation of the MAPK/ERK signalling pathway. In turn, high concentrations of Zn ions can inhibit the osteogenic differentiation via damaging intracellular Zn homeostasis, increasing intracellular reactive oxygen species, and inducing cell apoptosis [215]. Our study confirmed these published data and revealed similar results that suitable Zn ion concentrations play a critical role in cellular

response and osteogenic differentiation of immortalized periosteal cells. Although the exact mechanism should be more deeply analyzed and understood, the regulation of Zn ions in the extracellular microenvironment seems to be essential to promote new bone formation.

## 5.4. Limitations of the studies and outlook

The first two studies of the present thesis focus for the first time on the *in vitro* investigation of the interactions between 2D and 3D-cultivated JPCs and dendritic cells. The third study deals with the response of immortalized periosteal cells to degradation products of Zn/Zn alloys.

From the first two studies we can draw the conclusion that JPCs possess the capability to inhibit the DC maturation process regardless of the culture conditions as monolayers or growing within 3D-TCP scaffolds. Therefore, we could demonstrate for the first time that JPCs elicit immunosuppressive effects. The third study led to the conclusion that low Zn concentrations can enhance the osteogenic potential of immortalized periosteal cells. This result is relevant in the context of the generation of absorbable Zn alloys for the clinical application of dental implants.

By the performed studies described in the present study, we moved a small step further towards clinical applications. It seems that human JPCs represent a promising stem cell source for clinical applications. Nevertheless, translation of JPCs-based tissue engineering constructs from bench to bedside still remains a considerable challenge, as illustrated in Figure 5.2.
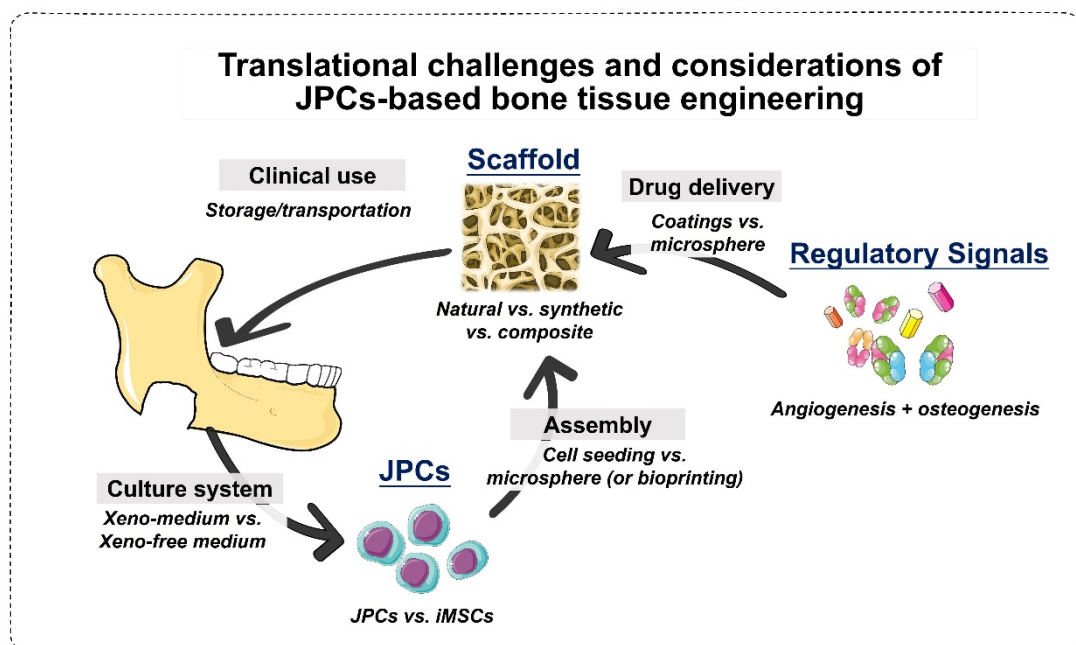


**Figure 5.2.** The schematic summarizing translational challenges and considerations of JPCs-based bone tissue engineering. JPCs were

reprogrammed to iPSCs which were differentiated to iMSCs.

Regarding future JPCs-based therapies, following scenario is conceivable: jaw periosteal cells will be isolated from human jaw periosteum and will be further expanded *in vitro*. Secondly, an ideal scaffold should provide conditions for good cell attachment, proliferation and differentiation. After the assembly between stem cells and scaffolds, constructs will undergo activation using regulatory signals and after the required time, sterile constructs will be implanted into the bone defect site.

Our lab achieved progress however, there are different obstacles we have to take. We compared JPC phenotype and osteogenic capacity under normal FCS-containing and animal-free culture conditions [15]. Further, we demonstrated that *in vitro* cultivation of JPCs with platelet lysate is a promising alternative to FCS culture conditions [23]. Regarding the cell source, we succeeded in generating "footprint-free" iPSCs from JPCs by using self-replicating RNA. In the next step, we produced induced pluripotent stem cell-derived mesenchymal stem cell-like cells (iMSCs) exhibiting even a stronger mineralization potential after induced osteogenic differentiation [225, 226]. However, we still have to deal with and solve some problems occurred during osteogenic differentiation of iMSCs such as poor adhesive capacity and elevated cellular stress.

Further, in order to optimize the assembly method for applicable BTE constructs it is of importance to include cell-laden microspheres and bioprinting. Moreover, the characteristics of scaffolds in terms of biodegradability, optimal size of micropores, chemical composition, surface topography and appropriate mechanical strength, ought to be improved, which parameters determine cellular behavior [18]. Considering regulatory signals and related delivery, it is still unclear which factors or carriers are optimal for the use of cell constructs. Finally, transportation and storage before implantation should be carefully standardized for safe clinical applications. Therefore, further research is required to bridge the gap between scientific advancements and clinical applications.

## 6. Summary

This thesis investigated the immunoregulatory properties of 2D-cultured human periosteal cells as well as their effects in the 3D culture within β-TCP constructs on monocyte-derived DC maturation. Furthermore, the impact of extracellular Zn ion concentrations on periosteal cell response was evaluated. Based on the experimental results, the principal findings can be summarized as follows:

1) After co-culturing with 2D-cultured JPCs, DC numbers were significantly decreased. At the same time, gene expressions of IL-12p35 and -p40 and pro-inflammatory cytokine (IFN-γ and TNF-α) levels were decreased while IL-8 mRNA levels were increased. These data showed that 2D-cultured JPCs elicit an overall immunosuppressive effect on monocyte-derived DC maturation.

2) After co-culturing with JPCs-seeded β-TCP scaffolds, lower dendritic cell densities and mature/immature DC ratios were detected, probably due to its overall inhibition of pro-inflammatory (IFN-γ) and induction of the anti-inflammatory cytokines (IL-10 and G-CSF). This study demonstrated an overall inhibitory effect of JPCs-seeded β-TCP constructs on monocyte-derived DC maturation.

3) The third study revealed that low extracellular Zn ion concentrations can significantly induce the osteogenesis of immortalized periosteal cells while the high Zn ion concentration seemed to inhibit its osteogenic differentiation, implying a dose-dependent effect of this element.

To sum up, JPCs exhibit excellent characteristics and can be considered as a promising stem cell source for bone tissue engineering. Further, appropriate Zn ion concentrations effectively improved osteogenic differentiation of immortalized periosteal cells. To continue this research topic, future investigations should focus the interactions of JPCs with other members of the innate immune system, e.g. macrophages and the analysis of the underlaying mechanism in more details. As a further aspect, the influence of Zn ions on primary periosteal cells should be elucidated.

## 7. German summary

In dieser Arbeit wurden die immunregulatorischen Eigenschaften menschlicher 2D-kultivierten Periostzellen sowie die Auswirkungen von Zellen, die auf β-TCP-Konstrukte gesät wurden, auf die von Monozyten abgeleitete DC-Reifung untersucht werden. Darüber hinaus, wurde der Einfluss der extrazellulären Zn-Ionen-Konzentration auf die zelluläre Antwort untersucht. Auf der Grundlage der experimentellen Ergebnisse, können diese wie folgt zusammengefasst werden:

1)  Nach der Ko-Kultivierung mit 2D-kultivierten JPCs, wurde die Zahl der DCs signifikant verringert. Gleichzeitig wurde die Genexpression von IL-12p35 und -p40 sowie die Levels der pro-inflammatorischen Zytokine (IFN-γ und TNF-α) reduziert, während die IL-8-mRNA Levels erhöht waren. Diese Daten zeigten, dass von den JPCs insgesamt eine immunsuppressive Wirkung auf die von Monozyten abgeleitete DC-Reifung ausging.

2)  Nach der Ko-Kultivierung mit JPCs-besiedelten β-TCP-Gerüsten, zeigten sich niedrigere Zelldichten und reife/unreife DC-Verhältnisse, vermutlich basierend auf der allgemeinen Inhibition der pro-inflammatorischen (IFN-γ) und der Induktion der anti-inflammatorischen Zytokine (IL-10 und G-CSF). Auch die Ergebnisse der zweiten Studie zeigten, dass insgesamt eine hemmende Wirkung von JPCs-besiedelten β-TCP-Konstrukten auf die DC-Reifung ausging.

3)  Die dritte Studie zeigte, dass niedrige extrazelluläre Zn-Konzentrationen die Osteogenese der immortalisierten Periostzellen signifikant induzieren, während die hohe Zn-Konzentration deren osteogene Differenzierung hinweist, was auf einen dosisabhängigen Effekt hinweist.

Zusammenfassend lässt sich sagen, dass JPCs exzellente Eigenschaften zeigen, um als eine vielversprechende Stammzellquelle für für das Knochen Tissue Engineering darstellen. Außerdem zeigte sich, dass geeignete Zn-Ionen Konzentrationen die osteogene Differenzierung von immortalisierten Periostzellen wirksam verbesserte. Um dieses Forschungsthema fortzuführen, sollen zukünftige Studien die Interaktionen

zwischen JPCs und anderen Komponenten des Immunsystems, beispielsweise Makrophagen und die Analyse der zugrunde liegenden Mechanismen, fokussieren. Als ein weiterer Aspekt, soll die Wirkung von Zn-Ionen auf primäre Periostzellen untersucht werden.

## 8. Bibliography

[1] C.M. Murphy, F.J. O'Brien, D.G. Little, A. Schindeler, Cell-scaffold interactions in the bone tissue engineering triad, EUR CELL MATER 26(4) (2013) 120-132.

[2] B.D. Smith, D.A. Grande, The current state of scaffolds for musculoskeletal regenerative applications, NATURE REVIEWS RHEUMATOLOGY 11(4) (2015) 213-222.

[3] S. Al-Himdani, Z.M. Jessop, A. Al-Sabah, E. Combellack, A. Ibrahim, S.H. Doak, A.M. Hart, C.W. Archer, C.A. Thornton, I.S. Whitaker, Tissue-engineered solutions in plastic and reconstructive surgery: principles and practice, FRONTIERS IN SURGERY 4 (2017) 4.

[4] P. Bianco, P.G. Robey, Stem cells in tissue engineering, NATURE 414(6859) (2001) 118-121.

[5] T. Zhao, Z.-N. Zhang, Z. Rong, Y. Xu, Immunogenicity of induced pluripotent stem cells, NATURE 474(7350) (2011) 212-215.

[6] S. Kargozar, M. Mozafari, S. Hamzehlou, P. Brouki Milan, H.-W. Kim, F. Baino, Bone tissue engineering using human cells: a comprehensive review on recent trends, current prospects, and recommendations, APPLIED SCIENCES 9(1) (2019) 174.

[7] C. Ferretti, M. Mattioli-Belmonte, Periosteum derived stem cells for regenerative medicine proposals: Boosting current knowledge, WORLD J STEM CELLS 6(3) (2014) 266-277.

[8] S.F. Evans, H. Chang, M.L. Knothe Tate, Elucidating multiscale periosteal mechanobiology: a key to unlocking the smart properties and regenerative capacity of the periosteum?, TISSUE ENGINEERING PART B: REVIEWS 19(2) (2013) 147-159.

[9] H. NAKAHARA, S.P. BRUDER, V.M. GOLDBERG, A.I. CAPLAN, *In vivo* osteochondrogenic potential of cultured cells derived from the periosteum, CLINICAL ORTHOPAEDICS AND RELATED RESEARCH 259 (1990) 223-232.

[10] Z. Lin, A. Fateh, D. Salem, G. Intini, Periosteum: biology and applications in craniofacial bone regeneration, JOURNAL OF DENTAL RESEARCH 93(2) (2014) 109-116.

[11] S. Debnath, A.R. Yallowitz, J. McCormick, S. Lalani, T. Zhang, R. Xu, N. Li, Y. Liu, Y.S. Yang, M. Eiseman, Discovery of a periosteal stem cell mediating intramembranous bone formation, NATURE 562(7725) (2018) 133.

[12] D. Alexander, J. Hoffmann, A. Munz, B. Friedrich, J. Geis-Gerstorfer, S. Reinert, Analysis of OPLA scaffolds for bone engineering constructs using human jaw periosteal cells, JOURNAL OF MATERIALS SCIENCE: MATERIALS IN MEDICINE 19(3) (2008) 965-974.

[13] E. Brauchle, D. Carvajal Berrio, M. Rieger, K. Schenke-Layland, S. Reinert, D. Alexander, Raman Spectroscopic Analyses of Jaw Periosteal

Cell Mineralization, STEM CELLS INT 2017 (2017) 1651376.

[14] D. Alexander, F. Schäfer, M. Olbrich, B. Friedrich, H.-J. Bühring, J. Hoffmann, S. Reinert, MSCA-1/TNAP selection of human jaw periosteal cells improves their mineralization capacity, CELLULAR PHYSIOLOGY AND BIOCHEMISTRY 26(6) (2010) 1073-1080.

[15] D. Alexander, M. Rieger, C. Klein, N. Ardjomandi, S. Reinert, Selection of osteoprogenitors from the jaw periosteum by a specific animal-free culture medium, PLOS ONE 8(12) (2013) e81674.

[16] N. Ardjomandi, C. Klein, K. Kohler, A. Maurer, H. Kalbacher, J. Niederländer, S. Reinert, D. Alexander, Indirect coating of RGD peptides using a poly‑L‑lysine spacer enhances jaw periosteal cell adhesion, proliferation, and differentiation into osteogenic tissue, JOURNAL OF BIOMEDICAL MATERIALS RESEARCH PART A 100(8) (2012) 2034-2044.

[17] H. Agata, I. Asahina, Y. Yamazaki, M. Uchida, Y. Shinohara, M. Honda, H. Kagami, M. Ueda, Effective bone engineering with periosteum-derived cells, JOURNAL OF DENTAL RESEARCH 86(1) (2007) 79-83.

[18] L. Schuster, N. Ardjomandi, M. Munz, F. Umrath, C. Klein, F. Rupp, S. Reinert, D. Alexander, Establishment of Collagen: Hydroxyapatite/BMP-2 Mimetic Peptide Composites, MATERIALS 13(5) (2020) 1203.

[19] N. Ardjomandi, J. Huth, D. Stamov, A. Henrich, C. Klein, H.-P. Wendel, S. Reinert, D. Alexander, Surface biofunctionalization of β-TCP blocks using aptamer 74 for bone tissue engineering, MATERIALS SCIENCE AND ENGINEERING: C 67 (2016) 267-275.

[20] D. Alexander, F. Schäfer, A. Munz, B. Friedrich, C. Klein, J. Hoffmann, H.-J. Bühring, S. Reinert, LNGFR induction during osteogenesis of human jaw periosteum-derived cells, CELLULAR PHYSIOLOGY AND BIOCHEMISTRY 24(3-4) (2009) 283-290.

[21] F. Umrath, C. Thomalla, S. Pöschel, K. Schenke-Layland, S. Reinert, D. Alexander, Comparative Study of MSCA-1 and CD146 Isolated Periosteal Cell Subpopulations, CELLULAR PHYSIOLOGY AND BIOCHEMISTRY 51(3) (2018) 1193-1206.

[22] M. Olbrich, M. Rieger, S. Reinert, D. Alexander, Isolation of osteoprogenitors from human jaw periosteal cells: a comparison of two magnetic separation methods, PLOS ONE 7(10) (2012) e47176.

[23] Y. Wanner, F. Umrath, M. Waidmann, S. Reinert, D. Alexander, Platelet lysate: the better choice for jaw periosteal cell mineralization, STEM CELLS INTERNATIONAL 2017 (2017).

[24] M. Danalache, S.-M. Kliesch, M. Munz, A. Naros, S. Reinert, D. Alexander, Quality Analysis of Minerals Formed by Jaw Periosteal Cells under Different Culture Conditions, INTERNATIONAL JOURNAL OF MOLECULAR SCIENCES 20(17) (2019) 4193.

[25] M.L. Heuzé, P. Vargas, M. Chabaud, M. Le Berre, Y.J. Liu, O. Collin, P. Solanes, R. Voituriez, M. Piel, A.M. Lennon‑Duménil, Migration of dendritic cells: physical principles, molecular mechanisms, and functional

implications, IMMUNOLOGICAL REVIEWS 256(1) (2013) 240-254.

[26] K. Turksen, Stem Cell Biology and Regenerative Medicine, SPRINGER (2013).

[27] B.S. Guerrouahen, H. Sidahmed, A. Al Sulaiti, M. Al Khulaifi, C. Cugno, Enhancing mesenchymal stromal cell immunomodulation for treating conditions influenced by the immune system, STEM CELLS INTERNATIONAL 2019 (2019).

[28] F. Dazzi, I. Marigo, The Immunosuppressive Properties of Adult Stem Cells: Mesenchymal Stem Cells as a Case Study, The Immunological Barriers to Regenerative Medicine, SPRINGER 2013, pp. 175-197.

[29] A. Augello, R. Tasso, S.M. Negrini, A. Amateis, F. Indiveri, R. Cancedda, G. Pennesi, Bone marrow mesenchymal progenitor cells inhibit lymphocyte proliferation by activation of the programmed death 1 pathway, EUROPEAN JOURNAL OF IMMUNOLOGY 35(5) (2005) 1482-1490.

[30] M. Di Nicola, C. Carlo-Stella, M. Magni, M. Milanesi, P.D. Longoni, P. Matteucci, S. Grisanti, A.M. Gianni, Human bone marrow stromal cells suppress T-lymphocyte proliferation induced by cellular or nonspecific mitogenic stimuli, BLOOD 99(10) (2002) 3838-3843.

[31] P. Fiorina, M. Jurewicz, A. Augello, A. Vergani, S. Dada, S. La Rosa, M. Selig, J. Godwin, K. Law, C. Placidi, Immunomodulatory function of bone marrow-derived mesenchymal stem cells in experimental autoimmune type 1 diabetes, THE JOURNAL OF IMMUNOLOGY 183(2) (2009) 993-1004.

[32] I. Rasmusson, O. Ringdén, B. Sundberg, K. Le Blanc, Mesenchymal stem cells inhibit the formation of cytotoxic T lymphocytes, but not activated cytotoxic T lymphocytes or natural killer cells, TRANSPLANTATION 76(8) (2003) 1208-1213.

[33] C. Prevosto, M. Zancolli, P. Canevali, M.R. Zocchi, A. Poggi, Generation of CD4+ or CD8+ regulatory T cells upon mesenchymal stem cell-lymphocyte interaction, HAEMATOLOGICA 92(7) (2007) 881-888.

[34] A.J. Nauta, A.B. Kruisselbrink, E. Lurvink, R. Willemze, W.E. Fibbe, Mesenchymal stem cells inhibit generation and function of both CD34+-derived and monocyte-derived dendritic cells, THE JOURNAL OF IMMUNOLOGY 177(4) (2006) 2080-2087.

[35] A. Uccelli, L. Moretta, V. Pistoia, Immunoregulatory function of mesenchymal stem cells, EUROPEAN JOURNAL OF IMMUNOLOGY 36(10) (2006) 2566-2573.

[36] M.B. Lutz, N.A. Kukutsch, M. Menges, S. Rößner, G. Schuler, Culture of bone marrow cells in GM‐CSF plus high doses of lipopolysaccharide generates exclusively immature dendritic cells which induce alloantigen‐specific CD4 T cell anergy *in vitro*, EUROPEAN JOURNAL OF IMMUNOLOGY 30(4) (2000) 1048-1052.

[37] H. Jonuleit, E. Schmitt, G. Schuler, J. Knop, A.H. Enk, Induction of interleukin 10–producing, nonproliferating CD4+ T cells with regulatory

properties by repetitive stimulation with allogeneic immature human dendritic cells, THE JOURNAL OF EXPERIMENTAL MEDICINE 192(9) (2000) 1213-1222.

[38] W.-X. Gao, Y.-Q. Sun, J. Shi, C.-L. Li, S.-B. Fang, D. Wang, X.-Q. Deng, W. Wen, Q.-L. Fu, Effects of mesenchymal stem cells from human induced pluripotent stem cells on differentiation, maturation, and function of dendritic cells, STEM CELL RESEARCH & THERAPY 8(1) (2017) 1-16.

[39] S. Beyth, Z. Borovsky, D. Mevorach, M. Liebergall, Z. Gazit, H. Aslan, E. Galun, J. Rachmilewitz, Human mesenchymal stem cells alter antigen-presenting cell maturation and induce T-cell unresponsiveness, BLOOD 105(5) (2005) 2214-2219.

[40] F. Djouad, L.M. Charbonnier, C. Bouffi, P. Louis‑Plence, C. Bony, F. Apparailly, C. Cantos, C. Jorgensen, D. Noël, Mesenchymal stem cells inhibit the differentiation of dendritic cells through an interleukin‑6‑dependent mechanism, STEM CELLS 25(8) (2007) 2025-2032.

[41] N. Ardjomandi, A. Henrich, J. Huth, C. Klein, E. Schweizer, L. Scheideler, F. Rupp, S. Reinert, D. Alexander, Coating of ß-tricalcium phosphate scaffolds—a comparison between graphene oxide and poly-lactic-co-glycolic acid, BIOMEDICAL MATERIALS 10(4) (2015) 045018.

[42] M. Geiger, R. Li, W. Friess, Collagen sponges for bone regeneration with rhBMP-2, ADVANCED DRUG DELIVERY REVIEWS 55(12) (2003) 1613-1629.

[43] W. Wang, K.W. Yeung, Bone grafts and biomaterials substitutes for bone defect repair: A review, BIOACTIVE MATERIALS 2(4) (2017) 224-247.

[44] T. Takizawa, N. Nakayama, H. Haniu, K. Aoki, M. Okamoto, H. Nomura, M. Tanaka, A. Sobajima, K. Yoshida, T. Kamanaka, Titanium fiber plates for bone tissue repair, ADVANCED MATERIALS 30(4) (2018) 1703608.

[45] J.E. Coleman, Structure and mechanism of alkaline phosphatase, ANNUAL REVIEW OF BIOPHYSICS AND BIOMOLECULAR STRUCTURE 21(1) (1992) 441-483.

[46] D. Zhu, Y. Su, M.L. Young, J. Ma, Y. Zheng, L. Tang, Biological responses and mechanisms of human bone marrow mesenchymal stem cells to Zn and Mg biomaterials, ACS APPLIED MATERIALS & INTERFACES 9(33) (2017) 27453-27461.

[47] H. Li, X. Xie, Y. Zheng, Y. Cong, F. Zhou, K. Qiu, X. Wang, S. Chen, L. Huang, L. Tian, Development of biodegradable Zn-1X binary alloys with nutrient alloying elements Mg, Ca and Sr, SCIENTIFIC REPORTS 5 (2015).

[48] K. Le Blanc, I. Rasmusson, B. Sundberg, C. Götherström, M. Hassan, M. Uzunel, O. Ringdén, Treatment of severe acute graft-versus-host disease with third party haploidentical mesenchymal stem cells, THE LANCET 363(9419) (2004) 1439-1441.

[49] K. Le Blanc, F. Frassoni, L. Ball, F. Locatelli, H. Roelofs, I. Lewis, E. Lanino, B. Sundberg, M.E. Bernardo, M. Remberger, Mesenchymal stem cells for treatment of steroid-resistant, severe, acute graft-versus-host

disease: a phase II study, THE LANCET 371(9624) (2008) 1579-1586.

[50] K. Le Blanc, L.C. Davies, MSCs—cells with many sides, CYTOTHERAPY 20(3) (2018) 273-278.

[51] S. Glennie, I. Soeiro, P.J. Dyson, E.W.-F. Lam, F. Dazzi, Bone marrow mesenchymal stem cells induce division arrest anergy of activated T cells, BLOOD 105(7) (2005) 2821-2827.

[52] K. Le Blanc, D. Mougiakakos, Multipotent mesenchymal stromal cells and the innate immune system, NATURE REVIEWS IMMUNOLOGY 12(5) (2012) 383.

[53] Z. Tu, Q. Li, H. Bu, F. Lin, Mesenchymal stem cells inhibit complement activation by secreting factor H, STEM CELLS AND DEVELOPMENT 19(11) (2010) 1803-1809.

[54] S. Manicassamy, B. Pulendran, Dendritic cell control of tolerogenic responses, IMMUNOLOGICAL REVIEWS 241(1) (2011) 206-227.

[55] G. Ceccarelli, A. Graziano, L. Benedetti, M. Imbriani, F. Romano, F. Ferrarotti, M. Aimetti, G.M. Cusella De Angelis, Osteogenic Potential of Human Oral‐Periosteal Cells (PCs) Isolated From Different Oral Origin: An *In Vitro* Study, JOURNAL OF CELLULAR PHYSIOLOGY 231(3) (2016) 607-612.

[56] C. Ferretti, M. Mattioli-Belmonte, Periosteum derived stem cells for regenerative medicine proposals: boosting current knowledge, WORLD JOURNAL OF STEM CELLS 6(3) (2014) 266.

[57] S.J. Roberts, N. van Gastel, G. Carmeliet, F.P. Luyten, Uncovering the periosteum for skeletal regeneration: the stem cell that lies beneath, BONE 70 (2015) 10-18.

[58] H.-Y. Hsiao, C.-Y. Yang, J.-W. Liu, E.M. Brey, M.-H. Cheng, Periosteal osteogenic capacity depends on tissue source, TISSUE ENGINEERING PART A 24(23-24) (2018) 1733-1741.

[59] P. Fang, X. Li, J. Dai, L. Cole, J.A. Camacho, Y. Zhang, Y. Ji, J. Wang, X.-F. Yang, H. Wang, Immune cell subset differentiation and tissue inflammation, JOURNAL OF HEMATOLOGY & ONCOLOGY 11(1) (2018) 97.

[60] D.J. Johnson, P.S. Ohashi, Molecular programming of steady‐state dendritic cells: impact on autoimmunity and tumor immune surveillance, ANNALS OF THE NEW YORK ACADEMY OF SCIENCES 1284(1) (2013) 46-51.

[61] K.N. Couper, D.G. Blount, E.M. Riley, IL-10: the master regulator of immunity to infection, THE JOURNAL OF IMMUNOLOGY 180(9) (2008) 5771-5777.

[62] S.E. Macatonia, N.A. Hosken, M. Litton, P. Vieira, C.-S. Hsieh, J.A. Culpepper, M. Wysocka, G. Trinchieri, K.M. Murphy, A. O'Garra, Dendritic cells produce IL-12 and direct the development of Th1 cells from naive CD4^{+} T cells, THE JOURNAL OF IMMUNOLOGY 154(10) (1995) 5071-5079.

[63] L. Stobie, S. Gurunathan, C. Prussin, D.L. Sacks, N. Glaichenhaus, C.-Y. Wu, R.A. Seder, The role of antigen and IL-12 in sustaining Th1 memory cells *in vivo*: IL-12 is required to maintain memory/effector Th1 cells sufficient to mediate protection to an infectious parasite challenge, PROCEEDINGS OF THE NATIONAL ACADEMY OF SCIENCES 97(15) (2000) 8427-8432.

[64] A. D'Andrea, M. Rengaraju, N.M. Valiante, J. Chehimi, M. Kubin, M. Aste, S. Chan, M. Kobayashi, D. Young, E. Nickbarg, Production of natural killer cell stimulatory factor (interleukin 12) by peripheral blood mononuclear cells, JOURNAL OF EXPERIMENTAL MEDICINE 176(5) (1992) 1387-1398.

[65] G. Trinchieri, Interleukin-12 and the regulation of innate resistance and adaptive immunity, NATURE REVIEWS IMMUNOLOGY 3(2) (2003) 133.

[66] S. Gillessen, D. Carvajal, P. Ling, F.J. Podlaski, D.L. Stremlo, P.C. Familletti, U. Gubler, D.H. Presky, A.S. Stern, M.K. Gately, Mouse interleukin‑12 (IL‑12) p40 homodimer: a potent IL‑12 antagonist, EUROPEAN JOURNAL OF IMMUNOLOGY 25(1) (1995) 200-206.

[67] M. Jana, K. Pahan, IL-12 p40 homodimer, but not IL-12 p70, induces the expression of IL-16 in microglia and macrophages, MOLECULAR IMMUNOLOGY 46(5) (2009) 773-783.

[68] P. Kaliński, P.L. Vieira, J.H. Schuitemaker, E.C. de Jong, M.L. Kapsenberg, Prostaglandin E2 is a selective inducer of interleukin-12 p40 (IL-12p40) production and an inhibitor of bioactive IL-12p70 heterodimer, BLOOD 97(11) (2001) 3466-3469.

[69] P. Kalinski, Regulation of immune responses by prostaglandin E2, THE JOURNAL OF IMMUNOLOGY 188(1) (2012) 21-28.

[70] Y. Zhang, X.-h. Ge, X.-J. Guo, S.-b. Guan, X.-m. Li, W. Gu, W.-g. Xu, Bone marrow mesenchymal stem cells inhibit the function of dendritic cells by secreting galectin-1, BIOMED RESEARCH INTERNATIONAL 2017 (2017).

[71] Y. Iwasaki, K. Fujio, T. Okamura, K. Yamamoto, Interleukin-27 in T cell immunity, INTERNATIONAL JOURNAL OF MOLECULAR SCIENCES 16(2) (2015) 2851-2863.

[72] R. Meisel, A. Zibert, M. Laryea, U. Göbel, W. Däubener, D. Dilloo, Human bone marrow stromal cells inhibit allogeneic T-cell responses by indoleamine 2, 3-dioxygenase–mediated tryptophan degradation, BLOOD 103(12) (2004) 4619-4621.

[73] S. Aggarwal, M.F. Pittenger, Human mesenchymal stem cells modulate allogeneic immune cell responses, BLOOD 105(4) (2005) 1815-1822.

[74] M.M.-J. Chang, M. Juarez, D.M. Hyde, R. Wu, Mechanism of dexamethasone-mediated interleukin-8 gene suppression in cultured airway epithelial cells, AMERICAN JOURNAL OF PHYSIOLOGY-LUNG CELLULAR AND MOLECULAR PHYSIOLOGY 280(1) (2001) L107-L115.

[75] H.-J. Lee, J.-W. Cho, S.-C. Kim, K.-H. Kang, S.-K. Lee, S.-H. Pi, S.-K. Lee, E.-C. Kim, Roles of p38 and ERK MAP kinases in IL-8 expression in

TNF-α-and dexamethasone-stimulated human periodontal ligament cells, CYTOKINE 35(1-2) (2006) 67-76.

[76] M. Toebak, J. De Rooij, H. Moed, T. Stoof, B. Von Blomberg, D. Bruynzeel, R. Scheper, S. Gibbs, T. Rustemeyer, Differential suppression of dendritic cell cytokine production by anti‐inflammatory drugs, BRITISH JOURNAL OF DERMATOLOGY 158(2) (2008) 225-233.

[77] N.K. Paschos, W.E. Brown, R. Eswaramoorthy, J.C. Hu, K.A. Athanasiou, Advances in tissue engineering through stem cell‐based co‐culture, JOURNAL OF TISSUE ENGINEERING AND REGENERATIVE MEDICINE 9(5) (2015) 488-503.

[78] L. Pomeraniec, D. Benayahu, Mesenchymal Cell Growth and Differentiation on a New Biocomposite Material: A Promising Model for Regeneration Therapy, BIOMOLECULES 10(3) (2020) 458.

[79] M. Akiyama, H. Nonomura, S.H. Kamil, R.A. Ignotz, Periosteal cell pellet culture system: a new technique for bone engineering, CELL TRANSPLANTATION 15(6) (2006) 521-532.

[80] D.W. Hutmacher, M. Sittinger, Periosteal cells in bone tissue engineering, TISSUE ENGINEERING 9(4, Supplement 1) (2003) 45-64.

[81] H. Nakahara, S. Bruder, S. Haynesworth, J. Holecek, M. Baber, V. Goldberg, A. Caplan, Bone and cartilage formation in diffusion chambers by subcultured cells derived from the periosteum, BONE 11(3) (1990) 181-188.

[82] H. Nakahara, V.M. Goldberg, A.I. Caplan, Culture‐expanded human periosteal‐derived cells exhibit osteochondral potential *in vivo*, JOURNAL OF ORTHOPAEDIC RESEARCH 9(4) (1991) 465-476.

[83] Y. Sakata, T. Ueno, T. Kagawa, M. Kanou, T. Fujii, E. Yamachika, T. Sugahara, Osteogenic potential of cultured human periosteum-derived cells–a pilot study of human cell transplantation into a rat calvarial defect model, JOURNAL OF CRANIO-MAXILLOFACIAL SURGERY 34(8) (2006) 461-465.

[84] D. Alexander, J. Hoffmann, A. Munz, B. Friedrich, J. Geis-Gerstorfer, S. Reinert, Comparison of three dimensional scaffolds for bone engineering constructs using human jaw periosteal cells, JOURNAL OF STEM CELLS & REGENERATIVE MEDICINE 2(1) (2007) 177.

[85] P. Eggli, W. Müller, R. Schenk, Porous hydroxyapatite and tricalcium phosphate cylinders with two different pore size ranges implanted in the cancellous bone of rabbits. A comparative histomorphometric and histologic study of bony ingrowth and implant substitution, CLINICAL ORTHOPAEDICS AND RELATED RESEARCH (232) (1988) 127-138.

[86] T. Okuda, K. Ioku, I. Yonezawa, H. Minagi, G. Kawachi, Y. Gonda, H. Murayama, Y. Shibata, S. Minami, S. Kamihira, The effect of the microstructure of β-tricalcium phosphate on the metabolism of subsequently formed bone tissue, BIOMATERIALS 28(16) (2007) 2612-2621.

[87] J. Zhou, H. Lin, T. Fang, X. Li, W. Dai, T. Uemura, J. Dong, The repair of large segmental bone defects in the rabbit with vascularized tissue engineered bone, BIOMATERIALS 31(6) (2010) 1171-1179.

[88] C.A. Vacanti, L.J. Bonassar, M.P. Vacanti, J. Shufflebarger, Replacement of an avulsed phalanx with tissue-engineered bone, NEW ENGLAND JOURNAL OF MEDICINE 344(20) (2001) 1511-1514.

[89] N. Romani, S. Gruner, D. Brang, E. Kämpgen, A. Lenz, B. Trockenbacher, G. Konwalinka, P.O. Fritsch, R.M. Steinman, G. Schuler, Proliferating dendritic cell progenitors in human blood, JOURNAL OF EXPERIMENTAL MEDICINE 180(1) (1994) 83-93.

[90] F. Sallusto, A. Lanzavecchia, Efficient presentation of soluble antigen by cultured human dendritic cells is maintained by granulocyte/macrophage colony-stimulating factor plus interleukin 4 and downregulated by tumor necrosis factor alpha, JOURNAL OF EXPERIMENTAL MEDICINE 179(4) (1994) 1109-1118.

[91] F. Chapuis, M. Rosenzwajg, M. Yagello, M. Ekman, P. Biberfeld, J.C. Gluckman, Differentiation of human dendritic cells from monocytes *in vitro*, EUROPEAN JOURNAL OF IMMUNOLOGY 27(2) (1997) 431-441.

[92] R.M. Steinman, D. Hawiger, M.C. Nussenzweig, Tolerogenic dendritic cells, ANNUAL REVIEW OF IMMUNOLOGY 21(1) (2003) 685-711.

[93] M. Krampera, S. Glennie, J. Dyson, D. Scott, R. Laylor, E. Simpson, F. Dazzi, Bone marrow mesenchymal stem cells inhibit the response of naive and memory antigen-specific T cells to their cognate peptide, BLOOD 101(9) (2003) 3722-3729.

[94] J. Dai, D. Rottau, F. Kohler, S. Reinert, D. Alexander, Effects of Jaw Periosteal Cells on Dendritic Cell Maturation, JOURNAL OF CLINICAL MEDICINE 7(10) (2018) 312.

[95] S.S. Jensen, N. Broggini, E. Hjørting‑Hansen, R. Schenk, D. Buser, Bone healing and graft resorption of autograft, anorganic bovine bone and β‑tricalcium phosphate. A histologic and histomorphometric study in the mandibles of minipigs, CLINICAL ORAL IMPLANTS RESEARCH 17(3) (2006) 237-243.

[96] D. Buser, B. Hoffmann, J.p. Bernard, A. Lussi, D. Mettler, R.K. Schenk, Evaluation of filling materials in membrane‑protected bone defects. A comparative histomorphometric study in the mandible of miniature pigs, CLINICAL ORAL IMPLANTS RESEARCH 9(3) (1998) 137-150.

[97] T. Ding, J. Sun, P. Zhang, Immune evaluation of biomaterials in TNF-α and IL-1β at mRNA level, JOURNAL OF MATERIALS SCIENCE: MATERIALS IN MEDICINE 18(11) (2007) 2233-2236.

[98] R.A. Horowitz, Z. Mazor, C. Foitzik, H. Prasad, M. Rohrer, A. Palti, β-tricalcium phosphate as bone substitute material: properties and clinical applications, JOURNAL OF OSSEOINTEGRATION 2(2) (2010) 61-68.

[99] H. Zhu, F. Yang, B. Tang, X.-M. Li, Y.-N. Chu, Y.-L. Liu, S.-G. Wang, D.-C. Wu, Y. Zhang, Mesenchymal stem cells attenuated PLGA-induced

inflammatory responses by inhibiting host DC maturation and function, BIOMATERIALS 53 (2015) 688-698.

[100] M. Zhang, H. Tang, Z. Guo, H. An, X. Zhu, W. Song, J. Guo, X. Huang, T. Chen, J. Wang, Splenic stroma drives mature dendritic cells to differentiate into regulatory dendritic cells, NATURE IMMUNOLOGY 5(11) (2004) 1124.

[101] X.-X. Jiang, Y. Zhang, B. Liu, S.-X. Zhang, Y. Wu, X.-D. Yu, N. Mao, Human mesenchymal stem cells inhibit differentiation and function of monocyte-derived dendritic cells, BLOOD 105(10) (2005) 4120-4126.

[102] J.J. Lee, K.A. Foon, R.B. Mailliard, R. Muthuswamy, P. Kalinski, Type 1‑polarized dendritic cells loaded with autologous tumor are a potent immunogen against chronic lymphocytic leukemia, JOURNAL OF LEUKOCYTE BIOLOGY 84(1) (2008) 319-325.

[103] M.M. Tiemessen, A.L. Jagger, H.G. Evans, M.J. van Herwijnen, S. John, L.S. Taams, CD4+ CD25+ Foxp3+ regulatory T cells induce alternative activation of human monocytes/macrophages, PROCEEDINGS OF THE NATIONAL ACADEMY OF SCIENCES 104(49) (2007) 19446-19451.

[104] D. Wang, T. Life, K. Chen, T. Life, W.T. Du, Z.-B. Han, T. Life, H. Ren, Y. Chi, T. Life, CD14+ monocytes promote the immunosuppressive effect of human umbilical cord matrix stem cells, EXPERIMENTAL CELL RESEARCH 316(15) (2010).

[105] C. Hawrylowicz, L. Guida, E. Paleolog, Dexamethasone up-regulates granulocyte-macrophage colony-stimulating factor receptor expression on human monocytes, IMMUNOLOGY 83(2) (1994) 274.

[106] L. Oehler, O. Majdic, W.F. Pickl, J. Stöckl, E. Riedl, J. Drach, K. Rappersberger, K. Geissler, W. Knapp, Neutrophil granulocyte– committed cells can be driven to acquire dendritic cell characteristics, JOURNAL OF EXPERIMENTAL MEDICINE 187(7) (1998) 1019-1028.

[107] M.L. McLemore, S. Grewal, F. Liu, A. Archambault, J. Poursine-Laurent, J. Haug, D.C. Link, STAT-3 activation is required for normal G-CSF-dependent proliferation and granulocytic differentiation, IMMUNITY 14(2) (2001) 193-204.

[108] T. Wang, G. Niu, M. Kortylewski, L. Burdelya, K. Shain, S. Zhang, R. Bhattacharya, D. Gabrilovich, R. Heller, D. Coppola, Regulation of the innate and adaptive immune responses by Stat-3 signaling in tumor cells, NATURE MEDICINE 10(1) (2004) 48.

[109] U. Bharadwaj, M. Li, R. Zhang, C. Chen, Q. Yao, Elevated interleukin-6 and G-CSF in human pancreatic cancer cell conditioned medium suppress dendritic cell differentiation and activation, CANCER RESEARCH 67(11) (2007) 5479-5488.

[110] C.Q. Xia, R. Peng, F. Beato, M. Clare‑Salzler, Dexamethasone induces IL‑10‑producing monocyte‑derived dendritic cells with durable immaturity, SCANDINAVIAN JOURNAL OF IMMUNOLOGY 62(1) (2005) 45-54.

[111] T. Lange, A.F. Schilling, F. Peters, F. Haag, M.M. Morlock, J.M. Rueger, M. Amling, Proinflammatory and osteoclastogenic effects of beta-tricalciumphosphate and hydroxyapatite particles on human mononuclear cells *in vitro*, BIOMATERIALS 30(29) (2009) 5312-5318.

[112] J. Dong, T. Uemura, Y. Shirasaki, T. Tateishi, Promotion of bone formation using highly pure porous β-TCP combined with bone marrow-derived osteoprogenitor cells, BIOMATERIALS 23(23) (2002) 4493-4502.

[113] S. Tai, J.-Y. Cheng, H. Ishii, K. Shimono, V. Zangiacomi, T. Satoh, T. Hosono, E. Suzuki, K. Yamaguchi, K. Maruyama, Effects of beta-tricalcium phosphate particles on primary cultured murine dendritic cells and macrophages, INTERNATIONAL IMMUNOPHARMACOLOGY 40 (2016) 419-427.

[114] I. Solaroglu, J. Cahill, T. Tsubokawa, E. Beskonakli, J.H. Zhang, Granulocyte colony-stimulating factor protects the brain against experimental stroke via inhibition of apoptosis and inflammation, NEUROLOGICAL RESEARCH (2008).

[115] C.W. Park, K.-S. Kim, S. Bae, H.K. Son, P.-K. Myung, H.J. Hong, H. Kim, Cytokine secretion profiling of human mesenchymal stem cells by antibody array, INTERNATIONAL JOURNAL OF STEM CELLS 2(1) (2009) 59.

[116] D.H. Kim, K.H. Yoo, K.S. Choi, J. Choi, S.-Y. Choi, S.-E. Yang, Y.-S. Yang, H.J. Im, K.H. Kim, H.L. Jung, Gene expression profile of cytokine and growth factor during differentiation of bone marrow-derived mesenchymal stem cell, CYTOKINE 31(2) (2005) 119-126.

[117] N.B. Azouna, F. Jenhani, Z. Regaya, L. Berraeis, T.B. Othman, E. Ducrocq, J. Domenech, Phenotypical and functional characteristics of mesenchymal stem cells from bone marrow: comparison of culture using different media supplemented with human platelet lysate or fetal bovine serum, STEM CELL RESEARCH & THERAPY 3(1) (2012) 6.

[118] C. Talarn, A. Urbano-Ispizua, R. Martino, M. Batlle, F. Fernandez-Aviles, C. Herrera, J. Perez-Simon, A. Gaya, M. Aymerich, J. Petriz, G-CSF increases the number of peripheral blood dendritic cells CD16^{+} and modifies the expression of the costimulatory molecule CD86^{+}, BONE MARROW TRANSPLANTATION 37(9) (2006) 873.

[119] V. Reddy, G.R. Hill, L. Pan, A. Gerbitz, T. Teshima, Y. Brinson, J.L. Ferrara, G-CSF modulates cytokine profile of dendritic cells and decreases acute graft-versus-host disease through effects on the donor rather than the recipient, TRANSPLANTATION 69(4) (2000) 691-693.

[120] M. Kondo, A.J. Wagers, M.G. Manz, S.S. Prohaska, D.C. Scherer, G.F. Beilhack, J.A. Shizuru, I.L. Weissman, Biology of hematopoietic stem cells and progenitors: implications for clinical application, ANNUAL REVIEW OF IMMUNOLOGY 21(1) (2003) 759-806.

[121] L.M. Souza, T.C. Boone, J. Gabrilove, P.H. Lai, K.M. Zsebo, D.C. Murdock, V.R. Chazin, J. Bruszewski, H. Lu, K.K. Chen, Recombinant human granulocyte colony-stimulating factor: effects on normal and leukemic myeloid cells, SCIENCE 232(4746) (1986) 61-65.

[122] W.P. Sheridan, R. Fox, C. Begley, D. Maher, K. McGrath, C. Juttner, L.B. To, J. Szer, G. Mostyn, Effect of peripheral-blood progenitor cells mobilised by filgrastim (G-CSF) on platelet recovery after high-dose chemotherapy, THE LANCET 339(8794) (1992) 640-644.

[123] N. Zhang, T.J. Rogers, M. Caterina, J.J. Oppenheim, Proinflammatory chemokines, such as CC chemokine ligand 3, desensitize μ-opioid receptors on dorsal root ganglia neurons, THE JOURNAL OF IMMUNOLOGY 173(1) (2004) 594-599.

[124] N. Tedla, H.-W. Wang, H.P. McNeil, N. Di Girolamo, T. Hampartzoumian, D. Wakefield, A. Lloyd, Regulation of T lymphocyte trafficking into lymph nodes during an immune response by the chemokines macrophage inflammatory protein (MIP)-1α and MIP-1β, THE JOURNAL OF IMMUNOLOGY 161(10) (1998) 5663-5672.

[125] A. Nehmé, J. Edelman, Dexamethasone inhibits high glucose–, TNF-α–, and IL-1β–induced secretion of inflammatory and angiogenic mediators from retinal microvascular pericytes, INVESTIGATIVE OPHTHALMOLOGY & VISUAL SCIENCE 49(5) (2008) 2030-2038.

[126] D. Vojtěch, J. Kubásek, J. Šerák, P. Novák, Mechanical and corrosion properties of newly developed biodegradable Zn-based alloys for bone fixation, ACTA BIOMATERIALIA 7(9) (2011) 3515-3522.

[127] H. Yang, X. Qu, W. Lin, C. Wang, D. Zhu, K. Dai, Y. Zheng, *In vitro* and *in vivo* studies on zinc-hydroxyapatite composites as novel biodegradable metal matrix composite for orthopedic applications, ACTA BIOMATERIALIA 71 (2018) 200-214.

[128] P. Li, W. Zhang, J. Dai, A.B. Xepapadeas, E. Schweizer, D. Alexander, L. Scheideler, C. Zhou, H. Zhang, G. Wan, Investigation of zinc‐copper alloys as potential materials for craniomaxillofacial osteosynthesis implants, MATERIALS SCIENCE AND ENGINEERING: C (2019) 109826.

[129] H. Yang, X. Qu, W. Lin, D. Chen, D. Zhu, K. Dai, Y. Zheng, Enhanced Osseointegration of Zn-Mg Composites by Tuning the Release of Zn Ions with Sacrificial Mg-Rich Anode Design, ACS BIOMATERIALS SCIENCE & ENGINEERING 5(2) (2018) 453-467.

[130] X. Wang, X. Shao, T. Dai, F. Xu, J.G. Zhou, G. Qu, L. Tian, B. Liu, Y. Liu, *In vivo* study of the efficacy, biosafety, and degradation of a zinc alloy osteosynthesis system, ACTA BIOMATERIALIA (2019).

[131] Q. Chen, G.A. Thouas, Metallic implant biomaterials, MATERIALS SCIENCE AND ENGINEERING: R: REPORTS 87 (2015) 1-57.

[132] P. Schumann, D. Lindhorst, M.E. Wagner, A. Schramm, N.-C. Gellrich, M. Rücker, Perspectives on resorbable osteosynthesis materials in craniomaxillofacial surgery, PATHOBIOLOGY 80(4) (2013) 211-217.

[133] J. Venezuela, M. Dargusch, The influence of alloying and fabrication techniques on the mechanical properties, biodegradability and biocompatibility of zinc: a comprehensive review, ACTA BIOMATERIALIA (2019).

[134] D. Zhu, I. Cockerill, Y. Su, Z. Zhang, J. Fu, K.-W. Lee, J. Ma, C. Okpokwasili, L. Tang, Y. Zheng, Mechanical strength, biodegradation, and *in vitro* and *in vivo* biocompatibility of Zn biomaterials, ACS APPLIED MATERIALS & INTERFACES 11(7) (2019) 6809-6819.

[135] Y. Su, I. Cockerill, Y. Wang, Y.-X. Qin, L. Chang, Y. Zheng, D. Zhu, Zinc-based biomaterials for regeneration and therapy, TRENDS IN BIOTECHNOLOGY (2018).

[136] E. Mostaed, M. Sikora-Jasinska, J.W. Drelich, M. Vedani, Zinc-based alloys for degradable vascular stent applications, ACTA BIOMATERIALIA 71 (2018) 1-23.

[137] E. O'Neill, G. Awale, L. Daneshmandi, O. Umerah, K.W.-H. Lo, The roles of ions on bone regeneration, DRUG DISCOVERY TODAY 23(4) (2018) 879-890.

[138] P. Li, C. Schille, E. Schweizer, F. Rupp, A. Heiss, C. Legner, U.E. Klotz, J. Geis-Gerstorfer, L. Scheideler, Mechanical characteristics, *in vitro* degradation, cytotoxicity, and antibacterial evaluation of Zn-4.0 Ag alloy as a biodegradable material, INTERNATIONAL JOURNAL OF MOLECULAR SCIENCES 19(3) (2018) 755.

[139] C. Hehrlein, B. Schorch, N. Kress, A. Arab, C. von Zur Mühlen, C. Bode, T. Epting, J. Haberstroh, L. Mey, H. Schwarzbach, Zn-alloy provides a novel platform for mechanically stable bioresorbable vascular stents, PLOS ONE 14(1) (2019) e0209111.

[140] M. Sikora-Jasinska, E. Mostaed, A. Mostaed, R. Beanland, D. Mantovani, M. Vedani, Fabrication, mechanical properties and *in vitro* degradation behavior of newly developed ZnAg alloys for degradable implant applications, MATERIALS SCIENCE AND ENGINEERING: C 77 (2017) 1170-1181.

[141] C. Shuai, L. Xue, C. Gao, Y. Yang, S. Peng, Y. Zhang, Selective laser melting of Zn–Ag alloys for bone repair: microstructure, mechanical properties and degradation behaviour, VIRTUAL AND PHYSICAL PROTOTYPING 13(3) (2018) 146-154.

[142] R. Marsell, T.A. Einhorn, The biology of fracture healing, INJURY 42(6) (2011) 551-555.

[143] H. Li, X. Xie, Y. Zheng, Y. Cong, F. Zhou, K. Qiu, X. Wang, S. Chen, L. Huang, L. Tian, Development of biodegradable Zn-1X binary alloys with nutrient alloying elements Mg, Ca and Sr, SCIENTIFIC REPORTS 5 (2015) 10719.

[144] N. Kirkland, N. Birbilis, M. Staiger, Assessing the corrosion of biodegradable magnesium implants: a critical review of current methodologies and their limitations, ACTA BIOMATERIALIA 8(3) (2012) 925-936.

[145] A. Bruinink, R. Luginbuehl, Evaluation of biocompatibility using *in vitro* methods: Interpretation and limitations, Tissue Engineering III: Cell-Surface Interactions for Tissue Culture, SPRINGER2011, pp. 117-152.

[146] Q. Tian, M. Deo, L. Rivera-Castaneda, H. Liu, Cytocompatibility of

magnesium alloys with human urothelial cells: a comparison of three culture methodologies, ACS BIOMATERIALS SCIENCE & ENGINEERING 2(9) (2016) 1559-1571

[147] A.F. Cipriano, A. Sallee, R.-G. Guan, Z.-Y. Zhao, M. Tayoba, J. Sanchez, H. Liu, Investigation of magnesium–zinc–calcium alloys and bone marrow derived mesenchymal stem cell response in direct culture, ACTA BIOMATERIALIA 12 (2015) 298-321.

[148] A.F. Cipriano, A. Sallee, M. Tayoba, M.C.C. Alcaraz, A. Lin, R.-G. Guan, Z.-Y. Zhao, H. Liu, Cytocompatibility and early inflammatory response of human endothelial cells in direct culture with Mg-Zn-Sr alloys, ACTA BIOMATERIALIA 48 (2017) 499-520.

[149] G.K. Levy, A. Kafri, Y. Ventura, A. Leon, R. Vago, J. Goldman, E. Aghion, Surface stabilization treatment enhances initial cell viability and adhesion for biodegradable zinc alloys, MATERIALS LETTERS 248 (2019) 130-133.

[150] P. Li, C. Schille, E. Schweizer, E. Kimmerle-Müller, F. Rupp, A. Heiss, C. Legner, U.E. Klotz, J. Geis-Gerstorfer, L. Scheideler, Selection of extraction medium influences cytotoxicity of zinc and its alloys, ACTA BIOMATERIALIA (2019).

[151] P. Li, N. Zhou, H. Qiu, M.F. Maitz, J. Wang, N. Huang, *In vitro* and *in vivo* cytocompatibility evaluation of biodegradable magnesium-based stents: a review, SCIENCE CHINA MATERIALS 61(4) (2018) 501-515.

[152] B.J. Luthringer, R. Willumeit-Römer, Effects of magnesium degradation products on mesenchymal stem cell fate and osteoblastogenesis, GENE 575(1) (2016) 9-20.

[153] D. Maradze, D. Musson, Y. Zheng, J. Cornish, M. Lewis, Y. Liu, High magnesium corrosion rate has an effect on osteoclast and mesenchymal stem cell role during bone remodelling, SCIENTIFIC REPORTS 8 (2018).

[154] H. Yang, C. Wang, C. Liu, H. Chen, Y. Wu, J. Han, Z. Jia, W. Lin, D. Zhang, W. Li, Evolution of the degradation mechanism of pure zinc stent in the one-year study of rabbit abdominal aorta model, BIOMATERIALS 145 (2017) 92-105.

[155] D. Alexander, R. Biller, M. Rieger, N. Ardjomandi, S. Reinert, Phenotypic characterization of a human immortalized cranial periosteal cell line, CELLULAR PHYSIOLOGY AND BIOCHEMISTRY 35(6) (2015) 2244-2254.

[156] J. Kubásek, D. Vojtěch, E. Jablonská, I. Pospíšilová, J. Lipov, T. Ruml, Structure, mechanical characteristics and *in vitro* degradation, cytotoxicity, genotoxicity and mutagenicity of novel biodegradable Zn–Mg alloys, MATERIALS SCIENCE AND ENGINEERING: C 58 (2016) 24-35.

[157] E. Jablonská, D. Vojtěch, M. Fousová, J. Kubásek, J. Lipov, J. Fojt, T. Ruml, Influence of surface pre-treatment on the cytocompatibility of a novel biodegradable ZnMg alloy, MATERIALS SCIENCE AND ENGINEERING: C 68 (2016) 198-204.

[158] International Organization for Standardization. ISO 10993-12: 2012.

Biological Evaluation of Medical Devices–Part 12: Sample Preparation and Reference Materials; International Organization for Standardization: Geneva, Switzerland, 2012.

[159] International Organization for Standardization. ISO 8407: 2009. Corrosion of metals and alloys–Removal of corrosion products from corrosion test specimens; International Organization for Standardization: Geneva, Switzerland, 2009.

[160] ASTM G31-12a. Standard Guide for Laboratory Immersion Corrosion Testing of Metals; American Section of the International Association for Testing Materials: West Conshohocken, PA, USA, 2017.

[161] International Organization for Standardization. ISO 10993–5: 2009 Biological Evaluation of Medical Devices–Part 5: Tests for *In Vitro* Cytotoxicity; International Organization for Standardization: Geneva, Switzerland, 2009.

[162] H. Hermawan, Updates on the research and development of absorbable metals for biomedical applications, PROGRESS IN BIOMATERIALS 7(2) (2018) 93-110.

[163] S. Johnston, M. Dargusch, A. Atrens, Building towards a standardised approach to biocorrosion studies: a review of factors influencing Mg corrosion *in vitro* pertinent to *in vivo* corrosion, SCIENCE CHINA MATERIALS 61(4) (2018) 475-500.

[164] R.-Q. Hou, N. Scharnagl, R. Willumeit-Römer, F. Feyerabend, Different effects of single protein vs. protein mixtures on magnesium degradation under cell culture conditions, ACTA BIOMATERIALIA (2019).

[165] R. Hou, R. Willumeit-Römer, V.M. Garamus, M. Frant, J. Koll, F. Feyerabend, Adsorption of Proteins on Degradable Magnesium—Which Factors are Relevant?, ACS APPLIED MATERIALS & INTERFACES 10(49) (2018) 42175-42185.

[166] Y. Xin, T. Hu, P. Chu, *In vitro* studies of biomedical magnesium alloys in a simulated physiological environment: a review, ACTA BIOMATERIALIA 7(4) (2011) 1452-1459.

[167] X. Liu, H. Yang, Y. Liu, P. Xiong, H. Guo, H.-H. Huang, Y. Zheng, Comparative Studies on Degradation Behavior of Pure Zinc in Various Simulated Body Fluids, JOM 71(4) (2019) 1414-1425.

[168] J. Gonzalez, R.Q. Hou, E.P. Nidadavolu, R. Willumeit-Römer, F. Feyerabend, Magnesium degradation under physiological conditions–best practice, BIOACTIVE MATERIALS 3(2) (2018) 174-185.

[169] M. Schinhammer, J. Hofstetter, C. Wegmann, F. Moszner, J.F. Löffler, P.J. Uggowitzer, On the immersion testing of degradable implant materials in simulated body fluid: active pH regulation using CO2, ADVANCED ENGINEERING MATERIALS 15(6) (2013) 434-441.

[170] J. Wang, F. Witte, T. Xi, Y. Zheng, K. Yang, Y. Yang, D. Zhao, J. Meng, Y. Li, W. Li, Recommendation for modifying current cytotoxicity testing standards for biodegradable magnesium-based materials, ACTA BIOMATERIALIA 21 (2015) 237-249.

[171] J. Fischer, D. Pröfrock, N. Hort, R. Willumeit, F. Feyerabend, Improved cytotoxicity testing of magnesium materials, MATERIALS SCIENCE AND ENGINEERING: B 176(11) (2011) 830-834.

[172] L. Scheideler, C. Füger, C. Schille, F. Rupp, H.-P. Wendel, N. Hort, H. Reichel, J. Geis-Gerstorfer, Comparison of different *in vitro* tests for biocompatibility screening of Mg alloys, ACTA BIOMATERIALIA 9(10) (2013) 8740-8745.

[173] O. Jung, R. Smeets, P. Hartjen, R. Schnettler, F. Feyerabend, M. Klein, N. Wegner, F. Walther, D. Stangier, A. Henningsen, Improved *In Vitro* Test Procedure for Full Assessment of the Cytocompatibility of Degradable Magnesium Based on ISO 10993-5/-12, INTERNATIONAL JOURNAL OF MOLECULAR SCIENCES 20(2) (2019) 255.

[174] Y. Zhang, Y. Yan, X. Xu, Y. Lu, L. Chen, D. Li, Y. Dai, Y. Kang, K. Yu, Investigation on the microstructure, mechanical properties, *in vitro* degradation behavior and biocompatibility of newly developed Zn-0.8% Li-(Mg, Ag) alloys for guided bone regeneration, MATERIALS SCIENCE AND ENGINEERING: C 99 (2019) 1021-1034.

[175] K.B. Törne, A. Örnberg, J. Weissenrieder, Characterization of the protective layer formed on zinc in whole blood, ELECTROCHIMICA ACTA 258 (2017) 1476-1483.

[176] T. Alhawi, M. Rehan, D. York, X. Lai, Hydrothermal synthesis of zinc carbonate hydroxide nanoparticles, PROCEDIA ENGINEERING 102 (2015) 356-361.

[177] J. Santana, B. Fernández-Pérez, J. Morales, H. Vasconcelos, R. Souto, S. González, Characterization of the corrosion products formed on zinc in archipelagic subtropical environments, INT. J. ELECTROCHEM. SCI 7 (2012) 12730-12741.

[178] M.M. Alves, T. Prošek, C.F. Santos, M.F. Montemor, Evolution of the *in vitro* degradation of Zn–Mg alloys under simulated physiological conditions, RSC ADVANCES 7(45) (2017) 28224-28233.

[179] C. Shuai, Y. Cheng, Y. Yang, S. Peng, W. Yang, F. Qi, Laser additive manufacturing of Zn-2Al part for bone repair: Formability, microstructure and properties, JOURNAL OF ALLOYS AND COMPOUNDS 798 (2019) 606-615.

[180] J. Ma, N. Zhao, D. Zhu, Bioabsorbable zinc ion induced biphasic cellular responses in vascular smooth muscle cells, SCIENTIFIC REPORTS 6 (2016) 26661.

[181] J. Ma, N. Zhao, D. Zhu, Endothelial cellular responses to biodegradable metal zinc, ACS BIOMATERIALS SCIENCE & ENGINEERING 1(11) (2015) 1174-1182.

[182] A. Yamamoto, R. Honma, M. Sumita, Cytotoxicity evaluation of 43 metal salts using murine fibroblasts and osteoblastic cells, JOURNAL OF BIOMEDICAL MATERIALS RESEARCH: A 39(2) (1998) 331-340.

[183] T. Ren, X. Gao, C. Xu, L. Yang, P. Guo, H. Liu, Y. Chen, W. Sun, Z. Song, Evaluation of as‐extruded ternary Zn–Mg–Zr alloys for biomedical

implantation material: *In vitro* and *in vivo* behavior, MATERIALS AND CORROSION 70(6) (2019) 1056-1070.

[184] Y. Yang, F. Yuan, C. Gao, P. Feng, L. Xue, S. He, C. Shuai, A combined strategy to enhance the properties of Zn by laser rapid solidification and laser alloying, JOURNAL OF THE MECHANICAL BEHAVIOR OF BIOMEDICAL MATERIALS 82 (2018) 51-60.

[185] W. Yuan, B. Li, D. Chen, D. Zhu, Y. Han, Y. Zheng, Formation Mechanism, Corrosion Behavior, and Cytocompatibility of Microarc Oxidation Coating on Absorbable High-Purity Zinc, ACS BIOMATERIALS SCIENCE & ENGINEERING 5(2) (2018) 487-497.

[186] Y. Zhang, J. Xu, Y.C. Ruan, M.K. Yu, M. O'Laughlin, H. Wise, D. Chen, L. Tian, D. Shi, J. Wang, Implant-derived magnesium induces local neuronal production of CGRP to improve bone-fracture healing in rats, NATURE MEDICINE 22(10) (2016) 1160.

[187] K. Yusa, O. Yamamoto, M. Fukuda, S. Koyota, Y. Koizumi, T. Sugiyama, *In vitro* prominent bone regeneration by release zinc ion from Zn-modified implant, BIOCHEMICAL AND BIOPHYSICAL RESEARCH COMMUNICATIONS 412(2) (2011) 273-278.

[188] W. Liu, J. Li, M. Cheng, Q. Wang, K.W. Yeung, P.K. Chu, X. Zhang, Zinc‑Modified Sulfonated Polyetheretherketone Surface with Immunomodulatory Function for Guiding Cell Fate and Bone Regeneration, ADVANCED SCIENCE 5(10) (2018) 1800749.

[189] Q. Wang, Q. Yang, Z. Wang, H. Tong, L. Ma, Y. Zhang, F. Shan, Y. Meng, Z. Yuan, Comparative analysis of human mesenchymal stem cells from fetal-bone marrow, adipose tissue, and Warton's jelly as sources of cell immunomodulatory therapy, HUMAN VACCINES & IMMUNOTHERAPEUTICS 12(1) (2016) 85-96.

[190] X. Qu, X. Liu, K. Cheng, R. Yang, R.C. Zhao, Mesenchymal stem cells inhibit Th17 cell differentiation by IL-10 secretion, EXPERIMENTAL HEMATOLOGY 40(9) (2012) 761-770.

[191] F. Baratelli, Y. Lin, L. Zhu, S.-C. Yang, N. Heuzé-Vourc'h, G. Zeng, K. Reckamp, M. Dohadwala, S. Sharma, S.M. Dubinett, Prostaglandin E2 induces FOXP3 gene expression and T regulatory cell function in human CD4^{+} T cells, THE JOURNAL OF IMMUNOLOGY 175(3) (2005) 1483-1490.

[192] F. Luk, L. Carreras-Planella, S.S. Korevaar, S.F. de Witte, F.E. Borràs, M.G. Betjes, C.C. Baan, M.J. Hoogduijn, M. Franquesa, Inflammatory conditions dictate the effect of mesenchymal stem or stromal cells on B cell function, FRONTIERS IN IMMUNOLOGY 8 (2017) 1042.

[193] C. Manferdini, F. Paolella, E. Gabusi, L. Gambari, A. Piacentini, G. Filardo, S. Fleury-Cappellesso, A. Barbero, M. Murphy, G. Lisignoli, Adipose stromal cells mediated switching of the pro-inflammatory profile of M1-like macrophages is facilitated by PGE2: *in vitro* evaluation, OSTEOARTHRITIS AND CARTILAGE 25(7) (2017) 1161-1171.

[194] G.M. Spaggiari, A. Capobianco, H. Abdelrazik, F. Becchetti, M.C.

Mingari, L. Moretta, Mesenchymal stem cells inhibit natural killer–cell proliferation, cytotoxicity, and cytokine production: role of indoleamine 2, 3-dioxygenase and prostaglandin E2, BLOOD, THE JOURNAL OF THE AMERICAN SOCIETY OF HEMATOLOGY 111(3) (2008) 1327-1333.

[195] Z. Selmani, A. Naji, I. Zidi, B. Favier, E. Gaiffe, L. Obert, C. Borg, P. Saas, P. Tiberghien, N. Rouas‑Freiss, Human leukocyte antigen-G5 secretion by human mesenchymal stem cells is required to suppress T lymphocyte and natural killer function and to induce CD4$^+$ CD25$^{high}$FOXP3$^+$ regulatory T cells, STEM CELLS 26(1) (2008) 212-222.

[196] C. Caux, B. Vanbervliet, C. Massacrier, C. Dezutter-Dambuyant, B. de Saint-Vis, C. Jacquet, K. Yoneda, S. Imamura, D. Schmitt, J. Banchereau, CD34$^+$ hematopoietic progenitors from human cord blood differentiate along two independent dendritic cell pathways in response to GM-CSF+ TNF alpha, THE JOURNAL OF EXPERIMENTAL MEDICINE 184(2) (1996) 695-706.

[197] R. Ramasamy, H. Fazekasova, E.W.-F. Lam, I. Soeiro, G. Lombardi, F. Dazzi, Mesenchymal stem cells inhibit dendritic cell differentiation and function by preventing entry into the cell cycle, TRANSPLANTATION 83(1) (2007) 71-76.

[198] W. Zhang, W. Ge, C. Li, S. You, L. Liao, Q. Han, W. Deng, R.C. Zhao, Effects of mesenchymal stem cells on differentiation, maturation, and function of human monocyte-derived dendritic cells, STEM CELLS AND DEVELOPMENT 13(3) (2004) 263-271.

[199] G.M. Spaggiari, H. Abdelrazik, F. Becchetti, L. Moretta, MSCs inhibit monocyte-derived DC maturation and function by selectively interfering with the generation of immature DCs: central role of MSC-derived prostaglandin E2, BLOOD, THE JOURNAL OF THE AMERICAN SOCIETY OF HEMATOLOGY 113(26) (2009) 6576-6583.

[200] L.C. Van Den Berk, H. Roelofs, T. Huijs, K.G. Siebers‑Vermeulen, R.A. Raymakers, G. Kögler, C.G. Figdor, R. Torensma, Cord blood mesenchymal stem cells propel human dendritic cells to an intermediate maturation state and boost interleukin‑12 production by mature dendritic cells, IMMUNOLOGY 128(4) (2009) 564-572.

[201] S. Tipnis, C. Viswanathan, A.S. Majumdar, Immunosuppressive properties of human umbilical cord‑derived mesenchymal stem cells: role of B7‑H1 and IDO, IMMUNOLOGY AND CELL BIOLOGY 88(8) (2010) 795-806.

[202] H.-W. Chen, H.-Y. Chen, L.-T. Wang, F.-H. Wang, L.-W. Fang, H.-Y. Lai, H.-H. Chen, J. Lu, M.-S. Hung, Y. Cheng, Mesenchymal stem cells tune the development of monocyte-derived dendritic cells toward a myeloid-derived suppressive phenotype through growth-regulated oncogene chemokines, THE JOURNAL OF IMMUNOLOGY 190(10) (2013) 5065-5077.

[203] F. de Sá Silva, R.N. Ramos, D.C. de Almeida, E.J. Bassi, R.P. Gonzales, S.P.H. Miyagi, C.P. Maranduba, O.A.B.E. Sant'Anna, M.M. Marques, J.A.M. Barbuto, Mesenchymal stem cells derived from human exfoliated

deciduous teeth (SHEDs) induce immune modulatory profile in monocyte-derived dendritic cells, PLOS ONE 9(5) (2014) e98050.

[204] J. Đokić, S. Tomić, M. Marković, P. Milosavljević, M. Čolić, Mesenchymal stem cells from periapical lesions modulate differentiation and functional properties of monocyte‐derived dendritic cells, EUROPEAN JOURNAL OF IMMUNOLOGY 43(7) (2013) 1862-1872.

[205] F.-j. Zhu, Y.-l. Tong, Z.-y. Sheng, Y.-m. Yao, Role of dendritic cells in the host response to biomaterials and their signaling pathways, ACTA BIOMATERIALIA 94 (2019) 132-144.

[206] B. Corradetti, The Immune Response to Implanted Materials and Devices, THE IMMUNE RESPONSE TO IMPLANTED MATERIALS AND DEVICES, (2017).

[207] S. Franz, S. Rammelt, D. Scharnweber, J.C. Simon, Immune responses to implants–a review of the implications for the design of immunomodulatory biomaterials, BIOMATERIALS 32(28) (2011) 6692-6709.

[208] D.P. Vasconcelos, A.P. Águas, M.A. Barbosa, P. Pelegrín, J.N. Barbosa, The inflammasome in host response to biomaterials: bridging inflammation and tissue regeneration, ACTA BIOMATERIALIA 83 (2019) 1-12.

[209] B.G. Keselowsky, J.S. Lewis, Dendritic cells in the host response to implanted materials, Seminars in immunology, ELSEVIER, 2017, pp. 33-40.

[210] J. Park, J.E. Babensee, Differential functional effects of biomaterials on dendritic cell maturation, ACTA BIOMATERIALIA 8(10) (2012) 3606-3617.

[211] S.P. Shankar, T.A. Petrie, A.J. García, J.E. Babensee, Dendritic cell responses to self-assembled monolayers of defined chemistries, JOURNAL OF BIOMEDICAL MATERIALS RESEARCH PART A 92(4) (2010) 1487-1499.

[212] Y. Liu, Y. Yin, L. Wang, W. Zhang, X. Chen, X. Yang, J. Xu, G. Ma, Surface hydrophobicity of microparticles modulates adjuvanticity, JOURNAL OF MATERIALS CHEMISTRY B 1(32) (2013) 3888-3896.

[213] P.M. Kou, Z. Schwartz, B.D. Boyan, J.E. Babensee, Dendritic cell responses to surface properties of clinical titanium surfaces, ACTA BIOMATERIALIA 7(3) (2011) 1354-1363.

[214] M. Yamaguchi, Role of zinc in bone formation and bone resorption, THE JOURNAL OF TRACE ELEMENTS IN EXPERIMENTAL MEDICINE 11(2‐3) (1998) 119-135.

[215] Y. Yu, K. Liu, Z. Wen, W. Liu, L. Zhang, J. Su, Double-edged effects and mechanisms of $Zn^{2+}$ microenvironments on osteogenic activity of BMSCs: osteogenic differentiation or apoptosis, RSC ADVANCES 10(25) (2020) 14915-14927.

[216] M. Yamaguchi, M.N. Weitzmann, Zinc stimulates osteoblastogenesis and suppresses osteoclastogenesis by antagonizing NF-κB activation,

MOLECULAR AND CELLULAR BIOCHEMISTRY 355(1-2) (2011) 179.

[217] H.-J. Seo, Y.-E. Cho, T. Kim, H.-I. Shin, I.-S. Kwun, Zinc may increase bone formation through stimulating cell proliferation, alkaline phosphatase activity and collagen synthesis in osteoblastic MC3T3-E1 cells, NUTRITION RESEARCH AND PRACTICE 4(5) (2010) 356-361.

[218] I.-S. Kwun, Y.-E. Cho, R.-A.R. Lomeda, H.-I. Shin, J.-Y. Choi, Y.-H. Kang, J.H. Beattie, Zinc deficiency suppresses matrix mineralization and retards osteogenesis transiently with catch-up possibly through Runx 2 modulation, BONE 46(3) (2010) 732-741.

[219] K. Yusa, O. Yamamoto, M. Iino, H. Takano, M. Fukuda, Z. Qiao, T. Sugiyama, Eluted zinc ions stimulate osteoblast differentiation and mineralization in human dental pulp stem cells for bone tissue engineering, ARCHIVES OF ORAL BIOLOGY 71 (2016) 162-169.

[220] G. Jin, H. Cao, Y. Qiao, F. Meng, H. Zhu, X. Liu, Osteogenic activity and antibacterial effect of zinc ion implanted titanium, COLLOIDS AND SURFACES B: BIOINTERFACES 117 (2014) 158-165.

[221] K. Huo, X. Zhang, H. Wang, L. Zhao, X. Liu, P.K. Chu, Osteogenic activity and antibacterial effects on titanium surfaces modified with Zn-incorporated nanotube arrays, BIOMATERIALS 34(13) (2013) 3467-3478.

[222] E. Thian, T. Konishi, Y. Kawanobe, P. Lim, C. Choong, B. Ho, M. Aizawa, Zinc-substituted hydroxyapatite: a biomaterial with enhanced bioactivity and antibacterial properties, JOURNAL OF MATERIALS SCIENCE: MATERIALS IN MEDICINE 24(2) (2013) 437-445.

[223] Y. Qiao, W. Zhang, P. Tian, F. Meng, H. Zhu, X. Jiang, X. Liu, P.K. Chu, Stimulation of bone growth following zinc incorporation into biomaterials, BIOMATERIALS 35(25) (2014) 6882-6897.

[224] S. Haimi, G. Gorianc, L. Moimas, B. Lindroos, H. Huhtala, S. Räty, H. Kuokkanen, G.K. Sándor, C. Schmid, S. Miettinen, Characterization of zinc-releasing three-dimensional bioactive glass scaffolds and their effect on human adipose stem cell proliferation and osteogenic differentiation, ACTA BIOMATERIALIA 5(8) (2009) 3122-3131.

[225] F. Umrath, H. Steinle, M. Weber, H.-P. Wendel, S. Reinert, D. Alexander, M. Avci-Adali, Generation of iPSCs from jaw periosteal cells using self-replicating RNA, INTERNATIONAL JOURNAL OF MOLECULAR SCIENCES 20(7) (2019) 1648.

[226] F. Umrath, M. Weber, S. Reinert, H.-P. Wendel, M. Avci-Adali, D. Alexander, iPSC-derived mscs versus originating jaw periosteal cells: comparison of resulting phenotype and stem cell potential, INTERNATIONAL JOURNAL OF MOLECULAR SCIENCES 21(2) (2020) 587.

## 9. Declaration of contribution of others

EBERHARD KARLS
UNIVERSITÄT
TÜBINGEN

Medizinische Fakultät

Version April 2019

### Declaration of contribution of all authors:

Herewith I, Jingtao Dai declare, that I have contributed to the mayor part of the following publication: Effects of Jaw Periosteal Cells on Dendritic Cell Maturation. Journal of Clinical Medicine, (2018) 7(10), 312.

The authors contributed to the publications as indicated in the following table (indicated in %):

| Contribution | Research concept | Selection of methods | Data acquisition | Results interpretation | Manuscript preparation |
|---|---|---|---|---|---|
| Jingtao Dai | 25 | 35 | 35 | 30 | 35 |
| Daniela Rottau | 10 | 10 | 15 | 15 | 10 |
| Franziska Kohler | 10 | 10 | 15 | 15 | 10 |
| Siegmar Reinert | 20 | 10 | 15 | 10 | 10 |
| Dorothea Alexander | 35 | 35 | 20 | 30 | 35 |

Signature of the doctoral candidate

As supervisor, I agree with the declarations by the candidate:

As corresponding author, agree with the declarations by the candidate:

As co-authors, we agree to the declarations above:

[Daniela Rottau]

[Franziska Kohler]

[Siegmar Reinert]

[Dorothea Alexander]

## 9. Declaration of contribution of others

**Declaration of contribution of all authors:**

Herewith I, Jingtao Dai declare, that I have contributed to the mayor part of the following publication: Jaw periosteal cells growing within beta-tricalcium phosphate scaffolds inhibit dendritic cell maturation. Biomolecules, Accepted.

The authors contributed to the publications as indicated in the following table (indicated in %):

| Contribution | Research concept | Selection of methods | Data acquisition | Results interpretation | Manuscript preparation |
|---|---|---|---|---|---|
| Jingtao Dai | 40 | 40 | 80 | 50 | 35 |
| Felix Umrath | - | 20 | 20 | 15 | 10 |
| Siegmar Reinert | - | - | - | - | 20 |
| Dorothea Alexander | 60 | 40 | - | 35 | 35 |

**Signature of the doctoral candidate**

**As supervisor, I agree with the declarations by the candidate:**

**As corresponding author, agree with the declarations by the candidate:**

**As co-authors, we agree to the declarations above:**

[Felix Umrach]                    [Siegmar Reinert]                    [Dorothea Alexander]

## 9. Declaration of contribution of others

**Declaration of contribution of all authors:**

Herewith I, Jingtao Dai declare, that I have contributed to the mayor part of the following publication: Response of human periosteal cells to degradation products of zinc and its alloy. Materials Science and Engineering: C, (2019) In Press, doi: 10.1016/j.msec.2019.110208. (Equally contributed first authors to this works).

The authors contributed to the publications as indicated in the following table (indicated in %):

| Contribution | Research concept | Selection of methods | Data acquisition | Results interpretation | Manuscript preparation |
|---|---|---|---|---|---|
| Ping Li | 15 | 20 | 35 | 20 | 20 |
| Jingtao Dai | 10 | 15 | 20 | 10 | 10 |
| Ernst Schweizer | 5 | 5 | 10 | 5 | 5 |
| Frank Rupp | 5 | 5 | 5 | 5 | 5 |
| Alexander Heiss | 10 | 5 | 5 | 10 | 10 |
| Andreas Richter | 5 | 5 | 5 | 5 | 5 |
| Ulrich E. Klotz | 5 | 5 | 5 | 5 | 5 |
| Jürgen Geis-Gerstorfer | 15 | 10 | 5 | 10 | 10 |
| Lutz Scheideler | 15 | 15 | 5 | 15 | 15 |
| Dorothea Alexander | 15 | 15 | 5 | 15 | 15 |

**Signature of the doctoral candidate**

**As supervisor, I agree with the declarations by the candidate:**

**As corresponding author, agree with the declarations by the candidate:**

**As co-authors, we agree to the declarations above:**

[Ping Li]

[Ernst Schweizer]

[Frank Rupp]

[Alexander Heiss]

[Andreas Richter]

[Ulrich E. Klotz]

[Jürgen Geis-Gerstorfer]

[Lutz Scheideler]

[Dorothea Alexander]

129

## Acknowledgements

My deepest gratitude goes first and foremost to my supervisor, Prof. Dr. Dorothea Alexander-Friedrich, for giving me the chance to work as a doctoral candidate in her group and providing such an interesting research topic. Her constant encouragement, support and guidance have greatly enlightened me not only in the research but also during daily life. Without her invaluable supervisions and useful suggestions, this thesis could not have reached the current state.

I am deeply grateful to my doctoral committee members, Prof. Dr. Andreas Nüssler and Prof. Dr. Hans Peter Wendel, for the professional advice in my thesis.

I would also like to express my gratitude to the dear group members Prof. Dr. Siegmar Reinert, Dr. Felix Umrath, Ms. Carol Cen, Ms. Suya Wang, Mr. Fang He, and former group members Ms. Yvonne Wanner, Ms. Franziska Kohler, Ms. Daniela Rottau, Dr. Liane Schuster, Ms. Marita Munz, Ms. Molly Lin, Ms. Marcella Engler, for providing technical assistance and help in my work.

My sincere appreciation also goes to Prof. Dr. Jürgen Geis-Gerstorfer, Prof. Dr. Frank Rupp, Dr. Lutz Scheideler, and Mr. Ernst Schweizer from the department of Section Medical Materials Science and Technology, for their good cooperation and scientific advice.

I acknowledge the contribution of Dr. Alexander Heiss, Dr. Ulrich E. Klotz and Dr. Andreas Richter from the fem Forschungsinstitut Edelmetalle & Metallchemie for their hard-working and cooperation.

I would like to express my heartfelt thanks to the China Scholarship Council for providing me with financial support.

I am particularly grateful to my lovely family, especially my parents, for their encouragement and support.

Most of all, I am deeply indebted to my beloved husband, Ping Li, who always willingly discussed with me, offered valuable insights and supported

me. I would also like to thank my son, Jasper Xiang Li, accompanies me these months while writing this thesis. Words cannot express how much their unconditional love and endless support means to me.

求学廿四春秋，光阴荏苒，日月如梭，书山浩浩，学海淼淼。感恩师者，其所传道、授业、解惑也。常思父母之恩，悠悠寸草心，难报三春晖。致爱人纸短情长，愿执子之手，与子偕老。忆芳华岁月，初心如故，路漫漫其修远兮，驾长风破万里浪，乘骐骥驰千里路，笑傲两侧万水千山！

<div align="right">

戴静桃

于内卡河畔

</div>

**Curriculum vitae**

**Personal Information:**

Name: Jingtao Dai

Gender: Female

Date of birth: 2nd June 1988

Nationality: Chinese

**Education:**

June 2012     Bachelor's degree, Jinan University, Guangzhou China

June 2015     Master's degree, Jinan University, Guangzhou China

Since February 2017 PhD degree, University of Tübingen, Germany

**Scholarships:**

Graduate scholarship from Jinan University, 2013 and 2014

Scholarship from the Chinese Scholarship Council, 2017-2019

**Certificates:**

Dental practitioner's qualification certificate in China (licensed since 2013)

**Full list of publications:**

- **Jingtao Dai**, Daniela Rottau, Franziska Kohler, Siegmar Reinert, Dorothea Alexander. Effects of Jaw Periosteal Cells on Dendritic Cell Maturation. Journal of Clinical Medicine, (2018) 7(10), 312.

- **Jingtao Dai**, Felix Umrath, Siegmar Reinert, Dorothea Alexander. Jaw Periosteal Cells Seeded in Beta-Tricalcium Phosphate Inhibit Dendritic Cell Maturation. Biomolecules (2020)10(6), 887.

- Ping Li, **Jingtao Dai**, Ernst Schweizer, Frank Rupp, Alexander Heiss, Andreas Richter, Ulrich E. Klotz, Jurgen Geis-Gerstorfer, Lutz Scheideler, Dorothea Alexander. Response of human periosteal cells to degradation products of zinc and its alloy. Materials Science and Engineering: C, (2020)108, 110208. (Equally contributed first authors to this works).

- Ping Li, Wentai Zhang, **Jingtao Dai**, Alexander Basileos Xepapadeas,

Ernst Schweizer, Dorothea Alexander, Lutz Scheideler, Chao Zhou, Haijun Zhang, Guojiang Wan, Jürgen Geis-Gerstorfer. Investigation of zinc-copper alloys as potential materials for craniomaxillofacial osteosynthesis implants. Materials Science and Engineering: C, 2019 (103), 109826.

**Academic Activities:**

- Poster presentation of "Effects of jaw periosteal cells on dendritic cells maturation" bone-tec 2017, Munich, Germany, 2017.

- Oral presentation of "Effects of jaw periosteal cells on dendritic cells maturation" 68th Kongress & Praxisfuehrungsseminar der Deutschen Gesellschaft fuer Mund-, Kiefer- und Gesichtschirurgie, Dresden, Germany, 2018.

- Oral presentation of "Jaw periosteal cells growing within β-tricalcium phosphate scaffolds reduce dendritic cells" 69th Kongress & Praxisfuehrungsseminar der Deutschen Gesellschaft fuer Mund-, Kiefer- und Gesichtschirurgie, Frankfurt am Main, Germany, 2019.

- Poster presentation of "Role of 3D growing jaw periosteal cells on dendritic cell maturation" Osteology Symposium Barcelona, Barcelona, Spain, 2019.